TECHNICAL REPORT

Date of first issue: 20 March 1998	Project No.: 76010057
Approved by: for Arne Edvin Løken Project Responsible	Organisational unit: Risers, Mooring and Foundations
Client: Joint Industry Project	Client ref.: Part 2, Activity 250

DET NORSKE VERITAS
Division Nordic Countries
Offshore

Veritasveien 1
N-1322 Høvik Norway
Tel: (47) 67 57 99 00
Fax: (47) 67 57 74 74
http://www.dnv.com
Org. No: NO 945 748 931 MVA

Summary:

A reliability analysis for the fluke anchor resistance has been developed and implemented. The failure event considered is the inception of drag due to extreme mooring line tension. The analysis accounts for the variation in anchor resistance R due applied anchor installation load, subsequent soil consolidation and cyclic loading effects following the application of extreme mooring line tension.

The analysis is initially developed for fluke anchors in a single layer of clay. The formulation is, however, generally defined such that it is extendable to reliability analyses involving multiple layers of clay, drag-in-plate anchors, and the possibility for updating the estimated reliability of the anchor resistance after installation based on measured penetration depth and/or drag length.

An initial design format for anchor installation has been developed, applying best estimates for the characteristic influence of consolidation effects and cyclic effects, and the characteristic extreme line tensions. Based on different choices for the partial safety factors, the required installation load with corresponding estimated annual failure probabilities are obtained.

See also conclusive summary on page 1.

Report No.: 98-3034	Subject Group: P5
Report title: Deep Water Anchors Pilot Reliability Analysis of Fluke Anchors (Technical Report TR 2-5)	
Work carried out by: Espen H. Cramer, Pål J. Strøm, Jan Mathisen, Knut O. Ronold and Rune Dahlberg	
Work verified by: Knut Arnesen and Gudfinnur Sigurdsson	
Date of this revision:	Rev. No.: 01 / Number of pages: 62+36

Indexing terms

Anchors
Clay
Technology Development
Structural Reliability

☒ No distribution without permission from the Client or responsible organisational unit

☐ Limited distribution within Det Norske Veritas

☐ Unrestricted distribution

Table of Contents *Page*

1 CONCLUSIVE SUMMARY 1

2 INTRODUCTION 2
2.1 About the Project 2
2.1.1 Participants 2
2.1.2 Brief Description of Project 2
2.1.3 Project Organisation 3
2.2 The Present Report 3

3 GLOSSARY AND DEFINITION OF TERMS 5
3.1 Basic Glossary and Terms 5
3.2 Case Convention for Variables in the Reliability Analysis 8

4 FORMULATION OF RELIABILITY ANALYSIS 9
4.1 General 9
4.2 Failure Event 9
4.3 Basic Limit State Function 9
4.4 Model Description 10
4.5 Probabilistic Formulation 12

5 RESPONSE SURFACE INTERFACE BETWEEN DIGIN AND PROBAN 15
5.1 Introduction to Response Surfaces 15
5.2 Interface File Specifications 15
5.3 Input Data Points 17

6 PHYSICAL MODELLING 19
6.1 Soil Description 19
6.1.1 Single Layer Clay 19
6.1.2 Double Layer Clay 20
6.2 Cyclic Loading Factor 22
6.2.1 Introduction 22
6.2.2 Technical approach 22
6.2.3 Analysis of two-way cyclic loading ($\tau_a = 0$) 25
6.2.4 Application of results to one-way cyclic loading ($\tau_a \neq 0$) 26
6.3 DIGIN Response Computation 28
6.3.1 Program Flow 28
6.3.2 Anchor Resistance 29
6.3.3 Failure Mode 30
6.3.4 Multiple DIGIN Calculations 30
6.3.5 Response Surface Representation of DIGIN Computations 30
6.4 Time Varying Loads 31
6.4.1 Annual Extreme Value Distribution of Mooring Line Tension 31

6.4.1.1 Short Term Stationary Tension 31
6.4.1.2 Annual Extreme Tension 31
6.4.2 Characteristic Tension 32

7 DESCRIPTION OF PILOT CASE 34
7.1 General 34
7.2 Probabilistic Analysis 34
7.2.1 Anchor Description 34
7.2.2 Shear Strength 34
7.2.3 Cyclic Loading Factor 35
7.2.4 DIGIN Computations 35
7.2.4.1 General 35
7.2.4.2 Penetration Depth and Installation Anchor Resistance R_{dip} 35
7.2.4.3 Drag Length 36
7.2.4.4 DIGIN Model Uncertainty 36
7.2.5 Time Varying Environmental Loads 36
7.2.6 Updated Estimates for the Failure Probability after Installation 36
7.2.7 Summary of Stochastic Variables 37

8 RELIABILITY ANALYSIS 38
8.1 Cumulative Distributions 38
8.1.1 Anchor Resistance 38
8.1.2 Penetration depth 38
8.1.3 Drag Length 38
8.2 Probabilistic Analysis 39
8.3 Discussion of Post Installation Resistance Uncertainty Model 39

9 DESIGN PROCEDURE 41
9.1 General 41
9.2 Design Equation 41
9.3 Characteristic Values 42
9.4 Partial Safety Factors 43
9.5 Target Installation Load 43
9.6 Annual Failure Probability 43

10 SUMMARY AND DISCUSSION 45

11 REFERENCES 47

12 FIGURES 49

13 APPENDICES 62

APPENDICES

A Linear Regression Analysis of Soil Data

B Analysis of two-way cyclic loading ($\tau_a = 0$)

C Response Surface Data

D Shear Strength Data

E Updated Estimates for the Failure Probability After Installation

F DWA Input File to PROBAN Run

G DWA Result File from PROBAN

1 CONCLUSIVE SUMMARY

A reliability analysis for the fluke anchor resistance has been developed and implemented. The failure event considered is the inception of drag due to extreme mooring line tension. The analysis accounts for the variation in anchor resistance R due applied anchor installation load, subsequent soil consolidation and cyclic loading effects following the application of extreme mooring line tension f_e.

The analysis is initially developed for fluke anchors in a single layer of clay. The formulation is, however, generally defined such that it is extendable to reliability analyses involving multiple layers of clay, drag-in-plate anchors, and the possibility for updating the estimated reliability of the anchor resistance after installation based on measured penetration depth and/or drag length. However, the drag length as such does not enter the design equations applied in the present pilot study, and has therefore not been addressed further herein.

The analysis is carried out in two steps. Step 1 involves multiple deterministic computations of the anchor response due to a wide range of input conditions for soil properties, anchor installation load, and extreme mooring line tension. The anchor installation phase and the subsequent effect of soil consolidation on anchor resistance is modelled and analysed with the DIGIN program. Step 2 is the computation of the probability of the failure event, with stochastic soil properties and stochastic extreme mooring line tension, applying the general probabilistic analysis program PROBAN. The effect of cyclic loading is accounted for in Step 2 of the analysis.

An interface file is used to transfer the DIGIN results from Step 1 to PROBAN, accounting for the anchor behaviour during installation and the subsequent consolidation effect expressed through R_{cons}. A response surface technique is used to interpolate between the discrete results computed by DIGIN, to obtain a continuous description of the anchor behaviour (penetration depth, drag length and resistance) for any soil properties and anchor installation load F_{dip}.

The approach for modelling and computing the various types of anchor resistance and the annual extreme line tension is described in this report, together with the applied uncertainty model. Based on different anchor installation loads, the estimated cumulative distribution functions for the penetration depth, the drag length and the holding capacity are derived for the anchor installation at a location with specified shear strength properties. Based on the modelled annual extreme line tension, the annual probability for failure (drag) of the anchor is further derived for different installation loads.

In order to show the possibilities available using probabilistic methods, a formulation for the updated estimated annual failure probability after installation depending on the measured actual penetration depth and/or drag length of the anchor is discussed.

An initial design format for anchor installation has been developed, applying best estimates for the characteristic influence of consolidation effects and cyclic effects, and the characteristic extreme line tensions. Based on different choices for the partial safety factors, the required installation load with corresponding estimated annual failure probabilities are obtained.

2 INTRODUCTION

2.1 About the Project

2.1.1 Participants

The project is organised as a joint industry project (JIP) with financial funding from the following twelve participants, which is gratefully acknowledged:

STATOIL, Norway
Saga Petroleum a.s, Norway
Det Norske Veritas, Norway
Health & Safety Executive, UK
Minerals Management Service, USA
Petrobras UK
Norsk Hydro ASA, Norway
Norske Conoco AS, Norway
BP Exploration Operating Company Limited, UK
Bruce Anchor Limited, UK
SOFEC, Inc., USA (only Part 1)
Shell Internationale Petroleum Maatschappij B.V., The Netherlands (only Part 1)

2.1.2 Brief Description of Project

The project is divided in three parts, and the objectives of the respective part-project are briefly summarised in the following.

Part 1, which was executed between August 1995 and February 1997 had the following main objectives:

- Development of a design procedure for fluke anchors in clay, utilising the results from fluke anchor tests compiled from different accessible sources and the offshore industry's general knowledge about fluke anchor performance in clay.
- Follow-up and compilation of data from drag-in plate anchor tests and identification of important design considerations and necessary further work to improve such anchors for deep water application.
- Writing a DNV Classification Note on fluke anchors based on the work on such anchors in Part 1 (after formal completion of Part 1).

Deliverables from Part 1 comprised a total of nine Interim Reports and seven Technical Reports, plus an executable version of the computer programme DIGIN.

Part 2, duration March 1997 - 1998, focuses further on deep water anchors in clay with the following main objectives:

- Further improvements to the DIGIN programme, e.g. better equilibrium solutions, and update of the fluke anchor back-fitting analyses from Part 1.
- Compilation of more drag-in plate anchor test data, e.g. from the DeepStar Project and Petrobras (through a confidentiality agreement).
- Back-fitting analysis of drag-in plate anchor tests to improve our understanding of this type of anchors both during installation and pull-out.

- Development of a design procedure for drag-in plate anchors.
- Specification and execution of a pilot reliability analysis of fluke anchors using the PROBAN system, with DIGIN providing the anchor-soil behaviour input and the DEEPMOOR project providing the extreme distribution of the line tension during storm.

Part 3 will comprise a full scope reliability analysis of a fluke anchors in clay with the objectives

- to develop a reliability-based design procedure for fluke anchor foundations and
- to perform a formal code calibration.

Only tentative plans have been presented to the Steering Committee, awaiting the conclusions from the pilot reliability analysis in Part 2.

2.1.3 Project Organisation

In DNV the project team consists of Rune Dahlberg (*Project Manager*), Pål J. Strøm, Trond Eklund (until 30.06.97), Jan Mathisen, Espen H. Cramer, Torfinn Hørte and Knut Olav Ronold with Knut Arnesen and Gudfinnur Sigurdsson as *Verifiers* and Øistein Hagen as *QA Responsible*. Arne E. Løken is *Project Responsible*.

The *Steering Committee*, composed of one representative from each participant with Asle Eide from Statoil as *Chairman*, contributes to a validation of the final products from the project by approving plans and reviewing and commenting on the Draft Final Reports.

2.2 The Present Report

This technical report, "Pilot Reliability Analysis of a Fluke Anchor", is the final result of the work covered by activity 250 of the joint industry project on "Design Procedures for Deep Water Anchors, Part 2: Further Work on Anchors in Clay."

Important work on the effects of cyclic loading was reported in Interim Report No. IR 203 (Dahlberg et al., 1997) covered by activity 251, which has been used as a basis for the same type of analysis reported herein. The formulation of the reliability analysis and software implementation is reported in Interim Report No. IR 204 (Mathisen et al., 1997) through activity 252.

The main work reported herein is covered by activities 253 and 254.

- The stipulated objectives of activity 253 are:

  Specify test case, compute response surface with DIGIN and do the load modelling.

- The stipulated objectives of activity 254 are:

  Perform a pilot reliability analysis of a fluke anchor for one test case.

The report presents a pilot study of a reliability analysis of a fluke anchor. The reliability analysis is carried out using the methods of structural reliability, in which the uncertain input variables to the anchor-soil interaction analysis program (DIGIN) are treated as stochastic variables, and the analysis results are linked to the reliability analysis program (PROBAN) applying a response surface description. In addition to the reliability study, a preliminary design equation is proposed, with associated partial safety factors and reliability levels.

The present work involves some modifications to the formulations presented in reports IR 203 and IR 204 with respect to the formulation of the response surface modelling the DIGIN results,

the influence of cyclic loading and the modelling of the intact and remoulded undrained shear strengths.

3 GLOSSARY AND DEFINITION OF TERMS

3.1 Basic Glossary and Terms

The glossary and definition of terms following is purposely somewhat extended, such that it may also serve as a quick reference for the relationship between different terms and safety aspects. More details about the respective terms are found in the relevant sections of the main text following immediately after this chapter.

	Dip-down point	The point on the seabed, where the anchor line starts to embed.
	Touch-down point	The point at the seabed, where the suspended catenary part of the anchor line first touches the seabed.
F	*Line tension*	The calculated line tension.
F_{char}	*Characteristic line tension*	The maximum calculated *line tension* at the touch-down point for the limit state under consideration
F_d	*Design line tension*	The characteristic *line tension* (F_{char}) multiplied by the appropriate load coefficient γ_f.
F_{dip}	*Target installation load*	The horizontal component of the line tension at the *dip-down* point during anchor installation, which gives the required installation resistance R_{dip} of the anchor.
F_{touch}	*Minimum installation load*	The target installation load F_{dip} *plus* the frictional force ($\mu W' L_s'$) along the anchor line (L_s') at seabed during installation *minus* post-installation effects ΔR_{cons} and ΔR_{cy}, with appropriate partial safety coefficients. The F_{touch} shall be maintained over a specified period of time and is equal to the minimum load level measured during this period. The uncertainty in the load measuring system and extra seabed friction due to misalignment of the installation line are to be accounted for.
F_{mbl}	*Minimum breaking load*	Manufacturer's rated breaking load of an anchor line segment.
R	*Resistance*	The resistance of the embedded anchor plus the embedded part of the anchor line
R_{ult}	*Ultimate resistance*	The holding capacity of the anchor at ultimate penetration, i.e. when the anchor does not penetrate any deeper during continuous penetration, but drags at a constant depth without further increase in the installation line tension.

R_{char}	*Characteristic resistance*	The installation resistance R_{dip} *plus* line seabed friction *plus* post-installation effects, i.e. $R_{char} = R_{dip} + \mu W' L_s' + \Delta R_{cons} + \Delta R_{cy}$
R_d	*Design resistance*	The design holding capacity with material coefficient on predicted contributions to R_{char},: $R_d = R_{dip} + (\mu W' L_s' + \Delta R_{cons} + \Delta R_{cy})/\gamma_m$
R_{dip}	*Installation resistance*	*Measured* part of the anchor resistance at *dip-down* point, equal to the target installation load F_{dip}
ΔR_{cons}	*Consolidation effect*	*Predicted* contribution to the anchor resistance from the effect of soil consolidation.
U_{cons}	*Soil consolidation factor*	Factor, which when multiplied with R_{dip} gives the consolidated anchor resistance R_{cons}.
R_{cons}	*Consolidated anchor resistance*	$R_{cons} = R_{dip} \cdot U_{cons} = R_{dip} + \Delta R_{cons}$
	Soil consolidation	A time dependent process, which leads to an increase in the anchor resistance as the undrained shear strength gradually regains its intact strength s_u after having been remoulded due to the disturbance from the penetrating anchor. The maximum possible increase is a function of the soil sensitivity (S_t) and the anchor geometry.
ΔR_{cy}	*Cyclic loading effect*	*Predicted* contribution to the anchor resistance from the effect of cyclic loading.
U_{cy}	*Cyclic loading factor*	Factor, which when multiplied with R_{cons} gives the characteristic anchor resistance R_{char}, i.e. $R_{char} = R_{cons} \cdot U_{cy} = R_{dip} \cdot U_{cons} \cdot U_{cy}$
	Cyclic loading	Affects the static undrained shear strength (s_u) in *two ways*: During a storm, the rise time from mean to peak load may be about 3 - 5 seconds (1/4 of a wave-frequency load cycle), as compared to 0.5 to 2 hours in a static consolidated undrained triaxial test, and this higher loading rate leads to an *increase* in the undrained shear strength As a result of repeated cyclic loading during a storm, the undrained shear strength will *decrease*, the degradation effect increasing with the overconsolidation ratio (OCR) of the clay. The cyclic shear strength $\tau_{f,cy}$ accounts for both these effects.

ΔR	*Post-installation effects*	Increase in anchor installation resistance R_{dip} due to soil consolidation and cyclic loading effects, i.e. $\Delta R = R_{dip}\,(U_{cons} \cdot U_{cy} - 1)$
γ_m	*Material coefficient*	Accounts for the uncertainty in • the predicted effect of soil consolidation ΔR_{cons} • the predicted effect cyclic loading ΔR_{cy} • the measured intact (static) undrained shear strength s_u and remoulded undrained shear strength s_{ur} (e.g. complexity of soil stratigraphy, scatter in/number of strength measurements, sample disturbance, etc.).
$\tau_{f,cy}$	*Cyclic shear strength*	Accounts for both the loading rate and the cyclic degradation effect and is the preferred characteristic soil strength for use in the design of fluke anchors. $\tau_{f,cy}$ is calculated according to the strain accumulation method, which utilises so-called strain-contour diagrams to describe the response of a clay to various types, intensities and duration of cyclic loading: Given a clay specimen with a certain s_u and OCR, which is subjected to a load history defined in terms of a sea state and a storm duration, the intensity of the storm is gradually increased until calculations according to the strain accumulation method show that the soil fails in cyclic loading. Depending on the average shear stress level in the applied storm history, the clay may fail either due to excessive cyclic shear strains or due to excessive accumulated average shear strains. In a catenary anchoring system the loads transmitted to the anchors through the mooring lines will always be in tension (one-way), which has a less degrading effect on the shear strength than two-way cyclic loading (stress reversal). The failure criterion for one-way cyclic loading is development of excessive accumulated average shear strains. The maximum shear stress the soil can sustain at that state of failure, is equal to the cyclic shear strength $\tau_{f,cy}$. The load history for use in the calculations should account for the combination of wave-frequency load cycles superimposed on low-frequency, slowly varying, load cycles, particularly the amplitude of cyclic loads relative to the average (or mean) load level.

OCR	*Overconsolidation ratio*	The ratio between the maximum past effective vertical stress on a soil element and the present effective vertical stress acting on the same soil element. The higher the *OCR* is the more strength degradation due to cyclic loading and the less strength increase due to an increase in loading rate. For a normally consolidated (*NC*) clay the *OCR* = 1
s_u	*Intact strength*	The static undrained shear strength, which is the best measure of the *in situ* undisturbed (intact) soil strength. For fluke anchor analysis the direct simple shear (DSS) strength or the unconsolidated undrained (UU) triaxial strength is assumed to be the most representative intact strength.
$s_{u,r}$	*Remoulded shear strength*	The undrained shear strength measured e.g. in a UU triaxial test after having remoulded the clay completely.
S_t	*Soil sensitivity*	The ratio between s_u and $s_{u,r}$, as determined e.g. by UU triaxial tests.
c_v	*Coefficient of consolidation*	Parameter derived from consolidation tests, which is used for calculation of rate of consolidation.

3.2 Case Convention for Variables in the Reliability Analysis

Using the established practice for reliability analysis, where an upper case format is used for stochastic variables and a lower case format for the realisation of the stochastic variable, is partly in conflict with the glossary and definition of terms as described in Section 3.1.

The objective of the report is to demonstrate how probabilistic methods can be applied to analyse a geotechnical problem, namely the geotechnical design of a fluke anchor. Bearing this in mind, it is logical to maintain the definitions and conventions agreed on previously in this project and only introduce the terms required for description of the reliability analysis as relevant. Therefore the reliability analysis terms used in the following will not be listed in Chapter 3 like those in Section 3.1, but will simply be defined in the text when they first appear. A summary of the stochastic variables used in the reliability analysis is presented in Table 7.1.

4 FORMULATION OF RELIABILITY ANALYSIS

4.1 General

The present analysis is limited to fluke anchors in a single layer of clay. A procedure for inclusion of a two-layer clay model has further been developed, and is presented at the end of this section. It is subsequently possible to extend the analysis to also include drag-in plate anchors. The mooring line may be attached to any type of offshore structure, in any water depth.

The modelling of the anchor resistance as described in IR 204 (Mathisen et al., 1997) has been modified in the present analysis. The present formulation requires only one single response surface transformation.

4.2 Failure Event

The primary function of an anchor, in an offshore mooring system, is to hold the lower end of a mooring line in place, under all environmental conditions. Since extreme environmental conditions give rise to the highest mooring line tensions, the designer must focus attention on these conditions. If the extreme line tension causes the anchor to drag, then the anchor has failed to fulfil its intended function.

Limited drag of an anchor need not lead to the complete failure of a mooring system. In fact, it may be a favourable event, leading to a redistribution of line tensions, and reducing the tension in the most heavily loaded line. However, this is not always the case. If the soil conditions are not completely homogeneous between the anchors, then a less heavily loaded anchor may drag first, and lead to an increase in the tension in the most heavily loaded line, which may cause failure in that line. Such a scenario would have to include a design analysis that allows anchors to drag, resulting in a much more complicated analysis, and is not recommended. Instead, the inherent safety margin in the proposed failure event should be taken into consideration when setting the target reliability level. Therefore, the event of inception of drag may be defined as a failure, and is the limit state definition used in the present reliability analysis.

4.3 Basic Limit State Function

The failure event must be expressed as a mathematical function in a structural reliability analysis. Such a function is termed a limit state function, usually denoted by *g(.)*, and should satisfy the following properties:

$$g(\vec{x}) \begin{cases} <0, & \text{for } \vec{x} \text{ in the failure set} \\ =0, & \text{for } \vec{x} \text{ on the failure boundary} \\ >0, & \text{for } \vec{x} \text{ in the safe set} \end{cases} \qquad (4.1)$$

where $\vec{x}$ is a realisation of the vector of stochastic variables $\vec{X}$ involved in the problem. There are usually a number of different possible formulations of the limit state function for any specific problem. In the present reliability analysis, the limit state function is taken as the difference between the anchor resistance *r* and the applied line tension *f*, i.e.

$$g(\vec{x}) = r(\vec{x}) - f(\vec{x}) \qquad (4.2)$$

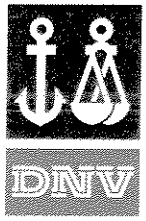

where the anchor resistance is the line tension at the *dip-down* point for which the anchor just starts to drag, and the load is the applied line tension at the same point. The anchor resistance r is built up step-wise from the installation resistance R_{dip} through the consolidated resistance R_{cons}, which includes the effect of consolidation ΔR_{cons}, and then superimposing the cyclic loading effect ΔR_{cy}, see the glossary in Chapter 3 for definition of these terms.

It is not relevant to use the term *characteristic* anchor resistance R_{char} when a detailed reliability analysis is performed. The characteristic resistance is normally calculated according to a detailed recipe, and is intended for use with a set of corresponding partial safety factors in a specified design equation. The same goes for the *characteristic* line tension F_{char}.

Therefore, for the purpose of this pilot study the stochastic variable F is used for the line tension and the stochastic variable R is used for the anchor resistance. The realisation value of these stochastic variables are denoted f and r, respectively, see Equation (4.2).

The result of a full scope reliability analysis, which is the subject of Part 3 of this project, will take the results from this pilot study up to a level, which opens for calibration of a simplified design equation with associated partial safety factors. The target reliability level will be defined after comparative analyses between the calibrated design equation and a wide range of likely design cases from practical design. The intention is then to set the target reliability level such that it is in reasonable harmony with the safety level that has been found acceptable for the type of structures covered by the agreed scope for the calibration.

The line is assumed to intersect the seabed under an uplift angle for the applied line tensions, i.e. seabed friction can be set to zero for the example case. Both anchor resistance and line tension are functions of the stochastic and the deterministic variables involved in the problem. The deterministic variables are sufficiently accurately determined so that there is no need to treat them as stochastic variables; e.g. the anchor geometry.

The drag limit state evaluated is an ultimate limit state, since it deals with anchor failure in an intact mooring system, where failure is defined as the inception of drag of the anchor, i.e. violation of the functional requirement of no motion of the anchor. However, the ultimate anchor resistance F_{ult} as defined in the glossary is not necessarily involved, since this is only reached at ultimate penetration of the anchor.

4.4 Model Description

The anchor performance (relationship between penetration depth, drag and anchor resistance at the dip-down point) is computed using the DIGIN program (Eklund and Strøm, 1996) for specified installation load, soil conditions and anchor geometry. The input variables to DIGIN provide the basis for the selection of the set of random variables that is appropriate to describe the stochastic nature of the installation anchor resistance with or without the superimposed consolidation effect.

The consolidated anchor resistances R_{cons} computed by DIGIN are modified in the probabilistic analysis in order to account for the influence of loading rate and cyclic degradation, or simpler the cyclic loading effect ΔR_{cy}, on the anchor resistance during a storm. In addition, uncertainties in the computed anchor resistance and line tension are accounted for in the probabilistic formulation.

The following parameters are modelled as stochastic variables in the probabilistic analysis:

s_u intact soil shear strength capacity, being depth dependent (s_{uD} = direct simple shear strength)

$s_{u,r}$ remoulded soil shear strength capacity, being depth dependent

U_{cy} factor accounting for the effect of cyclic loading on s_u

U_R model uncertainty factor on the computed increase in anchor resistance, primarily due to consolidation of the soil,

F the applied line load

U_F model uncertainty factor on the line tension.

The installation line load F_{dip} is not modelled as stochastic, as the anchor installation load is measured and thus well controlled. Making the anchor resistance a function of the installation load F_{dip}, implicit information about the actual soil properties is utilised in the evaluation of the anchor resistance.

The anchor resistance is also dependent on the sliding resistance between the soil and the anchor members. In DIGIN, this is modelled as an adhesion factor times the remoulded shear strength of the soil during installation. This factor has, to some extent, been used in the calibration of the DIGIN program with respect to measurements during anchor installations. A best estimate of the adhesion factor has been applied as a deterministic variable in the present analysis. Uncertainty about the results from DIGIN (excluding the uncertainty related to the soil shear strength) is handled by the model uncertainty factor U_R. The adhesion factor is eliminated after consolidation.

In general, the mooring line need not be horizontal at the dip-down point. There may be some non-zero uplift angle θ that defines the line inclination at that point, and which may differ between installation θ_i and extreme load situations θ_e. Mooring lines are usually designed with zero uplift, and this is simplest to handle in the analysis. However, non-zero uplift is a feature that may be useful in future designs, and which may be desirable to model. In the present analysis, it is assumed that the uplift angle during installation, if any, is specified deterministically through the configuration and geometry of the installation line. In the reliability analysis, it should be useful to allow for variation in the uplift angle under extreme line tension, either deterministically or as a random variable. In fact, the uplift angle is likely strongly correlated with the extreme line tension.

The installation anchor resistance r_{dip}, which depends on the intact undrained shear strength s_u, the remoulded undrained shear strength $s_{u,r}$, the penetration depth z, and the installation uplift angle θ_i, is computed in the first step of the anchor analysis with the DIGIN program

$$r_{dip} \rightarrow r(s_u, s_{u,r}, z, \theta_i) \tag{4.3}$$

The full effect of soil consolidation on the installation anchor resistance is obtained by setting the remoulded undrained shear strength equal to the intact undrained shear strength in the DIGIN analysis. This gives the consolidated anchor resistance r_{cons}, which should be combined with the uplift angle for extreme line load θ_e

$$r_{cons} \rightarrow r(s_u, z, \theta_e) \tag{4.4}$$

The dependency on the installation load f_{dip} is carried through the penetration depth, which is also a function of the intact and remoulded undrained shear strengths s_u and $s_{u,r}$ as well as the installation uplift angle θ_i

$$z \rightarrow z(s_u, s_{u,r}, f_{dip}, \theta_i) \tag{4.5}$$

Since the consolidated anchor resistance is defined as a function of the penetration depth, which again depends on the anchor installation load, the anchor resistance may be expressed directly through the functional description of the penetration depth, omitting the specification of the penetration depth in the formulation of the anchor resistance,

$$r_{cons} \rightarrow r(s_u, s_{u,r}, f_{dip}, \theta_i, \theta_e) \tag{4.6}$$

The effect of cyclic loading is assumed to apply to the situation after full consolidation of the clay surrounding the anchor through a factor u_{cy} on the consolidated anchor resistance, which gives the total anchor resistance,

$$r \rightarrow r(s_u, s_{u,r}, f_{dip}, \theta_i, \theta_e) \cdot u_{cy} \tag{4.7}$$

The model uncertainty u_R on the characteristic anchor resistance derived from the DIGIN analysis applies only to the predicted increase in the anchor resistance due to consolidation and cyclic loading effects, since the installation anchor resistance is well controlled through measurement of the installation load, see above. Hence, the anchor resistance to be applied in the limit state function in Equation (4.2) is

$$r \rightarrow \left| r(s_u, s_{u,r}, f_{dip}, \theta_i, \theta_e) \cdot u_{cy} - f_{dip} \right| \cdot u_R + f_{dip} \tag{4.8}$$

Again, with reference to Equation (4.2), inclusion of the model uncertainty u_F on the extreme line tension f_e leads to the line tension f to be applied in the limit state function

$$f \rightarrow f_e \cdot u_F \tag{4.9}$$

The drag length d is at present not applied in the probabilistic formulation, but could be utilised in a reassessment of the estimated anchor resistance after installation through a conditioning on the measured actual drag length.

The installation drag length d_i is a function of the same properties as the penetration depth, namely

$$d_i \rightarrow d(s_u, s_{u,r}, f_{dip}, \theta_i) \tag{4.10}$$

The installation anchor resistance r_{dip}, the penetration depth z and the drag length d are in the analysis expressed as functions of the installation load f_{dip}, the intact and the remoulded undrained shear strengths s_u and $s_{u,r}$, and the installation and extreme uplift angles θ_i and θ_e, applying a response surface description, see also Section 7.2.6.

4.5 Probabilistic Formulation

When including the details introduced above, the limit state function from Equation (4.2) may now be rewritten as

$$\begin{aligned} &g(s_u, s_{u,r}, f_{dip}, \theta_i, \theta_e, u_{cy}, u_R, f_{char}, u_F) = \\ &= \left| r(s_u, s_{u,r}, f_{dip}, \theta_i, \theta_e) \cdot u_{cy} - f_{dip} \right| \cdot u_R + f_{dip} - f_e \cdot u_F \end{aligned} \tag{4.11}$$

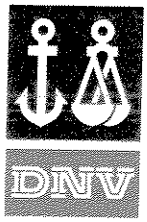

where the arguments of the *g*-function include all the stochastic variables envisaged for the analysis, and one deterministic variable, the installation load f_{dip}. Although the installation load is treated as deterministic, it is included in the list because the DIGIN calculation of the anchor resistance is a direct function of the installation depth, and thereby the installation load. This dependency is shown by Equation (4.5), which must be kept in mind when reading Equation (4.11).

All the stochastic variables involved in this formulation are time-invariant. Although the soil strengths vary with time between the intact and remoulded states, it is only these two states that are involved in the limit state function, and the probability of failure refers to the reconsolidated state with intact soil properties and with superimposed cyclic loading effects. The probability of failure in any intermediate state between anchor installation and reconsolidation of the soil is assumed negligible in this analysis. The applied line tension also varies with time, but the time dependency is taken into account by applying the annual extreme value distribution of the line tension.

The annual probability of failure may then simply be expressed as the probability mass associated with the failure state

$$P_f = \int_{g(\vec{x})<0} f_{\vec{X}}(\vec{x})\, d\vec{x} \tag{4.12}$$

where $f_{\vec{X}}(\vec{x})$ is the joint probability density function of the stochastic variables involved in the limit state function. This probability integral may be computed with the PROBAN program (DNV Sesam, 1996). First or Second Order Reliability Methods (FORM or SORM), may be applied in the computation. The program requires input of the probability distributions of the stochastic variables, and must be able to compute the value of the limit state function for any realisation of the stochastic variables. If the stochastic variables are all independent, then the joint probability density is simply expressed by the product of the marginal densities of the individual stochastic variables. If two or more variables are interdependent, then their joint density can be modelled using additional input about the correlation coefficients between them.

The realisations of the applied line tension, the two model uncertainties, and the cyclic loading factor are simply taken from their respective distribution functions by PROBAN, to compute the value of the limit state function. However, resistance, penetration depth and drag length of the anchor are relatively complex functions of the input variables, which are normally computed by DIGIN. PROBAN needs to have the values of these intermediate variables available for any set of input variables, as PROBAN searches through the domain of the input variables to find the point most likely to lead to failure (the design point). Other software programs needed in the evaluation of the limit state function are commonly linked directly to PROBAN. This approach, however, does not seem suitable in the present case, because DIGIN requires relatively lengthy calculations, and because its computations are not completely stable for all input sets. Instead, a different approach is used, in which a response surface is interposed between the calculations in DIGIN and in PROBAN. The response surface is described in detail in the next chapter.

Two failure modes are considered in DIGIN: (a) drag in the fluke direction, and (b) breakout, roughly normal to the fluke direction. Experience with DIGIN so far indicates that the drag mode is associated with a lower anchor resistance in the majority of cases. Hence, this initial reliability

analysis is limited to the drag mode only. DIGIN will be set to only give resistance for the drag mode, and to flag any instances where failure in the breakout mode precedes the drag mode.

If both modes should need full consideration, then DIGIN should be used to compute the anchor resistance for both modes independently, and the two modes should be modelled with separate limit state functions, arranged as a series system in PROBAN. The system then fails if one or both of the two limit state functions in the system fails.

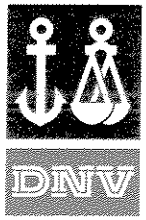

5 RESPONSE SURFACE INTERFACE BETWEEN DIGIN AND PROBAN

5.1 Introduction to Response Surfaces

Suppose you have the values of a response y_i defined for a set of values of a single input variable x_i , $i=1,...,n$, and require the response at some intermediate input value. If the response is a fairly linear function of the input, or the input values are closely spaced, then linear interpolation may be an appropriate approach. Otherwise, you may try to fit some suitable function to the data, and use this fitted function to obtain the interpolated response value. The fitted function forms a curved line in a two-dimensional space.

Let us expand this situation to a single response to two input variables. A fitted interpolation function may now be seen as a surface in a three dimensional space. Further generalisation to more than 2 input variables takes us out of range of simple geometrical descriptions, but it is still convenient to refer to the fitted interpolation function as a response surface.

The need for this type of interpolation technique arises frequently in structural reliability analysis, when complicated algorithms are involved in the limit state function, which may be dependent on many input variables. By interposing a response surface between the detailed response analysis and the reliability analysis, the two parts of the analysis are decoupled, and usually handled more efficiently. To aid convergence of the reliability analysis, it is important that the response surface is continuous, and has continuous derivatives with respect to all the input variables.

The structural reliability group at DNV has mainly used two types of functions for response surfaces:

(a) Sequential splines, which require data points filling a matrix grid in the input space, and are relatively accurate for limited dimensions of input variables.

(b) Ordinary polynomials, generalised to multi-dimensional input, which can handle arbitrarily spaced input data, and larger dimensions of input variables.

In both cases, it is important that the input data set spans the relevant domain of input variables well. It is also essential to carefully check the accuracy of the response surface approximation, particularly in the vicinity of the design point. Type (b) response surfaces, as described by Mathisen (1993), are applied in the present application. A detailed specification of the interface files that are used to transfer results from DIGIN to the response surface module in PROBAN is required.

5.2 Interface File Specifications

The DIGIN program calculates, for specified anchor geometry, soil properties and uplift angle, the relationship between the penetration depth and line tension. For installation, DIGIN computes the required installation tension as a function of the given penetration depth, and for a holding capacity evaluation, DIGIN computes the holding capacity for given penetration depth. The installation analysis requires both intact and remoulded soil properties, whereas the latter only requires intact soil properties. DIGIN is, at present, not able to compute both the required

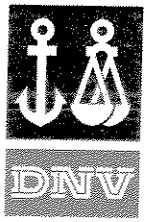

installation tension and corresponding holding capacity in the same run for specified penetration depth, which would be of interest for the reliability analysis of an anchor.

Initially, this was taken care of applying two response surfaces defining the interface between DIGIN and PROBAN. One response surface defining the relationship between the installation tension and the penetration depth, for different soil properties, and one response surface defining the relationship between the penetration depth and the holding capacity. Although this approach works satisfactory, a more computational stable approach is to describe the relationship between the installation tension and the holding capacity directly, applying only one response surface. In the present analysis, however, a response surface for the holding capacity is defined directly for specified soil properties, uplift angles and installation tension. In addition to the holding capacity, also the penetration depth and the drag length are outputs from this single response surface.

The data material required for specifying the single response surface for the holding capacity is obtained by combining the DIGIN results from the installation and holding capacity analyses for corresponding soil properties. At a later stage DIGIN may be re-modified in order to be able to compute the holding capacity directly for specified installation tension.

The standard file format for an interface file is specified in detail in Chapter 5 of Mathisen (1993). The interface file starts with a header portion in which the data is identified and the input and output variables are defined. The remainder of the file comprises a series of data records, in which each data record specifies one point on the response function; i.e. input values and the corresponding output values for one point. As a minimum, there must be a sufficient number of points to allow the coefficients of the interpolation polynomial to be computed. For a second order polynomial, with 3 input variables, this minimum is 10 points. A much larger number of points are usually required in practice, to obtain an adequate description of the response.

The following input variables are specified in the response surface interface file for a single layer of clay:

1. Intact, soil shear strength intercept at zero depth, $s_{u,0}$
2. Intact, soil shear strength gradient, k_u
3. Remoulded, soil shear strength intercept at zero depth, $s_{u,r,0}$
4. Remoulded, soil shear strength gradient, $k_{u,r}$
5. Installation tension at the dip-down point, f_{dip}
6. Uplift angle under extreme load, θ_e

The following output variables are obtained from the response surface interface file:

1. Penetration depth during installation, z
2. Drag length during installation, d_i
3. Consolidated anchor resistance at the dip down point (which for the case studied coincides with the touch-down point), r_{cons}

The following functional relationship then exist for the response surface,
Penetration depth:

$$z = f_1\left(s_{u,0}, k_u, s_{u,r,0}, k_{u,r}, f_{dip}\right) \tag{5.1}$$

Drag length:

$$d_i = f_2\left(s_{u,0}, k_u, s_{u,r,0}, k_{u,r}, f_{dip}\right) \tag{5.2}$$

Consolidated anchor resistance:

$$r_{cons} = f_3\left(s_{u,0}, k_u, s_{u,r,0}, k_{u,r}, f_{dip}, \theta_e\right) \tag{5.3}$$

The drag length during installation is not absolutely essential, but is a useful by-product of the DIGIN installation computation that can be utilised to obtain extra results.

In the present version of DIGIN, the installation process is followed through in stepwise increments of the penetration depth, and the corresponding drag length and line tension required for force equilibrium is computed as a result at each position. The anchor resistance calculation is carried out in the same manner through stepwise increments of the penetration depth, where the necessary anchor resistance at dip down point for specified uplift angle results in a corresponding drag of the anchor.

5.3 Input Data Points

The data points must span the relevant part of the domain of the input variables, which includes both the mean value, and the location of the design point. The majority of points should be located around the design point. To aid visualisation of the fit of the response surface to the data points, a small number of values of each input variable should be employed in defining the entire set of data points.

Table 5.1 indicates an initial set of corresponding points for 6 input stochastic variables, resulting in a total of 23 cases. The values specified describe the number of standard deviations away from the mean value in the direction of the design point (smaller for resistance variables and larger for load variables) a functional evaluation is to be made. It is usually convenient to round off the actual numerical values to 2 or 3 significant digits, rather than the exact values defined by Table 5.1.

In the present analysis, the up-lift angle under extreme load is specified and deterministic. The up-lift angle is therefore to be specified for the values of interest. The installation tension is further deterministic, and is to be given for the corresponding values available from the DIGIN runs based on specified penetration depths.

Table 5.1 Example on suggestion for data points for 6 input stochastic variables, given as numbers of standard deviations away from the mean value, in the direction likely to lead to failure.

X_1	X_2	X_3	X_4	X_5	X_6
-1	-1	-1	-1	-1	-1
0	0	0	0	0	0
1	1	1	1	1	1
2	2	2	2	2	2
3	3	3	3	3	3
2	1	1	1	1	1
3	1	1	1	1	1
4	1	1	1	1	1
1	2	1	1	1	1
1	3	1	1	1	1
1	4	1	1	1	1
...					
1	1	1	1	1	2
1	1	1	1	1	3
1	1	1	1	1	4

6 PHYSICAL MODELLING

6.1 Soil Description

In the following, the intact and remoulded undrained shear strength of the Troll clay is modelled. The shear strength profile is modelled through an intercept at the seabed and a gradient with depth, for single and double layers. In the following reliability analysis, only single layer clay is considered. The shear strength data are from fall cone tests on soil samples from the Troll field.

6.1.1 Single Layer Clay

For single layer clay, the intact and remoulded shear strengths are modelled through a linear trend line with associated residuals, ε. It is here implicitly assumed that the standard deviation of the shear strengths around the trend line (subscript t) is constant over the depth.

The intact and remoulded shear strengths at depth z is then defined as,

$$s_u(z) = s_{u,0,t} + z \cdot k_{u,t} + \varepsilon_u \tag{6.1}$$

$$s_{u,r}(z) = s_{u,r,0,t} + z \cdot k_{u,r,t} + \varepsilon_{u,r} \tag{6.2}$$

There is typically uncertainty associated with the modelling of the trend line due to lack of sufficient data for describing the shear strength at different depths. The modelling uncertainty for the trend lines are defined through a stochastic modelling of the two intercept shear strengths and the two gradients for the intact and remoulded shear strength, where the four stochastic variables are correlated. The marginal distributions for each of these four stochastic variables $s_{u,0,t}$, $k_{u,t}$, $s_{u,r,t}$ and $k_{u,r,t}$ are Normally distributed with correlation matrix,

	$s_{u,0,t}$	$k_{u,t}$	$s_{u,r,0,t}$	$k_{u,r,t}$
$s_{u,0,t}$	1	-	-	-
$k_{u,t}$	$\rho_{ku,su}$	1	-	-
$s_{u,r,0,t}$	$\rho_{sur,su}$	$\rho_{sur,ku}$	1	-
$k_{u,r,t}$	$\rho_{kur,su}$	$\rho_{kur,ku}$	$\rho_{kur,sur}$	1

The residuals of the shear strengths around the trend line for the intact and remoulded shear strengths are typically correlated due to common soil properties. The residuals for the intact and remoulded shear strengths are therefore defined to be 2-dimensional Normal distributed with mean value zero, standard deviation and correlation as obtained from the linear regression analysis.

$$\varepsilon_u, \varepsilon_{u,r} \in N_2\left(0.,0.,\sigma_{\varepsilon_u},\sigma_{\varepsilon_{u,r}},\rho_{\varepsilon_u,\varepsilon_{u,r}}\right) \tag{6.3}$$

The intact and remoulded shear strengths at depth z are then described through 4 variables in the response surface,

$$s_u(z) = s_{u,0} + z \cdot k_u \tag{6.4}$$

$$s_{u,r}(z) = s_{u,r,0} + z \cdot k_{u,r} \tag{6.5}$$

where;

- intact soil shear strength intercept at zero depth:

$$s_{u,0} = s_{u,0,t} + \varepsilon_u \tag{6.6}$$

- intact soil shear strength gradient:

$$k_u = k_{u,t} \tag{6.7}$$

- remoulded soil shear strength intercept at zero depth:

$$s_{u,r,0} = s_{u,r,0,t} + \varepsilon_{u,r} \tag{6.8}$$

- remoulded soil shear strength gradient:

$$k_{u,r} = k_{u,r,t} \tag{6.9}$$

6.1.2 Double Layer Clay

For double layer clay, the same linear modelling approach as for single layer of clay is applied, where the clay is assumed to consist of two layers with independent soil properties above and below the intersecting depth h. The depth of intersection h is deterministic.

The intact and remoulded shear strengths at depth z is then defined as,

$$s_u(z) = \begin{cases} s_{u,0,t} + z \cdot k_{u,1,t} + \varepsilon_{u,1} & z \le h \\ s_{u,h,t} + (z-h) \cdot k_{u,2,t} + \varepsilon_{u,2} & z > h \end{cases} \tag{6.10}$$

$$s_{u,r}(z) = \begin{cases} s_{u,r,0,t} + z \cdot k_{u,r,1,t} + \varepsilon_{u,r,1} & z \le h \\ s_{u,r,h,t} + (z-h) \cdot k_{u,r,2,t} + \varepsilon_{u,r,2} & z > h \end{cases} \tag{6.11}$$

The modelling uncertainty for the trend lines for the intact and remoulded shear strength for the two layers are defined in the same manner as for one layer. The two layers are, however, assumed to be independent.

The stochastic modelling of the two intercept shear strengths and the two gradients for the intact and remoulded shear strength are defined through correlated stochastic variables for each layer. The marginal distributions for each of these four stochastic variables are Normally distributed with correlation matrix,

The marginal distributions for each of the four stochastic variables $s_{u,0,t}$, $k_{u,t}$, $s_{u,r,t}$ and $k_{u,r,t}$ within each layer are Normally distributed with correlation matrix,

Layer 1

	$s_{u,0,1,t}$	$k_{u,1,t}$	$s_{u,r,0,1,t}$	$k_{u,r,1,t}$
$s_{u,0,1,t}$	1	-	-	-
$k_{u,1,t}$	$\rho_{ku1,su1}$	1	-	-
$s_{u,r,0,1,t}$	$\rho_{sur1,su1}$	$\rho_{sur1,ku1}$	1	-
$k_{u,r,1,t}$	$\rho_{kur1,su1}$	$\rho_{kur1,ku1}$	$\rho_{kur1,sur1}$	1

Layer 2

	$s_{u,0,2,t}$	$k_{u,2,t}$	$s_{u,r,0,2,t}$	$k_{u,r,2,t}$
$s_{u,0,2,t}$	1	-	-	-
$k_{u,2,t}$	$\rho_{ku2,su2}$	1	-	-
$s_{u,r,0,2,t}$	$\rho_{sur2,su2}$	$\rho_{sur2,ku2}$	1	-
$k_{u,r,2,t}$	$\rho_{kur2,su2}$	$\rho_{kur2,ku2}$	$\rho_{kur2,sur2}$	1

The residuals of the shear strengths for around the trend line for the intact and remoulded shear strengths for each layer are typically correlated due to common soil properties. The residuals are assumed independent for the two layers. The residuals are then modelled as,

$$\varepsilon_{u1}, \varepsilon_{ur1} \in N_2\left(0.,0.,\sigma_{\varepsilon_{u1}},\sigma_{\varepsilon_{ur1}},\rho_{\varepsilon_{u1},\varepsilon_{ur1}}\right) \tag{6.12}$$

$$\varepsilon_{u2}, \varepsilon_{ur2} \in N_2\left(0.,0.,\sigma_{\varepsilon_{u2}},\sigma_{\varepsilon_{ur2}},\rho_{\varepsilon_{u2},\varepsilon_{ur2}}\right) \tag{6.13}$$

The intact and remoulded shear strengths at depth z are then defined through 8 variables in the response surface (for given intersecting depth h) as,

$$s_u(z) = \begin{cases} s_{u,0} + z \cdot k_{u,1} & z \le h \\ s_{uh} + (z-h) \cdot k_{u2} & z > h \end{cases} \tag{6.14}$$

$$s_{u,r}(z) = \begin{cases} s_{u,r,0} + z \cdot k_{u,r,1} & z \le h \\ s_{u,r,h} + (z-h) \cdot k_{u,r,2} & z > h \end{cases} \tag{6.15}$$

where

- intact soil shear strength intercept at zero depth:

$$s_{u,0} = s_{u,0,t} + \varepsilon_{u,1} \tag{6.16}$$

- intact soil shear strength intercept at depth h:

$$s_{u,h} = s_{u,h,t} + \varepsilon_{u,2} \tag{6.17}$$

- intact soil shear strength gradient for layer 1:

$$k_{u,1} = k_{u,1,t} \tag{6.18}$$

- intact soil shear strength gradient for layer 2:

$$k_{u,2} = k_{u,2,t} \tag{6.19}$$

- remoulded soil shear strength intercept at zero depth:

$$s_{u,r,0} = s_{u,r,0,t} + \varepsilon_{u,r,1} \tag{6.20}$$

- remoulded soil shear strength intercept at depth h:

$$s_{u,r,h} = s_{u,r,h,t} + \varepsilon_{u,r,2} \tag{6.21}$$

- remoulded soil shear strength gradient for layer 1:

$$k_{u,r,1} = k_{u,r,1,t} \tag{6.22}$$

- remoulded soil shear strength gradient for layer 2:

$$k_{u,r,2} = k_{u,r,2,t} \tag{6.23}$$

The theoretical background for development of two correlated linear regression lines for two sets of data points is described in Appendix A.

6.2 Cyclic Loading Factor

6.2.1 Introduction

The cyclic shear strength $\tau_{f,cy}$, accounting for both the loading rate and strength degradation effects on the intact undrained shear strength, is a function of the applied load history, containing both low-frequency (LF) and wave-frequency (WF) environmental load components. The load history used in this study for assessment of $\tau_{f,cy}$ is based on reliability analysis for a mooring system in 350 m water depth as considered in the DEEPMOOR project (Mathisen et al., 1996). The influence of cyclic effects for catenary loading is based on an evaluation for two-way cyclic loading for Troll clay, where a transformation of these results for one-way cyclic loading is based on the results from a study of Drammen clay by Andersen et al, 1988. The Troll clay behaviour for one-way cyclic loading is here 'predicted' by combining the results from analysis of two-way cyclic loading of Troll clay with the published behaviour of Drammen clay for one-way cyclic loading. After completion of the reliability analysis using the 'predicted' Troll curves for one-way cyclic loading, site specific Troll data for one-way cyclic loading became available. In Chapter 10, where the results from the reliability analysis are discussed, the effects of cyclic loading is addressed particularly in light of the post-analysis information obtained about the Troll clay.

The cyclic loading factor U_{cy} accounts for the change in the cyclic shear strength $\tau_{f,cy}$ relative to the undrained shear strength s_u. Uncertainties are, however, related to the determination of this factor due to uncertainties in the prediction of the acting load history and modelling uncertainties in the prediction of the influence of the load history on the cyclic shear strength. With the intention to get an idea of how the load history and modelling uncertainties may influence the cyclic shear strength a total of nine load cases have been defined, see Section 6.2.2 below.

6.2.2 Technical approach

The background for modelling of the cyclic shear strength is described in the interim report IR-203 (Dahlberg et al, 1997). The effects of cyclic loading on the undrained shear strength of clay is initially evaluated for two-way cyclic loading which will give the distribution of the cyclic

shear strength $\tau_{f,cy}$ for an average shear stress $\tau_a = 0$. Through simulations for different possible loading conditions, the distribution of $\tau_{f,cy}$ based on the strain accumulation method (Andersen and Lauritzen, 1988) with uncertainties in strain-contour diagram and strain accumulation accounted for, is obtained.

A total of nine load cases have been defined for analysis of the effects of cyclic loading on the undrained shear strength of clay. The mooring line tension in a stationary, environmental state is composed of 4 components:

$$z = z_0 + z_M + z_L + z_W \tag{6.24}$$

- z_0 the mooring line pretension,
- z_M the mean tension due to quasi-static mooring line response to mean platform offset caused by mean wind, wave, and current loads,
- z_L the low-frequency tension due to quasi-static mooring line response to low-frequency platform motions, excited by wind gusts and second order wave forces,
- z_W the wave-frequency tension from dynamic mooring line response to platform motions excited by first order wave loads.

The relative magnitude of these components varies widely, dependent on water depth, type of floating platform, and details of the mooring system. Table 6.1 gives some indication of the magnitude of these tension components for a few mooring systems.

Table 6.1 Examples of line tension components. The environmental conditions E1, E2, E3 are defined in Table 6.2.

Environ-mental conditions	Pretension	Mean tension	Std. dev. low-freq. tension	Std. dev. wave-freq. tension	Mean period low-freq. component	Mean period wave-freq. component
	kN	kN	kN	kN	s	s
Ship 70m						
E1	400	644	427	606	90	15.3
E2	400	1011	1258	2017	80	18.0
E3	400	1487	1941	3770	72	20.4
Ship 350m						
E1	750	973	129	158	265	12.6
E2	750	1288	402	416	263	13.8
E3	750	1743	745	935	233	16.4
Ship 2000m						
E1	1400	1618	41	247	640	13
E2	1400	1924	127	438	569	13.8
E3	1400	2375	256	644	509	14.6

In the reliability analysis reported herein the line tensions are assumed to represent the mooring tensions for a ship in 350 m water depth with a sea state characterised by a significant wave height equal to 15 m, 20 m and 20 m, respectively. These sea states are termed load condition E1, E2 and E3, respectively, in the following. The environmental components for these load conditions are defined in Table 6.2 following. The calculated line tensions for load conditions

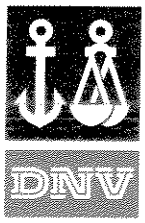

E1, E2 and E3 were for the purpose of this study split into a low-frequency (LF) component and a wave-frequency (WF) component, denoted z_L and z_W, respectively, in Eq. (6.24).

For each load condition E1, E2 and E3 three different time histories were defined. It is assumed that the line tension can be represented by

1) Time history represented by the WF-component only (800 cycles)
2) Time history represented by the LF-component only (46 cycles)
3) Time history represented by the LF-component *plus* the WF-component (46 cycles)

This gave a total of nine load cases, which were analysed for the effect of cyclic loading. For further information about the modelling of time-varying loads reference is made to IR-203 (Dahlberg et al, 1997).

Table 6.2. Environmental conditions.

Environmental state id.:	E1	E2	E3
Significant wave height (m)	10	15	20
Peak wave period (s)	15.2	19.6	24.5
Wind velocity, 1 hour mean (m/s)	22.0	31.5	40.9
Current velocity (m/s)	0.30	0.36	0.43
Wave direction (deg)	180	180	180
Wind direction (deg)	180	180	180
Current direction (deg)	180	180	180

The evaluation of cyclic effects for catenary one-way cyclic loading follows basicly the same approach as that proposed in IR-203 (Dahlberg et al, 1997), although significantly improved from a reliability analysis point of view. Having the distribution of the cyclic shear strength for two-way cyclic loading, the distribution of the equivalent number of cycles leading to failure, N_{eq}, of the cyclic shear strength ratio $\tau_{f,cy}/s_u$ may be obtained. The distribution for equivalent number of cycles to failure is then applied directly to determine the cyclic shear strength for catenary mooring one-way cyclic loading ($\tau_a \neq 0$), dependent on the average shear stress level (τ_a/s_u).

In this modelling, it is assumed that the equivalent number of cycles leading to failure N_{eq} is not affected by the average shear stress level (τ_a/s_u). This may be a slightly non-conservative assumption, as it is believed that N_{eq} may increase somewhat with increasing average shear stress level.

In addition to the influence of N_{eq} on $\tau_{f,cy}/s_u$ for one-way cyclic loading, the uncertainty in the determination of the acting average stress ratio for catenary mooring one-way cyclic loading is accounted for in the uncertainty modelling. An extra modelling uncertainty accounting for the uncertainty in the determination of the cyclic shear strength ratio $\tau_{f,cy}/s_u$ for specified N_{eq} and τ_a/s_u is also included in the formulation.

The mean and coefficient of variation of the static (intact) undrained shear strength s_u is defined separately, and is combined with the obtained cyclic shear strength ratio $\tau_{f,cy}/s_u$ to define the cyclic shear strength.

In the proposed design procedure for fluke anchors, the cyclic shear strength ratio $\tau_{f,cy}/s_u$ is set equal to U_{cy} and termed cyclic loading factor.

6.2.3 Analysis of two-way cyclic loading ($\tau_a = 0$)

A detailed description of the calculations performed for estimation of the mean and standard deviation of the cyclic shear strength $\tau_{f,cy}$ for each of the nine load cases considered is included in Appendix B. The simulation procedure is repeated for all nine load histories to get the distributions and statistical moments for the cyclic shear strength that corresponds to each of them normalised with respect to the intact undrained shear strength, s_u. The results are given in Table 6.3 below.

Table 6.3 Results of simulation of $\tau_{f,cy}/s_u$ distribution for 350 m water depth (for description of load cases see Section 6.2.2).

Load case	Description	$\tau_{f,cy}/s_u$				
		Mean	St.dev.	Skewness	Kurtosis	CoV (%)
1	E1 WF	0.94	0.026	–1.64	7.1	2.8
2	E1 LF	1.02	0.045	–0.40	4.0	4.4
3	E1 LF+WF	1.01	0.041	–0.46	3.7	4.1
4	E2 WF	0.95	0.026	–1.51	6.8	2.7
5	E2 LF	1.01	0.044	–0.47	3.6	4.4
6	E2 LF+WF	1.01	0.043	–0.52	3.4	4.2
7	E3 WF	0.97	0.030	–1.30	5.5	3.1
8	E3 LF	1.01	0.042	–0.32	3.5	4.2
9	E3 LF+WF	1.01	0.041	–0.60	3.7	4.1

The results in Table 6.3 indicates that the cyclic shear strength ratio $\tau_{f,cy}/s_u$ has a distribution with a coefficient of variation of about 3 to 5 %, which represents a fairly small uncertainty. This is considerably less than the uncertainty found for normally consolidated Drammen clay. Since one of the major sources of uncertainty in $\tau_{f,cy}/s_u$ is the uncertainty in the strain-contour coefficients $a_1,\ldots a_4$ (see Appendix B), this difference between the Troll clay and the Drammen clay may to a great extent be explained by the significantly larger uncertainty in a_2 found for Drammen clay relative to Troll clay. These findings are not totally unexpected, because more data are available for the estimation of Troll clay properties than there were for the estimation of Drammen clay properties, so the statistical uncertainty should be less for Troll clay properties than for Drammen clay properties.

The distribution of the equivalent number of cycles N_{eq} of the maximum shear stress in the load history leading to failure is also calculated for all the nine load cases considered. The results of these simulations are presented in Table 6.4 in terms of the first four statistical moments of the equivalent number of cycles N_{eq}. Note that even if $\tau_{f,cy}/s_u$ has a coefficient of variation of only 3-5%, N_{eq} comes out with a much higher uncertainty. The skewness and kurtosis values reported in

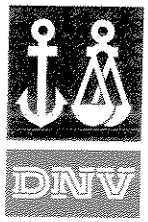

Table 6.4 should be used with care. They are encumbered with considerable uncertainty owing to the limited number of simulations used for their estimation.

Table 6.4 Results of simulation of N_{eq} distribution for 350 m water depth.

Load case	Description	N_{eq}				
		Mean	St.dev.	Skewness	Kurtosis	CoV (%)
1	E1 WF	6.04	2.10	1.25	6.1	35
2	E1 LF	3.03	1.71	1.26	6.2	56
3	E1 LF+WF	3.15	1.59	0.90	4.2	51
4	E2 WF	5.52	1.85	0.84	4.9	34
5	E2 LF	3.16	1.73	1.05	4.5	55
6	E2 LF+WF	3.16	1.61	0.74	3.3	51
7	E3 WF	4.19	1.67	0.72	3.8	40
8	E3 LF	3.20	1.81	1.40	6.9	56
9	E3 LF+WF	3.29	1.69	1.14	4.7	52

6.2.4 Application of results to one-way cyclic loading ($\tau_a \neq 0$)

The results from the analysis of a situation with two-way cyclic loading ($\tau_a = 0$) in Section 6.2.3 are used to estimate how the undrained shear strength of a normally consolidated clay may be affected by one-way catenary cyclic loading. It is assumed that the clay, which was remoulded due to penetration of the anchor at the installation stage, is fully re-consolidated before the anchor becomes subjected to the cyclic loading (storm loading).

The cyclic shear strength $\tau_{f,cy}$ is defined as the sum of the average shear stress component τ_a and the cyclic shear stress component τ_{cy}, which satisfies a specified failure criterion (shear strain γ) for the clay, when it is subjected to a specified storm loading, i.e.

$$\tau_{f,cy} = (\tau_a + \tau_{cy})_{\max} \tag{6.25}$$

At the time when the reliability analysis was performed no data were available for the Troll clay, presenting the cyclic shear strength as a function of the average shear stress level τ_a/s_u, only cyclic test data for $\tau_a = 0$, as used for the analyses reported in Section 6.2.3. As a basis for prediction of the Troll clay behaviour for $\tau_a/s_u \neq 0$, Drammen clay data published by Andersen and Lauritzen (1988) were used in combination with the results for Troll clay reported in Section 6.2.3. A slightly elaborated version of a diagram for Drammen clay from the paper by Andersen and Lauritzen is presented in Figure 6.1, which shows how the cyclic shear strength ratio $\tau_{f,cy}/s_{u,D}$ varies with the average shear stress level $\tau_a/s_{u,D}$ for different values of N_{eq}. A similar set of curves for Troll clay was predicted knowing the N_{eq} for $\tau_a/s_u = 0$ for Troll clay and the shape of such curves for the Drammen clay. The 'predicted' curves for Troll clay are presented in Figure 6.2. It should be mentioned that in the present study the two layers (Unit I and II) of the Troll clay was modelled as one single layer, which means that the prediction leads to a cyclic shear strength ratio applicable for *average* Troll clay properties.

It should also be mentioned that the Drammen clay results are for OCR = 1, whereas the Troll results are for OCR = 1.2 - 1.4. No correction has been made for this. However, the effect of OCR is likely to decrease with increasing average shear stress level τ_a/s_u.

It has been assumed in this analysis that the uncertainty in $\tau_{f,cy}$ due to the effect of cyclic loading, as determined for a situation with two-way cyclic loading, see Table 6.3, decreases linearly from that value to zero for $\tau_a/s_u = 1.0$. In other words, the higher the average stress component is, the less influence the uncertainty on the cyclic contribution will have on the cyclic shear strength.

It may be seen from Figure 6.2 that the ratio $\tau_{f,cy}/s_u$ does not vary significantly when the average shear stress level varies between 0.6 and 0.8, which is a reasonable range. The most conservative results are obtained for the upper bound of this range.

According to Table 6.4 the calculated range of N_{eq} for $\tau_a/s_u = 0$ varies between about 3 and 6 for the nine investigated load cases. Experience has shown that N_{eq} is higher when the failure is caused by accumulated *permanent* shear strain (one-way cyclic loading) compared to a situation when the specimen fails due to excessive *cyclic* shear strains (two-way cyclic loading). No correction for this has been made in the prediction of the Troll clay behaviour.

Uncertainties in the predicted cyclic shear strength for the Troll clay is further discussed in Chapter 10.

The initial approach in IR-203 (Dahlberg et al., 1997), was to apply the cyclic shear strength $\tau_{f,cy}$ for two-way cyclic loading as a reference for determination of the cyclic shear strength for one-way cyclic loading. The present approach uses, however, the equivalent number of cycles to failure N_{eq} as reference, resulting in a more precise modelling of the one-way cyclic shear strength. The estimated distribution of the equivalent number of cycles of amplitude $\tau_{f,cy}/s_u$ for two-way cyclic loading leading to failure, N_{eq}, is then applied directly in the determination of the cyclic shear strength for catenary mooring one-way cyclic loading ($\tau_a \neq 0$) for specified average shear stress level.

As mentioned above it is in the modelling assumed that the equivalent number of cycles N_{eq} is not affected by the average shear stress level (τ_a/s_u). This may be a slightly non-conservative assumption, as it is believed that N_{eq} may increase somewhat with increasing average stress level. By assuming the number of stress cycles leading to failure not being dependent on the average shear stress level, the dependence of the cyclic shear strength on the actual modelling of the combined low-frequency and wave-frequency amplitudes may, however, be done separately and thereby simplify the computational effort.

If a pure cyclic loading situation is considered, then $\tau_a = 0$ and $\tau_{f,cy} = (\tau_{cy})_{max}$, which is the case studied in Section 6.2.3. The results from load case 6, considered herein, with combined low-frequency and wave-frequency loading, gave a mean value for $\tau_{f,cy}/s_u$ of 1.0, a coefficient of variation around 5%, and a slightly negative skewness. The equivalent number of load cycles to failure had mean value 3.2, a CoV of 51% and a slightly positive skewness.

Based on the 'predicted' Troll clay behaviour for $\tau_a \neq 0$ in Figure 6.2, the functional relationship between N_{eq} and $\tau_{f,cy}/s_u$ is established applying a power function. For an average shear stress level $\tau_a/s_u = 0.7$, the following expression obtained for $\tau_{f,cy}/s_u$ as a function of the number of cycles to failure is obtained,

$$\hat{U}_{f,cy-0.7} = 1.52 \cdot \left(N_{eq}\right)^{-8.83 \cdot 10^{-2}} \tag{6.26}$$

The average shear stress level, $b = \tau_a / s_u$, applicable for one-way catenary mooring is difficult to predict, but will typically be in the range 0.6-0.8. For an average shear stress level varying within this range, the following equivalent relative variation in the cyclic shear strength is established (based on Troll data combined with Drammen clay data as explained above),

$$\hat{U}_{f,cy} = X_{\tau_a / s_u}(b) \cdot \hat{U}_{f,cy-0.7} \tag{6.27}$$

where

$$X_{\tau_a / s_u}(b) = -0.383 \cdot b^2 + 0.230 \cdot b + 1.027 \tag{6.28}$$

and $b = \tau_a / s_u$. $X_{\tau_a / s_u}(b) = 1.0$ for b=0.7.

The empirical expressions for the influence of cyclic effects and the average shear stress for one-way catenary loading as defined through Equations 6.26 and 6.27, are dependent on the soil conditions and the environmental load characteristic for different locations.

By specifying the equivalent number of cycles to failure for two-way cyclic loading, the predicted cyclic shear strength may be directly obtained for one-way cyclic loading for specified rate of average shear stress. By modelling the distribution of the equivalent number of cycles to failure from two-way cyclic loading, the corresponding distribution for the predicted cyclic shear strength to be applied in the probabilistic analysis is obtained. In the probabilistic analysis, the estimated equivalent number of load cycles to failure N_{eq} is modelled through a Weibull distribution with moments from load case 6.

The line tension during a storm is due to line pretension and wave- and low-frequency components. It is not easy to split this relatively complex loading history into an average and a cyclic component for use in the probabilistic analysis. The average shear stress level τ_a/s_u is in the probabilistic analysis assumed to vary uniformly within the range [0.6-0.8].

In the uncertainty modelling, also the prediction uncertainty in the determination of the cyclic shear strength from specified N_{eq} and τ_a/s_u is account for. This prediction uncertainty is dependent on both N_{eq} and τ_a/s_u and is modelled as an unbiased uncertainty factor $X_{f,cy}$ with CoV 2.5%.

The modelled loading rate and strength degradation factor is then defined as,

$$U_{f,cy} = X_{f,cy} \cdot \hat{U}_{f,cy} \tag{6.29}$$

6.3 DIGIN Response Computation

6.3.1 Program Flow

DIGIN is applied to define the relationship between the penetration depth, the drag length and the resistance of an anchor for specified anchor geometry, soil shear strength profile and installation load.

DIGIN is performing these computations in step-increments of the penetration depth, defining the corresponding drag length, the installation anchor resistance R_{dip} at the dip-down point for the specified installation load F_{dip} at the same point and the resulting consolidated anchor resistance after reconsolidation of the clay with the anchor at the installation depth. The installation load (equal to the installation anchor resistance) and the consolidated anchor resistance are in the present version of DIGIN computed in separate runs, but could through a modification of DIGIN be computed simultaneously at each iteration step.

Through multiple computations with parameter variations over areas of interest, it is then possibly to express the installation depth, drag length and anchor resistance as a function of the selected installation load and soil shear strength profile applying a response surface.

The calculations in DIGIN are performed in steps of equal depth from seabed and down to a defined maximum depth. Calculations are terminated when the maximum depth is reached or the lowest equilibrium force is found for an anchor orientation giving horizontal flukes (for which the anchor cannot penetrate deeper down into the soil).

At a specified depth it is possible to recalculate the anchor equilibrium with consolidated shear strength close to the anchor. This is done for one depth only. In the following depth steps, the remoulded shear strength is applied for sliding resistance and the embedded anchor line catenary is constrained to follow partly the one from the previous calculation. This is done until the combination of tension and new anchor position is such that the catenary will be unaffected by previous anchor line position.

For all other situations than the one described above, each of the depth increments is calculated independently from the previous step.

In the DIGIN computations, the installation phase and (post-installation) consolidation phase are separated, since the calculations at each depth increment is independent of the calculations / results from the previous depth increment. This approach only affects the anchor analysis if the installation is performed with an uplift angle being less than the one associated with the line tension leading to the design event. This is not obvious, but the explanation for this is simple. After installation the embedded curvature of the anchor line will restrain the embedded curvature associated with the higher uplift angle as illustrated in Figure 6.3 (copied from IR 204 (Mathisen and Strøm, 1997)), and with the DIGIN model of the same in Figure 6.4 (copied from the same report). To neglect this is somewhat conservative for that combination in the anchor analysis, yet this approach is accepted, at least at this stage, as a model uncertainty.

6.3.2 Anchor Resistance

In this study, it is the anchor resistance and the embedded part of anchor line (at dip-down point) that is considered. The fact that this is not a fixed point will be neglected in the analysis as the response in the mooring line is by far dominated of the suspended anchor line (compared to the part of the mooring line embedded in the soil and lying on the seabed).

The uplift angle at the dip-down point is not given as an input to the program today, but is a result of the tension in the mooring line at anchor equilibrium. Thus the user has only been able to vary the uplift angle indirectly, by adjusting mooring line length, line characteristics and anchor depth. In the present work it is found convenient to be able to specify a constant uplift angle, and include this as an input to the DIGIN program.

6.3.3 Failure Mode

For normally consolidated clays and a one-layer system, it will be sufficient to look at the restraint mode as basis for both the installation and consolidated anchor resistance analyses. For the most unfortunate combinations of undrained and remoulded shear strength and also for high uplift angles, spot checks of the results with the failure mode are made.

6.3.4 Multiple DIGIN Calculations

DIGIN produces all necessary results needed for response surface interface files in its present version. In establishing the response surface, it is, however, necessary to carry out multiple DIGIN calculations. Repeated restarting of DIGIN with modified input variables in a batch file is the present approach for doing this.

The interface file for the response surface will be accessed after each depth step with the following write statement:

```
WRITE (IFF,'(7F10.3)')Su,Ku,Sur,Kur,Depth(I),Drag(I),teta0,TDD(I)
```

Where

`Su`	= Intact shear strength intercept
`Ku`	= Shear strength gradient
`Sur`	= Remoulded shear strength intercept
`Kur`	= Remoulded shear strength gradient
`Depth(I)`	= Depth in question (of anchor shackle
`Drag(I)`	= Drag experienced from set position of the anchor to the depth in question
`teta0`	= Uplift angle at dip-down point
`TDD(I)`	= Line tension at dip-down point for the depth in question

In establishing the required installation tension and drag length for specified penetration depths, it is the individual intact and remoulded shear strength profile that are given for a specified zero uplift angle. In the computation of the consolidated anchor resistance R_{cons} for a given penetration depth, the remoulded shear strength is specified as intact, together with a selected up-lift angle under extreme loading. (The computed corresponding drag length for the consolidated anchor resistance analysis is not relevant)

6.3.5 Response Surface Representation of DIGIN Computations

The DIGIN computations of the installation anchor resistance R_{dip} (equal to the installation load) and the subsequently computed consolidated anchor resistance R_{cons} at the depth of penetration are made for corresponding set of input variables (shear strength data), and are combined into one response surface interface file consisting of hundreds of data lines with the set up given in Table 6.4. The data file applied in the response surface modelling is presented in Appendix C.

Table 6.4 Response surface interface file.

Variable	Type	Dimensions	Description
su	Input	kPa	Intact shear strength intercept
ku	Input	kPa/m	Intact shear strength gradient
sur	Input	kPa	Remoulded shear strength intercept
kur	Input	kPa	Remoulded shear strength gradient
fdip	Input	kN	Installation tension
teta	Input	degrees	Uplift angle at dip-down point under extreme loading
z	Output	m	Penetration depth
di	Output	m	Installation drag length
rcons	Output	kN	Consolidated anchor resistance

The response surface description of the DIGIN results is based on linear interpolation using PROBAN, as it was found that a linear interpolation gave the best modelling. The centre point for the polynomial fitting was selected to be close to the design point. See IR-204 (Mathisen and Strøm, 1997) for a closer description of the response surface modelling.

6.4 Time Varying Loads

6.4.1 Annual Extreme Value Distribution of Mooring Line Tension

6.4.1.1 Short Term Stationary Tension

The mooring line tension may be treated as a stationary stochastic process in a stationary environmental state of short duration τ , say a few hours. This is the basic building block in the computation of the tension.

The tension includes the following components:

- pretension
- mean tension due to mean environmental loads on the platform
- low-frequency tension due to low-frequency horizontal motions of the platform, excited by wind gusts and second order wave force,
- wave-frequency tension due to wave-frequency motions of the platform, excited by first order wave forces, and including the dynamic response of the line to these motions.

The short term extreme value distribution of the tension Z may be denoted by $F_{Z|\Psi}(z\,|\,\Psi;\tau)$, where Ψ is a stochastic vector that describes the short term environmental parameters, including significant wave height, peak wave period, mean wind speed, current speed, and heading angles of these environmental actions.

6.4.1.2 Annual Extreme Tension

The theorem of total probability is applied to compute the extreme value distribution of the line tension in a single, random environmental state

$$F_Z(z;\tau) = \int F_{Z|\Psi}(z|\psi;\tau)\, f_\Psi(\psi)\, d\psi \qquad (6.30)$$

where $f_\Psi(\psi)$ is the joint probability density of the environmental parameters. This integral is often computed by ordinary numerical integration when the environmental vector only includes two components; viz. the significant wave height and the peak wave period. When wind and current effects are also modelled stochastically, then more sophisticated integration techniques are required. This is provided by the First Order Reliability Method (FORM), or the Second Order Reliability Method (SORM).

The number of environmental states in a long term duration of $\lambda = 1$ year, is taken into account by assuming the tension response in each state is independent, giving

$$F_Z(z;\lambda) = [F_Z(z;\tau)]^{\lambda/\tau} \tag{6.31}$$

The annual extreme value distribution of the line tension in one line was also computed using the same reliability analysis that is applied in the DEEPMOOR project (Mathisen et al., 1996). Turkstra's hypothesis was applied to obtain the combined tension due to wave-frequency and low-frequency effects. The pretension and the mean tension due to environmental effects was also included. A uniform probability was applied for the direction of wave actions relative to the mooring, for all directions from 0 to 360 degrees. The position 450 meters from anchor was considered as reference point.

A fitted Weibull distribution is applied fit to represent the annual extreme line tension, given by,

$$F_Z(z) = 1 - \exp\left\{ -\left(\frac{z-\gamma}{\alpha}\right)^{\beta} \right\} \tag{6.32}$$

where the distribution parameters were fitted to be. $\alpha = 120\text{kN}, \beta = 0.6, \gamma = 1300\text{kN}$. The corresponding mean value and standard deviation of Z,

$$\text{mean}(Z) = \alpha\,\Gamma\left(1 + 1/\beta\right) + \gamma = 1480\,\text{kN} \tag{6.33}$$

$$\text{Std.Deviation}(Z) = \alpha\left[\Gamma\left(1 + 2/\beta\right) - \Gamma\left(1 + 1/\beta\right)\right] = 317\,\text{kN} \tag{6.34}$$

The distribution function parameters are defined based on a fitting to fractile values being relevant in the determination of the annual failure probability of the anchor. The corresponding mean values and standard deviation applying the fitted distribution parameters does therefore not necessarily reflect the mean value and standard deviation of the annual extreme line tension.

Note, especially that a Weibull distribution with shape parameter β being as low as 0.6 has a considerable curvature and a long tail, extending to high tensions. The annual extreme line tension is therefore not well described applying the mean vale and standard deviation alone.

6.4.2 Characteristic Tension

When a simpler analysis is applied to determine the line tension in order avoid the difficulties of a detailed analysis of several stochastic variables, then the tension is usually referred to as a characteristic tension.

A characteristic response is usually calculated according to a detailed recipe, and is intended for use with a set of corresponding partial safety factors in a specific design equation. Such recipes,

safety factors and design equations for mooring lines may be found in DNV's POSMOOR rules or in API RP2SK. These 3 items:

(i) design equation,

(ii) recipes for characteristic values,

(iii) partial safety factors, and

should ideally be calibrated by reliability methods, so that they provide the desired safety level in the ensuing design. They are inter-dependent, and cannot necessarily be used separately with any confidence that they separately represent particular probability levels.

Recipes for characteristic values should ideally provide each response at a clearly defined probability level, usually somewhere in the tail end of the corresponding distribution function, choosing the tail that is most likely to lead to failure; i.e. low values of strength and high values of load. In the case of mooring line tension, there are a large number of tension components to be included, and the long-term environment needs to be taken into account to determine the tension distribution, as described above. This is considered to be too complicated for the routine computation of characteristic tensions. Hence, the recipe is simplified, the probability level of the resulting characteristic value is not precisely known, and this level varies somewhat from case to case.

The aim of a calibration of a design rule, is to evaluate a number of different design conditions in order to define a design equation. This involves a recipe for determination of the characteristic values and a set of partial safety factors that results in a uniform safety level for different designs based on the design equation.

In IR 203 (Dahlberg et al., 1997), the annual extreme value distribution of the line tension in the most heavily loaded line is given for a turret-positioned ship 8 symmetrically spread lines at 350 meters of water depth.

The initial anchor characteristic load was calculated for a 100-year environmental state as follows:

- Significant wave height: 16.5 m
- Peak wave period: 20.8 s
- Wind velocity (1 hour mean) 19 m/s
- Current velocity 0.51 m/s.
- All environmental actions are assumed to encounter the ship from the same direction.

The characteristic line tension in the most heavily loaded line 450 meters from the anchor was for these conditions computed to be 4900 kN.

7 DESCRIPTION OF PILOT CASE

7.1 General

A reliability analysis of a fluke anchor in Troll clay has been carried out. The soil data has been interpreted as a single soil layer.

Based on a range of installation loads, the corresponding installation depth and anchor resistance is estimated.

The reliability analysis is aiming at determining the annual probability for drag of the anchor. This is requiring the modelling of the annual extreme line tension.

The modelling of the annual extreme line tension is a computational cumbersome process, and the resulting characteristic line tension value to be applied in design is based on the (most likely) 100 years line tension value.

7.2 Probabilistic Analysis

7.2.1 Anchor Description

The modelled anchor used for the pilot reliability analysis is a Vryhof Stevpris 18 tonnes anchor with a fluke/shank angle of 50 degrees. The background for selecting this anchor for the test analysis is described in IR 203 (Dahlberg, et.al., 1997). The dimension of the embedded anchor chain has been balanced with respect to the breaking strength of the other mooring line components.

7.2.2 Shear Strength

The soil data is defined as single soil layer. In the reliability study, it was desirable to have data available that represented the interdependence between the intact and remoulded shear strength for different depths, in order to be able to account for the correlation between the intact and remoulded shear strength in the modelling.

In Figure 7.1, the applied shear strength data from the Troll field is presented together with the fitted trend line assuming that the data may be represented as a single soil layer. In Figure 7.2 the same data are presented together with trend lines for two-layer soil, assuming the soil boundary at depth 16.5m. The linear modelling of the trend lines are given in the figures, and are also defined in Table 7.1 for the single soil layer.

The probabilistic analysis is only evaluated using single soil layer, resulting in a rather high standard deviation for the residuals, see Table 7.1. A modelling based on two-layer soil would reduce the residual standard deviations, and result in a more exact description of the shear strength and thereby the holding capacity.

In Appendix D, numerical values for the intact and remoulded shear strength are given together with the mean values, standard deviations and correlation matrix for the intact and remoulded trend lines, and the standard deviations and correlation for the intact and remoulded residuals.

The trend lines are defined through linear regression analysis. The correlation between the trend lines and residuals for the intact and remoulded shear strength are obtained applying the program code REGRESS-2, (Ronold, K. 1997).

7.2.3 Cyclic Loading Factor

The cyclic loading factor is defined from the estimated equivalent number of cycles to failure, accounting for the average stress ratio.

The influence of varying average stress level for one-way catenary loading is accounted for by assuming the relative average stress level τ_a/s_u to vary uniformly between 0.6-0.8.

The model uncertainty associated with the estimated increase in the anchor resistance based on known number of cycles to failure and average stress level is here assumed to be low, modelled with a CoV of 2.5%. In other cases, where less information about the soil characteristics exists, this modelling uncertainty should be defined larger. This uncertainty, however, comes in addition to the uncertainty associated with the increase in the anchor resistance from the installation stage, due to consolidation and cyclic effects, having a CoV of 15%.

The probability density function for the cyclic loading factor U_{cy} is presented in Figure 7.3 for different average shear stresses ratios τ_a/s_u being 0.6, 0.7 and 0.8. The distribution function is obtained through a modelling of the equivalent number of stress cycles to failure being Gamma distributed, see Table 7.3.

Evaluating the influence of the average shear stress ratio, it is from Figure 7.3, based on load case 6, observed that the most likely value for the cyclic loading factor is decreasing from 1.40 to 1.32 when the average shear stress ratio increases from 0.6 to 0.8. The here estimated high values for the cyclic loading factors are caused by the predicted relatively low number of equivalent cycles to failure. The distribution functions for the cyclic loading factors are close to Gaussian (a positive skewness of approximately 0.8) with a coefficient of variation (CoV) of around 5%.

The influence of cyclic effects may therefore be accounted for in the probabilistic modelling by defining the mean value for the cyclic loading factor from the mean value for the equivalent number of stress cycles to failure. The CoV on the cyclic part of the cyclic loading factor, i.e. subtracted the average shear stress ratio, is taken equal to the CoV from two-way cyclic loading.

7.2.4 DIGIN Computations

7.2.4.1 General

The penetration depth, drag length and resistance of the anchor is estimated through DIGIN and represented through response surface model for various parameter combinations of the installation tension and soil shear strength.

The line tension under installation is controlled, and the installation anchor resistance is therefore not associated with any prediction uncertainty in the analysis.

Uncertainties associated with the shear strength of the soil are accounted for directly in the modelling of the soil data.

7.2.4.2 Penetration Depth and Installation Anchor Resistance R_{dip}

There are larger uncertainties associated with the DIGIN computation of the penetration depth than for the anchor resistance for specified installation loads and soil characteristics.

The penetration depth is, however, only implicitly utilised in determination of the installation anchor resistance R_{dip}. There are direct connections between the installation load and the

penetration depth, and the penetration depth and the anchor resistance, making it possibly to describe the anchor resistance directly as a function of the installation load through the defined response-surface function. The penetration depth is then only a corresponding value for the estimated installation anchor resistance, but is associated with an estimated CoV uncertainty of 15%.

The required installation load for different installation depths is computed in DIGIN for different combinations of intercept and gradient values for the intact and remoulded shear strength (combinations in accordance to Table 5.1).

7.2.4.3 Drag Length

The uncertainty in drag length will generally not affect the anchor resistance, but is an effect of the uncertainty in the achieved penetration depth for a given target installation load F_{dip}. Although clearly a matter of interest when it comes to selecting the most suitable anchor for an actual design, the drag length as such is not considered further in the present study, see however Sections 7.2.6 and 8.1.3.

7.2.4.4 DIGIN Model Uncertainty

The model uncertainty u_R is considered to be basically connected to the consolidation effects. Part of the uncertainty in the consolidation effects is caused by the uncertainty allocated to the remoulded undrained shear strength $s_{u,r}$. In the DIGIN analysis model the skin friction during penetration is related to $s_{u,r}$. In comparison with the uncertainty in $s_{u,r}$ as such, the uncertainty in the factor relating the skin friction to $s_{u,r}$ contributes more to the DIGIN model uncertainty , at least with the moderate CoV on the $s_{u,r}$ obtained in this analysis example. The CoV on DIGIN model uncertainty is here estimated to be 15%.

7.2.5 Time Varying Environmental Loads

The distribution of the annual extreme loading at the area of interest was found in Mathisen et al., (1997) to be described by a Weibull distribution,

$$F_Z(z) = 1 - \exp\left\{ -\left(\frac{z-\gamma}{\alpha}\right)^{\beta} \right\} \tag{7.1}$$

with the following parameters $\alpha = 120\,\text{kN}$, $\beta = 0.6$, $\gamma = 1300\,\text{kN}$. The distribution function describing the exceedance probability of the line tension is given in Figure 7.8, together with a corresponding, but separately derived, characteristic line tension. The characteristic line tension is to be applied in the design equation proposed later in Section 9.

The line tension is defined from a combination of WF and LF contributions, resulting in some modelling uncertainty in determining the distribution of the combined annual extreme tension. The modelling uncertainty is defined to be 15%.

7.2.6 Updated Estimates for the Failure Probability after Installation

It is likely that measurements during and/or after the installation can be used for a post-installation reassessment of the anchor resistance. The predicted resistance based only on the information available before the installation will then be reevaluated based on the additional information available through the installation measurements. Some preliminary thoughts related to the use of updating based on measurements are included in Appendix E.

7.2.7 Summary of Stochastic Variables

The distribution functions for the stochastic input variables applied in the probabilistic evaluation are summarised in Table 7.1.

Table 7.1 Distribution functions of input stochastic variables, for a storage tanker in 350 m water depth, and soil conditions based on Troll soil data.

Symbol	Variable	Marginal Distribution
	Soil Shear Strength Model:	
$s_{u,0,t}$	intact shear strength intercept trend line	Normal, mean = -1.30, st.d. = 1.78 (kPa)
$k_{u,t}$	intact shear strength trend line gradient	Normal, mean = 2.22, st.d. = 0.08 (kPa)
$s_{u,r,0,t}$	remoulded shear strength intercept trend line	Normal, mean = -6.68, st.d. = 2.35 (kPa)
$k_{u,r,t}$	remoulded shear strength trend line gradient	Normal, mean = 1.31, st.d. = 0.11 (kPa)
ε_u	intact shear strength residual	Normal, mean = 0.0, st.d. = 4.1 (kPa)
$\varepsilon_{u,r}$	remoulded shear strength residual	Normal, mean = 0.0, st.d. = 5.4 (kPa)
	Cyclic Loading Factor U_{cy}:	
N_{eq}	equivalent number of cycles to failure	Weibull, mean = 3.16, st.d. = 1.61, low = 0.25
τ_d/s_u	average shear stress for catenary loading	Uniform, lower = 0.6, upper = 0.8
$\tau_{f,cy}/s_u$	resulting cyclic loading factor U_{cy}	Function of N_{eq}, τ_d/s_u and OCR
$X_{f,cy}$	model uncertainty on U_{cy} for given N_{eq}	Normal, mean = 1.0, c.o.v. = 2.5%
	Anchor Resistance:	
F_{dip}	installation load at dip-down point	Fixed, 4000 (kN)
U_R	model uncertainty on anchor resistance R	Normal, mean = 1.0, c.o.v. 15 %
θ	uplift angle of line for anchor resistance	Fixed, 0 (degrees)
	Line Tension:	
F_e	annual extreme line tension	Weibull, a = 120., b = 0.6, low 1300 (kN)
U_F	model uncertainty on annual line tension	Normal, mean = 1.0, c.o.v. 15 %

Correlation matrix for soil shear strength model is defined in Table 7.2 for the trend line. The residuals are correlated as for the intercept values for intact and remoulded shear data.

Table 7.2 Correlation matrix for description of trend lines for intact and remoulded trend lines based on Troll soil data. (Residuals: $\rho(\varepsilon_i, \varepsilon_i) = 0.44$)

	$s_{u,0,t}$	$k_{u,t}$	$s_{u,r,0,t}$	$k_{u,r,t}$
$s_{u,0,t}$	1	-	-	-
$k_{u,t}$	-0.91	1	-	-
$s_{u,r,0,t}$	0.44	-0.40	1	-
$k_{u,r,t}$	-0.40	0.44	-0.91	1

8 RELIABILITY ANALYSIS

8.1 Cumulative Distributions

8.1.1 Anchor Resistance

Based on the applied uncertainty model, the cumulative distribution function for the anchor resistance is defined in Figure 8.1. The figure presents the probability that the anchor resistance should be equal to or smaller than a specified anchor resistance for different target installation loads. The modelling uncertainty is accounted for in the representation of the cumulative distribution of the anchor resistance.

The figure shows that for an installation load of 3500 kN, the estimated probability that the anchor resistance should be less or equal to 4900 kN is approximately 4.0E-3.

Figure 8.2 presents the relative importance of the different uncertainty contributions in the determination of the probability that the anchor resistance should be less or equal to 4900kN for an installation load of 3500 kN. The figure shows that the uncertainty associated with the modelling of the residual shear strength around the trend lines contributes to the majority of the uncertainty modelling for the anchor resistance (85%). As the shear strength data indicates that a two-layer soil model would represent the shear strength more adequately, it is no surprise that the single-layer soil model with the larger residuals contributes so much to the overall uncertainty.

8.1.2 Penetration depth

Figure 8.3 presents the cumulative distribution of the penetration depth for different target installation loads. The curve presents the probability that the penetration depth should be equal to or smaller than a specified depth for different installation loads. The equivalent probability that the penetration depth should be larger than a given value is obtained as 1.0 minus the cumulative probability.

For an installation load of 3500 kN, the probability that the penetration depth should be less than 13 meters is approximately 0.6, and the corresponding probability that the penetration depth should be larger than 13 meters approximately 0.4.

No modelling uncertainty is accounted for in the cumulative representation of the penetration depth, implying that the uncertainty associated with the estimated penetration depth is due to uncertainty in the modelling of the trend lines and the residuals for the intact and remoulded shear strength.

8.1.3 Drag Length

In a similar manner as for the penetration depth a cumulative distribution function of the drag length can be established, i.e. a curve representing the probability that the drag length should be equal to or smaller than specified values for different installation loads. This information does not enter the anchor resistance equations and has therefore been given less attention in the analysis performed for this pilot study. In an actual design situation it is, however, expected that such information would be useful, if the acceptable drag length during installation is a matter of concern.

8.2 Probabilistic Analysis

Based on the presented uncertainty model for the anchor resistance and the annual extreme line tension, the annual probability of failure (dragging of anchor) is estimated. In Figure 8.4, the estimated annual failure probability for different installation loads is presented. It is seen that for an installation load of 3500 kN, the estimated annual failure probability is found to be approximately 4.6E-5. The input file to PROBAN and the corresponding result file for this installation load of 3500 kN are included in Appendix F and Appendix G, respectively.

The design-point for the penetration depth, being the penetration depth for the combination of stochastic variables most likely resulting in failure, is 10.2 meters.

Figure 8.5 presents the relative importance of the different uncertainty contributions in the determination of the annual failure probability for an installation load of 3500 kN. The figure shows that the uncertainty associated with the modelling of the annual extreme line tension contributes to the majority of the uncertainty for the annual failure probability, with (85%) for the description of the annual extreme line tension and with (5%) for the modelling uncertainty. The residual uncertainty on the shear strength around the trend lines contributes to (7%).

The uncertainty associated with the description of the annual extreme line tension therefore has a much higher influence on the total uncertainty picture than the uncertainty associated with the description of the anchor resistance.

8.3 Discussion of Post Installation Resistance Uncertainty Model

A prediction of the deterministic "best guess" post installation resistance, applying mean values (predicted values) for all the stochastic variables involved in the resistance model and not accounting for the residuals in the shear strength predictions, gave a post installation contribution to the anchor resistance of 4680 kN.

A modelling of obtained anchor resistance based on the applied uncertainty model, indicated that the total anchor resistance could be described through a Normal distribution with a mean value of 8180 kN and a standard deviation of 1330 kN for a target installation load of 3500 kN. As the installation resistance is 3500, the obtained mean value for the post installation effects is also (8180kN-3500kN) 4680 kN.

The coherence between the deterministic derived post installation resistance and the mean value for the obtained stochastic post installation resistance indicates that the non-linear effects in the capacity formulation is of minor importance.

As the installation resistance is deterministic, the coefficient of variation on the post installation resistance is CoV = 1330/4680 = 28%.

In Figure 8.6 the influence of the uncertainty on the post installation effect with respect to the derived annual failure probability is investigated. It is observed that for a pure deterministic anchor resistance model (CoV = 0), the predicted annual failure probability is around 2.0E-5, close to the estimated annual failure probability of 4.6E-5 for the full probabilistic analysis. Due to the high uncertainty associated with the description of the annual extreme line tension, the influence of the uncertainty on the anchor resistance capacity model is only having minor importance.

By increasing the uncertainty associated to the predicted post installation resistance, it is observed from Figure 8.6 that also the estimated annual failure probability is increasing. However, this increase is not significant, and results in an estimated annual failure probability of 4.6E-5 for a CoV of 28%, as also predicted from the discussion on the uncertainty on the post installation resistance above.

These results indicate again that the majority of the uncertainty is associated with the description of the annual extreme line tension, and that good estimates for the annual failure probability may be obtained by simply applying the "best guess" predicted estimates for the anchor resistance.

Such an approach would greatly simplify probabilistic analysis of anchor installations, as the deterministic predicted anchor resistance (installation resistance + consolidation effects from DIGIN + cyclic effects) may be combined directly with the estimated distribution for the annual extreme line tension.

If a more accurate, but still simplified, approach is desired, the deterministically derived post installation effect may be associated with a CoV of around 30%. The annual failure probability may be estimated only having one single stochastic variable for the anchor resistance.

However, further studies should be carried out prior to simplifying the probabilistic approaches for obtaining the annual failure probabilities for anchor installations.

9 DESIGN PROCEDURE

9.1 General

In the following, an initial proposed design equation with selected characteristic values is presented. A set corresponding partial safety factors for the characteristic anchor resistance and the characteristic loading is evaluated with respect to the corresponding reliability level for the design case studied.

9.2 Design Equation

The anchor resistance is defined as the resistance of the embedded anchor *plus* the embedded part of the anchor line. The design equation should be defined in such a way that it results in comparable safety levels for different designs based on the same design equation.

The *characteristic anchor resistance* of the line is defined as,

$$R_{char} = R_{dip} + \Delta R_{cons} + \Delta R_{cy} \tag{9.1}$$

where

R_{dip} is the *installation anchor resistance*, being the *measured* part of the anchor resistance at the *dip-down* point, equal to the target installation load F_{dip} at the same point.

ΔR_{cons} is the *consolidation effect*, being the *predicted* contribution to the anchor resistance from the effect of soil consolidation

ΔR_{cy} is the *cyclic load effect*, being the *predicted* contribution to the anchor resistance from the effect of cyclic loading.

The most significant line loads from an anchor design point of view are:

F_{dip} the *target installation load*, being the horizontal component of the line tension at *dip-down* point during anchor installation.

F_{char} the maximum calculated line tension at the *touch-down* point.

If no line is lying on the seabed during at target installation load and during extreme loading the touch-down point coincides with the dip-down point.

The *design anchor resistance* is defined as,

$$R_d = R_{dip} + [\Delta R_{cons} + \Delta R_{cy}]/\gamma_m \tag{9.2}$$

and the *design line tension* is defined as,

$$F_d = \gamma_f \cdot F_{char} \tag{9.3}$$

where

γ_m is the partial safety factor (*material* factor), accounting for the prediction uncertainty in the determination of the consolidation effect and the cyclic load effect.

γ_f is the partial safety factor (*load* factor), accounting for the prediction uncertainty in the maximum calculated line tension.

The selection of partial safety factors is directly linked to the procedure for obtaining characteristic values for the consolidation effect, the cyclic loading effect and the maximum line tension.

9.3 Characteristic Values

The characteristic values should be defined such that comparable safety levels are obtained for different designs based on the same design equation.

In the following, the characteristic values for the installation anchor resistance, the consolidation effect and the cyclic load effect are based on best estimates for these effects.

The installation anchor resistance is defined from the minimum target installation load, assumed to be controlled during installation,

$$R_{dip} = F_{dip} \tag{9.4}$$

The consolidation effect is the *predicted* increase in the anchor resistance after installation based on DIGIN calculations using the intact (consolidated) undrained shear strength s_u. Based on best estimates for the shear strength parameters (*trend lines*), the consolidated anchor resistance R_{cons} was found to be 1.69 times the installation resistance R_{dip} (= the installation load F_{dip}), see Figure 9.1. The increase in the anchor resistance due to consolidation is then 69% for the soil condition considered, and the consolidation effect expressed as a function of the target installation load is,

$$\Delta R_{cons} = 0.69 \cdot R_{dip} = 0.69 \cdot F_{dip} \tag{9.5}$$

The cyclic loading effect is derived from predicted equivalent number of cycles to failure for two-way cyclic loading, N_{eq}. The corresponding cyclic loading effect for catenary one-way cyclic loading is based on the results from the study of the Drammen clay, modified of these data to estimated equivalent results for the Troll clay has been made. For equivalent number of cycles $N_{eq} = 4$ (conservative best estimate) and an average shear stress level τ_a/s_u for one-way catenary loading equal to 0.7, the predicted anchor resistance accounting from cyclic effects is found from equations 6.26 and 6.27 to be 1.34. The increase in the anchor resistance due to cyclic effects expressed as a function of the target installation load is then,

$$\Delta R_{cy} = 0.34 \cdot \left(R_{dip} + \Delta R_{cons}\right) = 0.34 \cdot 1.69 \cdot R_{dip} = 0.57 \cdot R_{dip} = 0.57 \cdot F_{dip} \tag{9.6}$$

The characteristic anchor resistance for the maximum calculated line tension is based on the most likely occurring line load having 100 years extreme environmental description. Final procedures for establishing the characteristic value for the maximum line tension is, however, still to be defined in the DEEPMOOR project. In the present project, the characteristic value for the line load was derived to be

$$F_{char} = 4900 \text{ kN} \tag{9.7}$$

9.4 Partial Safety Factors

The set of partial safety factors for the anchor resistance and the line loading is linked directly to the shape of the design equation and the selection of the characteristic values. The partial safety factors are to be selected such that comparable safety levels with known reliability is obtained for different designs. At present, these partial safety factors have not been defined. However, a parameter study is carried out in order to investigate the obtained safety level, defined through the annual failure probability, for different selections of safety factors for the case studied.

In order to obtain a corresponding set of characteristic values and partial safety factor resulting in comparable safety levels for different designs applying the design equation, a calibration study involving a relevant set of design cases (environmental conditions, depth, anchor geometry, etc.) must be considered. Such a calibration study has been proposed for Part 3 of this project.

9.5 Target Installation Load

The target installation load F_{dip} at the *dip-down* point is the minimum installation load F_{touch} at the *touch-down* point minus the line sliding resistance along between the two points, see the Glossary in Chapter 2 for details. Since the case studied here assumes that no line is lying on the seabed during installation or extreme loading the $F_{dip} = F_{touch}$. This again means that the ULS and PLS requirements are to be satisfied in the dip-down point, meaning that design anchor resistance R_d shall be equal to the design line tension F_d, i.e.

$$R_d = F_d \tag{9.9}$$

$$R_{dip} + \left(\Delta R_{cons} + \Delta R_{cy}\right)\frac{1}{\gamma_m} = \gamma_f \cdot F_{char} \tag{9.10}$$

$$F_{dip} + \left(0.57F_{dip} + 0.69F_{dip}\right)\frac{1}{\gamma_m} = \gamma_f \cdot F_{char} \tag{9.11}$$

The target installation load is now defined directly as a function of the set of partial safety factors for given characteristic line tension,

$$F_{dip} = \frac{\gamma_f \cdot \gamma_m}{\gamma_m + 1.26} \cdot F_{char} \tag{9.12}$$

where 1.26 is the increase in the installation anchor resistance due to consolidation and cyclic loading effects. By playing around with the safety factors, it is found that the target installation load increases from 44% of the characteristic line tension to 71% of the characteristic line tension when the safety factors increase from 1.0 to e.g. $\gamma_f = 1.3$ and $\gamma_m = 1.5$.

In Figure 9.2, the target installation load is given as a function of different combinations of load γ_f and material factors γ_m.

9.6 Annual Failure Probability

The choice of partial safety factors, for given characteristic values, will greatly affect the safety level of the design. In Figure 9.3, the estimated annual failure probability for the evaluated design case is presented for different choices of partial safety factors for the anchor resistance and the line load.

Figure 9.3 shows that by increasing the load factor γ_f from 1.0 to 1.3 and the material factor γ_m from 1.0 to 1.5, the estimated annual failure probability decreases from 10^{-3} to approximately $6 \cdot 10^{-5}$.

10 SUMMARY AND DISCUSSION

A probabilistic formulation of the reliability of a fluke anchor installation against drag has been defined as a function of the anchor installation load F_{dip}. The anchor resistance as a function of the installation load has been defined through a response surface applying computed values from DIGIN. The consolidation and cyclic loading effects have been accounted for. The line tension is expressed through the annual extreme line tension.

The majority of uncertainty associated with the modelling of the distribution of the anchor resistance was from the residuals around the trend lines in the description of the shear strength for intact and remoulded soil (85 %).

The modelling of the annual failure probability showed that the majority of the uncertainty contribution (90 %) came from the modelling of the annual extreme line tension. The uncertainty contribution from the anchor resistance was 10 %, dominated by the contribution from the residual shear strength (7%).

The uncertainty modelling associated with the anchor resistance has considerably less importance than the uncertainty on the annual extreme line tension in the evaluation of the annual failure probability. This is because the consolidated anchor resistance is defined directly from a specified installation load and not the penetration depth, which would have resulted in a larger uncertainty with respect to the modelling of the consolidated anchor resistance. The uncertainty in the cyclic loading factor was also low for the considered soil study.

It should be mentioned that the uncertainty in the anchor resistance in the analysed case is 'favourably' low, partly due to the rather homogeneous clay used (low COV on s_u and $s_{u,r}$), but mainly due to the assumption that the clay considered is well documented by cyclic strain contour and cyclic strength diagrams, which is rarely the case in 'real life'.

In the present case, the Troll clay behaviour for one-way cyclic loading ($\tau_a \neq 0$) was 'predicted' by combining available Troll cyclic loading clay data for two-way cyclic loading with more complete data for Drammen clay as shown in Figures 6.1 and 6.2. After completion of the reliability analysis cyclic loading data for the Troll field was obtained, which allows for a comparison between the predicted and reported behaviour of the Troll clay.

In Figure 10.1 the contour lines for N_{eq} = 1, 3, 6 and 10 have been plotted for Drammen clay, Troll Unit I, Troll Unit II and the predicted Troll Unit (I + II). It may be seen that the prediction for Troll Unit (I+II) compares fairly well with the reported results for Troll clay, the match improving with increasing N_{eq}. The cyclic shear strength versus average shear stress for Drammen clay (Andersen and Lauritzen, 1988) has a much steeper shape for N_{eq} = 1 than that reported for the Troll clay, which has influenced the shape of the predicted curves for the Troll clay. As N_{eq} increases the effect of this decreases, however. From a practical design and reliability analysis point of view it would be possible to estimate how much uncertainty that has to be accounted for and to investigate how much this would influence the annual failure probability for the anchor.

The uncertainty increases also as a result of the additional uncertainty attached to the influence of the overconsolidation ratio OCR. As an example of this effect, Figure 10.2 for Drammen clay is shown. The figure, which is from Andersen and Lauritzen (1988), shows that the cyclic shear

strength decreases with increasing OCR. However, if the cyclic shear strength in Figure 10.2 is normalised is with respect to the intact undrained shear strength it may be seen that the effect of OCR decreases with increasing average shear stress level.

Another uncertainty is that the N_{eq} for one-way cyclic loading may be higher than for two-way cyclic loading, but this is also an effect which can be estimated and accounted for.

There will also be some uncertainty in the cyclic shear strength for a given *OCR* due to the limited data base from different types of clay. The cyclic shear strength for a given N_{eq} and *OCR* may likely be different for different types of clay. These uncertainties should be looked further into in Part 3 of this project.

However, preliminary calculations indicate that the annual failure probability for the anchor analysed in this study will not change significantly if the 10 % contribution from the anchor resistance shown in Figure 8.5 is increased moderately, see Figure 8.6. This means that rather large uncertainties can be accepted in the predicted anchor resistance without changing much of the picture that is drawn based on this pilot study due to the large uncertainties that are associated with the description and modelling of the annual extreme line tension.

The large uncertainty associated with the annual extreme line tension indicates that in order to increase the reliability of the fluke anchor, focus should be on a more precise description and modelling of the annual extreme line tension. The annual extreme line tension is at present expressed through a single variable, accounting for the pre-tension contribution, the mean loading contribution, the low-frequency contribution and wave-frequency induced contribution to the annual extreme line tension. A splitting of these load contributions could result in a more exact description of the annual extreme line tension. These aspects are evaluated in DEEPMOOR.

The proposed design equation should be calibrated to a series of design cases in order to assure that a satisfactory safety level is reached for different realistic design conditions. The set of characteristic values with corresponding partial safety factors should be selected to assure uniform safety levels for different design based on the same formulation of the design code.

A more detailed modelling of the characteristic line tension should be introduced, such that different partial safety factors could be applied for the load contribution from the pre-tension and line-tension due to mean offset, and the load contribution from the low-frequency and wave-frequency line tension. The relative influence of the pre-tension and the mean tension increases with increasing water depth. As the uncertainties associated with the pre-tension and mean tension is lower than for the combined LF and WF tension, a calibration of the design rules for moderate water depths will result in conservative designs for deeper waters applying only one partial safety factors for the design tension.

11 REFERENCES

Andersen, K. H. and Lauritzsen, R. (1988), "Bearing capacity for foundations with cyclic loads", Journal of Geotechnical Engineering, Vol. 114, No. 5, May, 1988, pp. 540-555.

Dahlberg, R., Hørte, T., Mathisen, J., Ronold, K., Strøm, P., (1997), "Deep Water Anchors, Loading Rate and Degradation Factor and Other Stochastic Variables (Interim Report No. IR-203)," DNV Report No. 97-3303, Høvik.

Strøm, P. and Eklund, T. (1996), "Back-fitting analyses of fluke anchor tests in clay, " DNV Report No. 96-3385, Rev. 02, dated 28.08.96.

Eklund, T., Strøm, P., (1996), "Deep Water Anchors, User's Manual DIGIN Ver.5.1 (Technical Report No. TR 1-1)," DNV report No. 96-3637, Høvik.

Degenkamp, G. (1996), "Towards vertical loaded anchor technology", Paper presented to the International Offshore Mooring Seminar, October, 1996, Houston.

DNV (1995), "Certification of Offshore Mooring Steel Wire Ropes", Det Norske Veritas Certification Note No. 2.5.

DNV Sesam, (1996), "User's manual: PROBAN, General Purpose Probabilistic Analysis Program," report no. 92-7049/Rev.1, Det Norske Veritas, Høvik.

Efron, B., and R.J. Tibshirani, (1993), *An Introduction to the Bootstrap*, Chapman and Hall, Inc., New York, N.Y.

Foss,I., Dahlberg,R., Kvalstad,T., (1978), "Design of Foundations of Gravity Structures against Failure in Cyclic Loading", Offshore Technology Conf., paper no. OTC 3114, Houston.

Fylling, I., Larsen, K., (1993), "Anchor Systems Analyses in PROMOOR," report no.513033.00.01, Marintek, Trondheim.

Lie, H., (1990), "User's Documentation MIMOSA-2, Version 2," report no. 519616.00.01, Marintek, Trondheim.

Madsen, H.O., Krenk, S., Lind, N.C., (1986), "Methods of Structural Safety," Prentice-Hall, Englewood Cliffs, New Jersey.

Mathisen, J., Strøm P. (1997) "Deep Water Anchors. Formulation of Reliability Analysis and Software Implementation (Interim Report No. IR-204)", DNV Report No. 97-3490, DNV

Mathisen, J., Hørte, T., Larsen, K., Sogstad, B., (1996), "DEEPMOOR - Design Methods for Deep Water Mooring Systems, Calibration of an Ultimate Limit State," report no. 96-3583, DNV

Mathisen, J., (1993), "A Polynomial Response Surface Module for Use in Structural Reliability Computations," DNV Report No. 93-2030, Høvik.

NGI, (1975), "Research project, Repeated loading on clay: Summary and interpretation of test results", NGI Report No. 74037-9, 15 October 1975, Oslo.

Ronold, K, (1997), "REGRESS2", Fortran software code for linear regression analysis of 2 series of data

Ronold, K.O., and H.O. Madsen, (1987), "A Probabilistic Approach to Failure of a Clay in Cyclic Loading", *Proceedings*, ICASP5, Vancouver, B.C., Canada.

Ronold, K.O., (1993), *Reliability of Marine Clay Foundations in Cyclic Loading*, Ph.D. Thesis, Dept. of Civil Engineering, Stanford University, Stanford, California.

Stansberg, C.T., (1991), "A Simple Method for Estimation of Extreme Values of Non-Gaussian Slow-Drift Responses," Proc. 1st Int. Offshore and Polar Engineering Conf. - ISOPE, Edinburgh.

Stansberg, C.T., (1992), "Basic Statistical Uncertainties in Predicting Extreme Second Order Slow Drift Motion," 2nd Int. Offshore and Polar Engineering Conf. - ISOPE, San Francisco.

Stansberg, C.T., (1996), "DEEPMOOR - Reliability-Based Design Methods for Deep Water Mooring Systems, Nonlinear Mooring Stiffness Influence on Extreme Slow-Drift Responses," report no. 513085.05.01, Marintek, Trondheim.

12 FIGURES

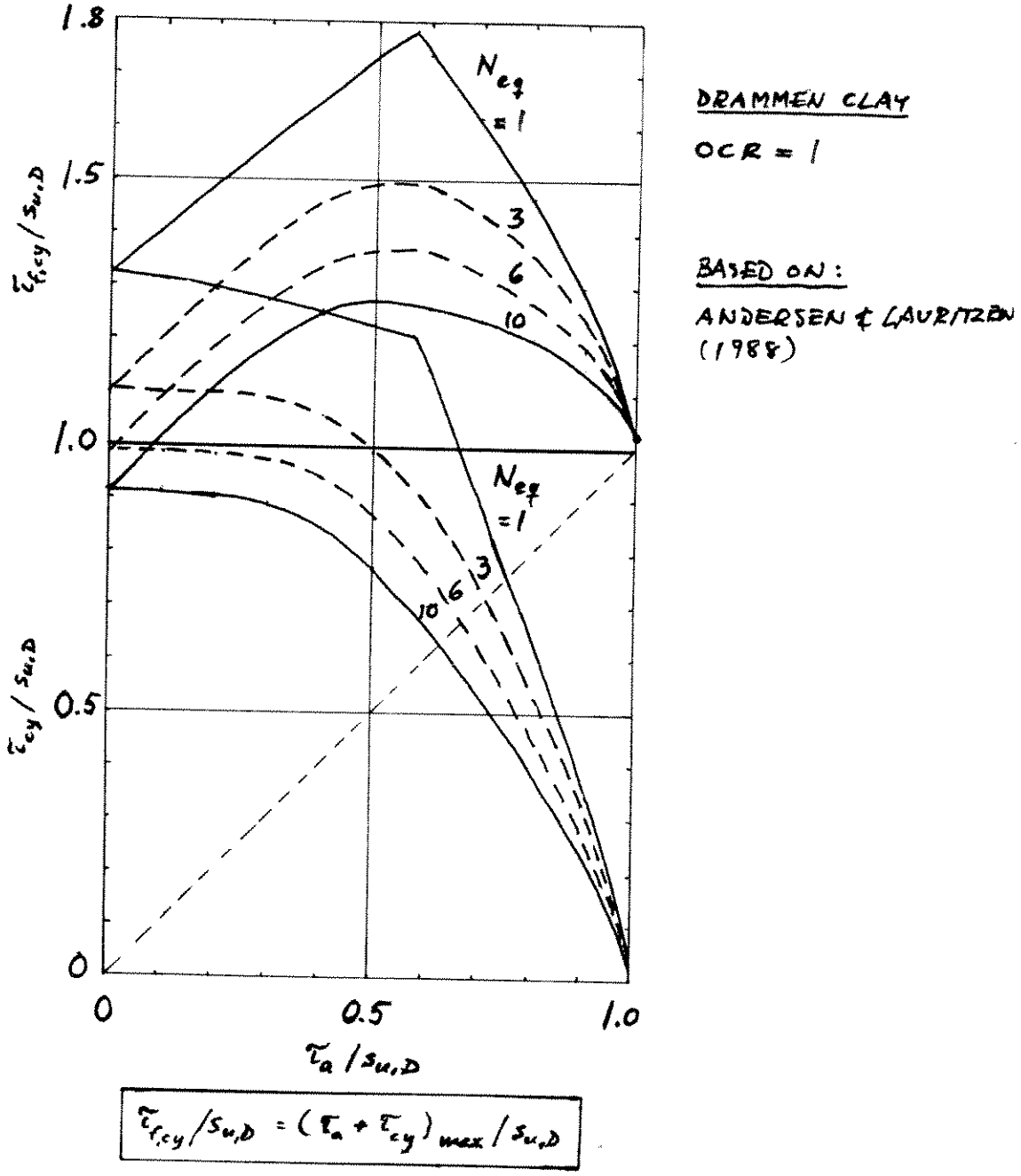

Figure 6.1 Cyclic shear strength data for Drammen clay, OCR = 1.

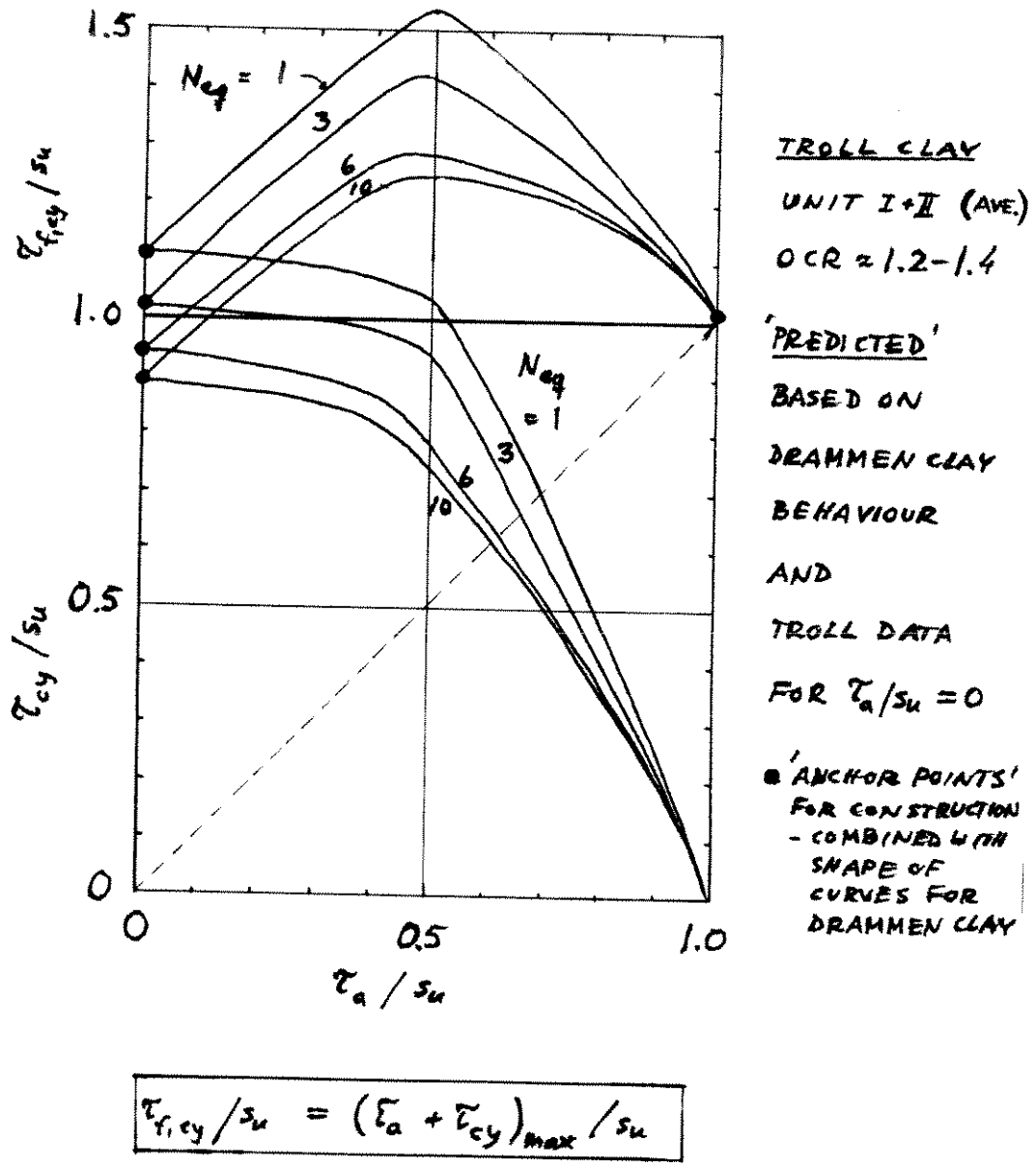

Figure 6.2 'Predicted' cyclic shear strength behaviour of Troll clay for $\tau_a \neq 0$ based on Drammen clay data, see Figure 6.1.

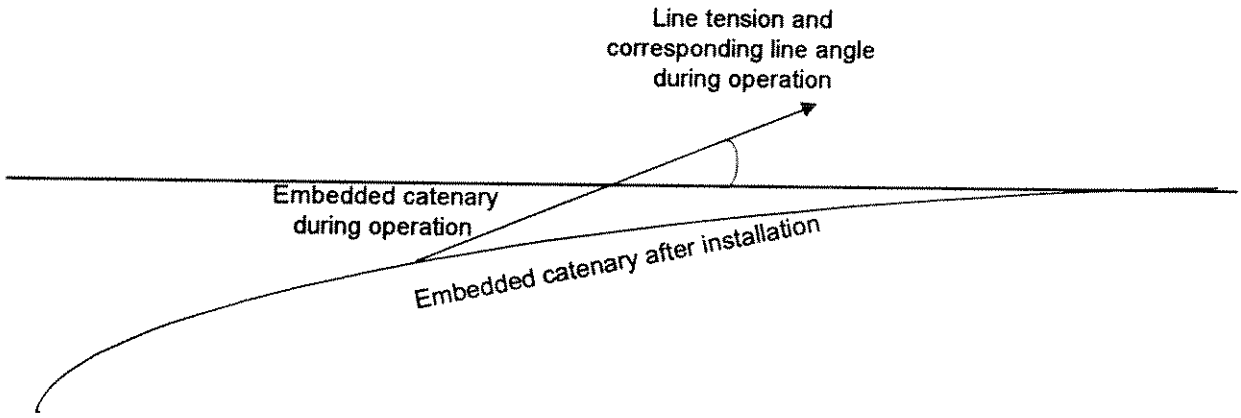

Figure 6.3 Effect of increasing uplift angle from installation to operation.

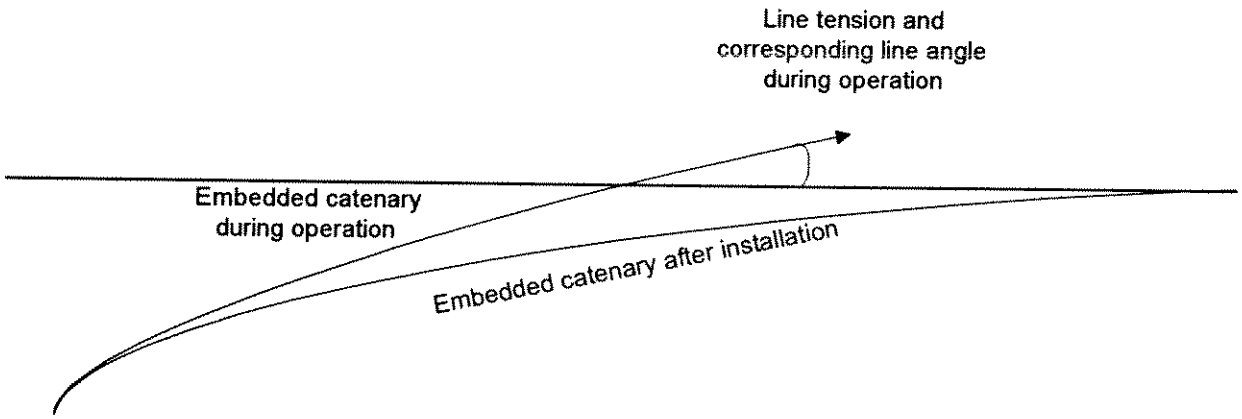

Figure 6.4 DIGIN model for increasing uplift angle.

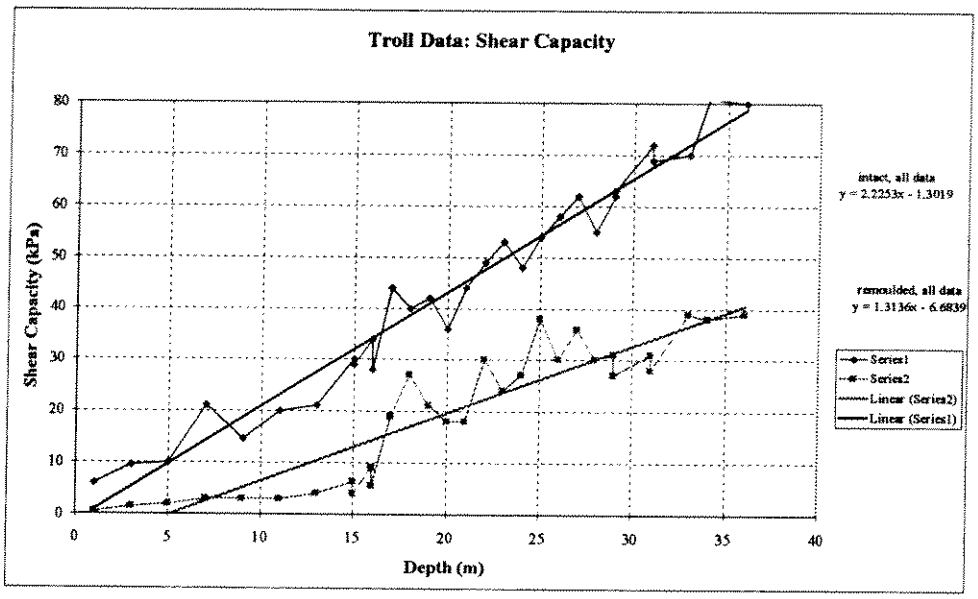

Figure 7.1 Shear strength model for single-layer soil.

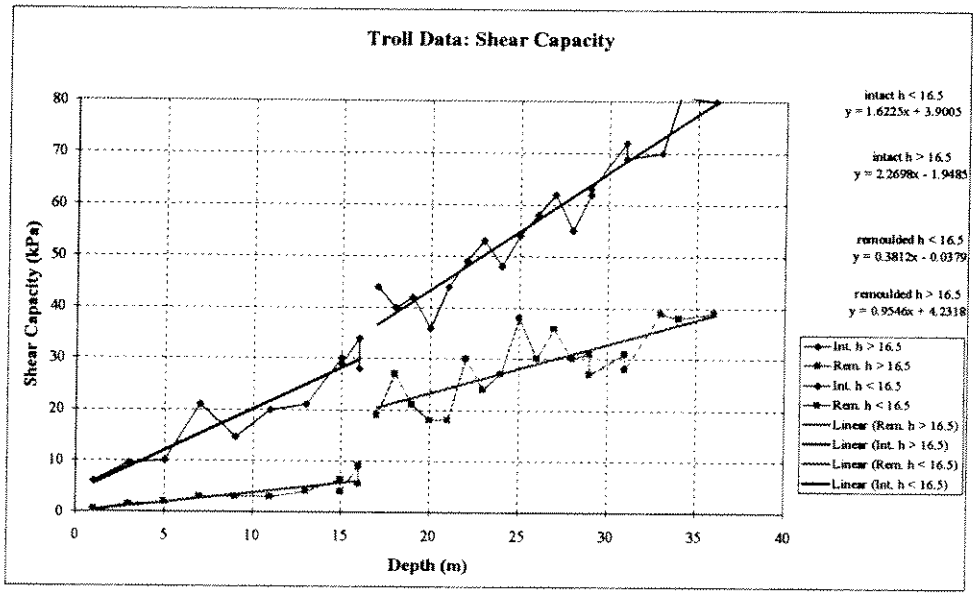

Figure 7.2 Shear strength model for double-layer soil.

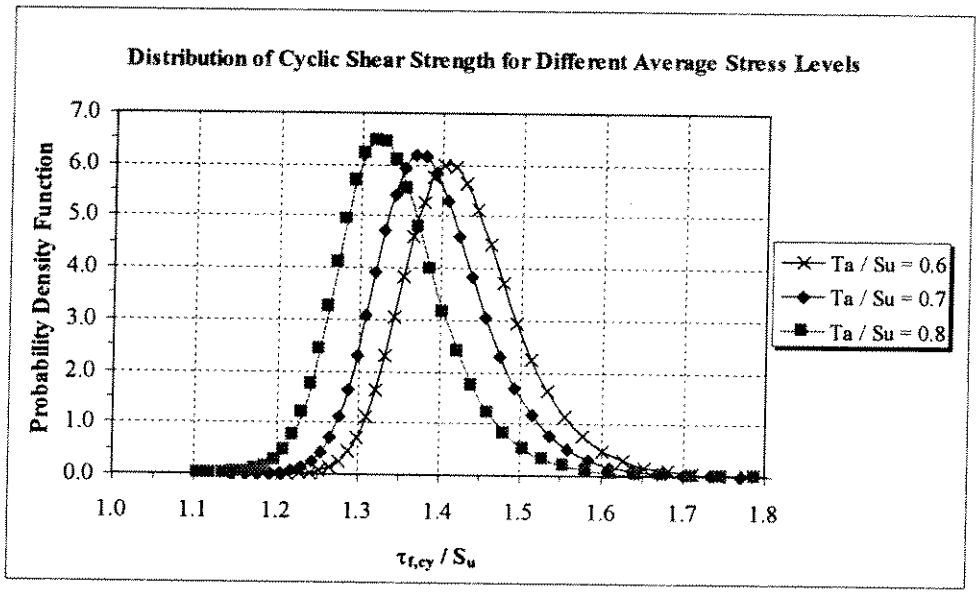

Figure 7.3 Estimated cyclic shear strength ratio dependent on average stress level.

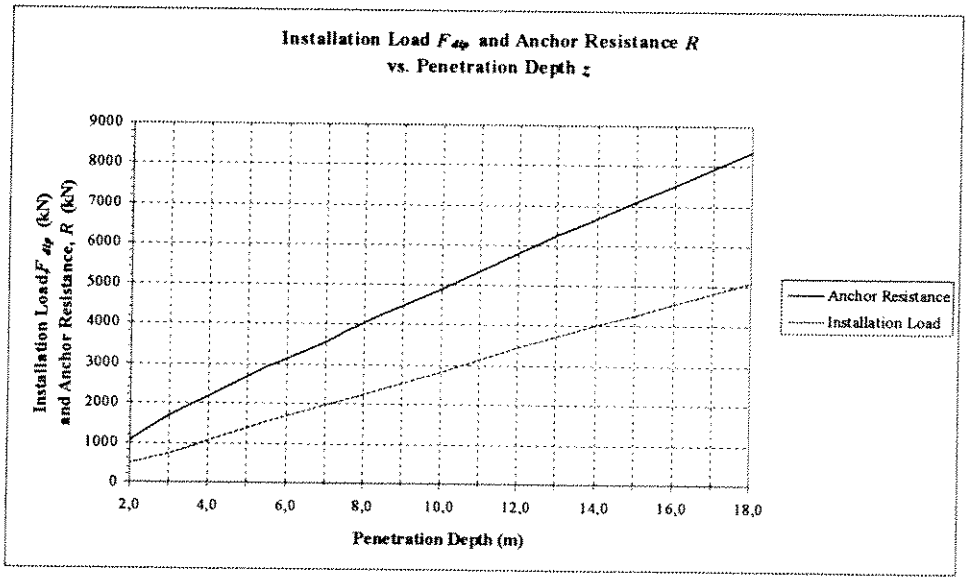

Figure 7.4 DIGIN computations of required installation load and anchor resistance for different penetration depths, based on best-estimates of intact and remoulded shear strength and zero uplift angle.

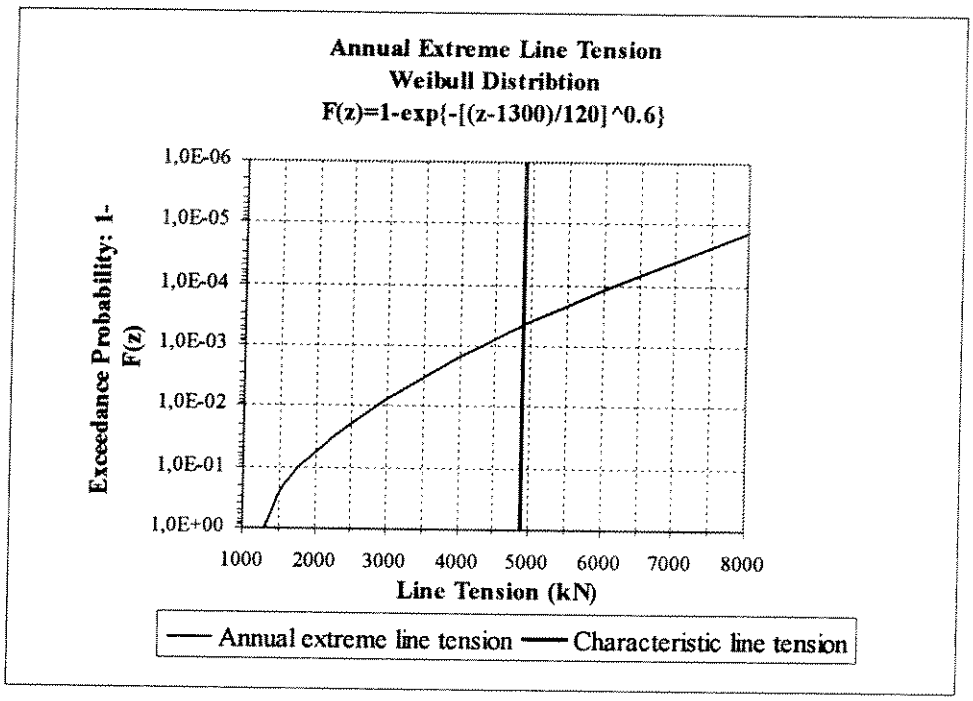

Figure 7.5 Distribution of annual extreme line tension for the probabilistic analysis together

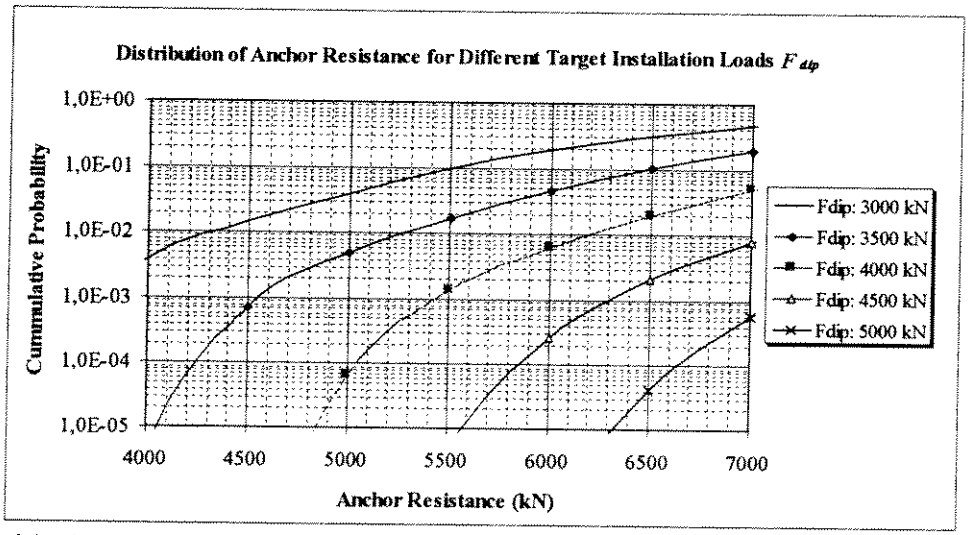

with characteristic line tension for the design equation.

Figure 8.1 Cumulative distribution of estimated holding capacity for different target installation loads. The cumulative distribution function defines the probability that the holding capacity is equal to or less than the considered value.

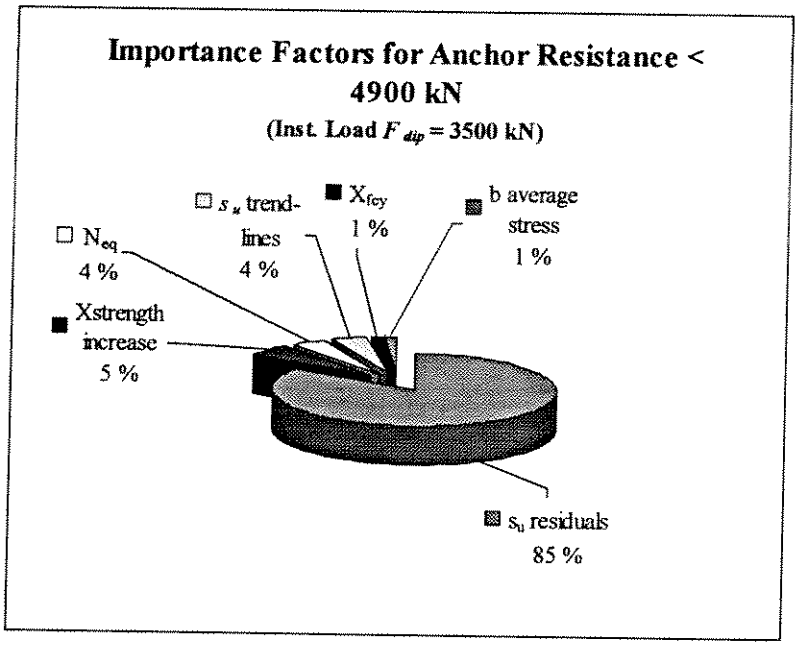

Figure 8.2 Importance of uncertainty contributions from the different uncertain variables in the determination of the holding capacity being larger than 4900kN for an installation load of 3500 kN.

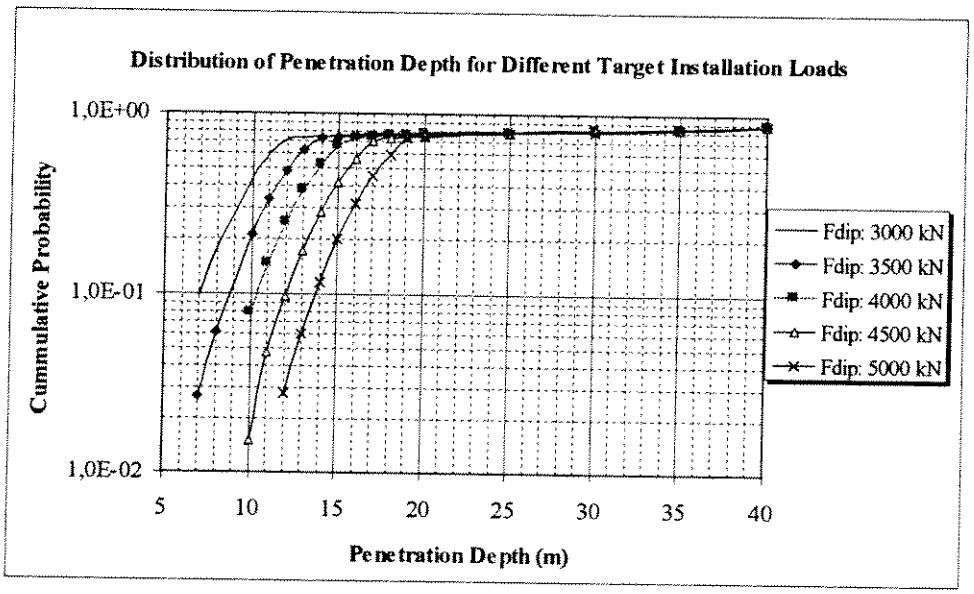

Figure 8.3 Cumulative distribution of estimated penetration depth for different target installation loads. The cumulative distribution function defines the probability that the penetration depth is equal to or less than the considered value.

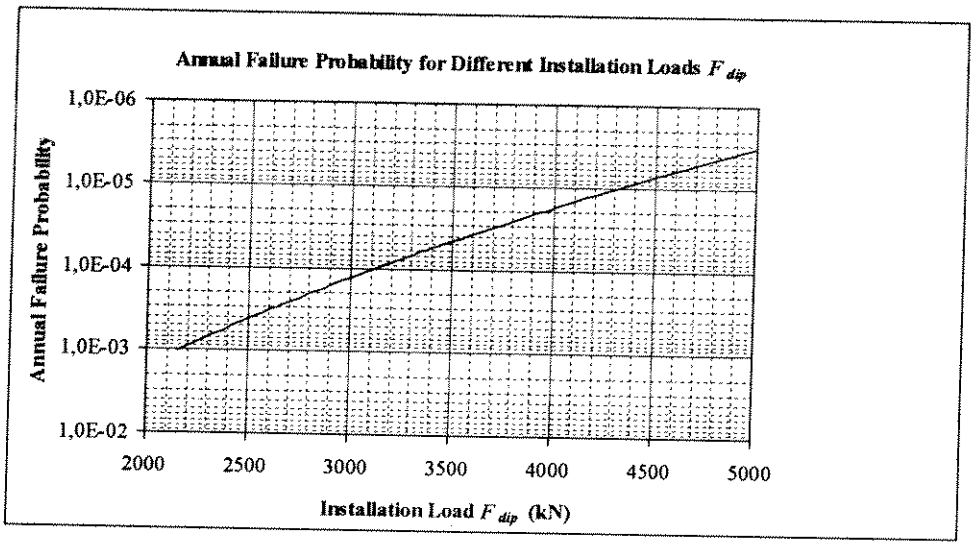

Figure 8.4 Estimated annual probability of failure (drag) of the anchor dependent on the installation load.

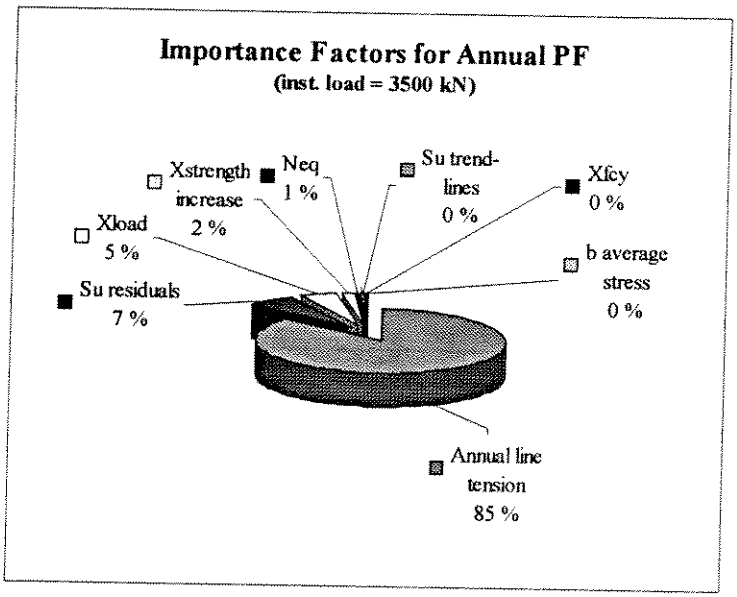

Figure 8.5 Importance of uncertainty contributions from the different uncertain variables in the determination of the annual probability of failure (drag) of the anchor for an installation load of 3500 kN.

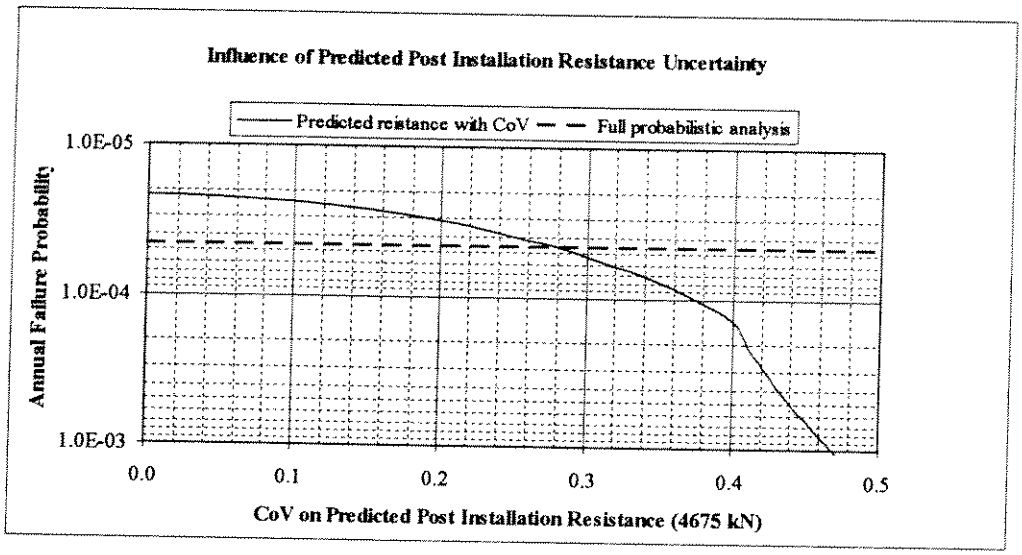

Figure 8.6 Influence of uncertainty associated to the "best guess" predicted post installation resistance on the estimated annual failure probability. The dashed-solid line defines the estimated annual failure probability obtained through the complete probabilistic analysis.

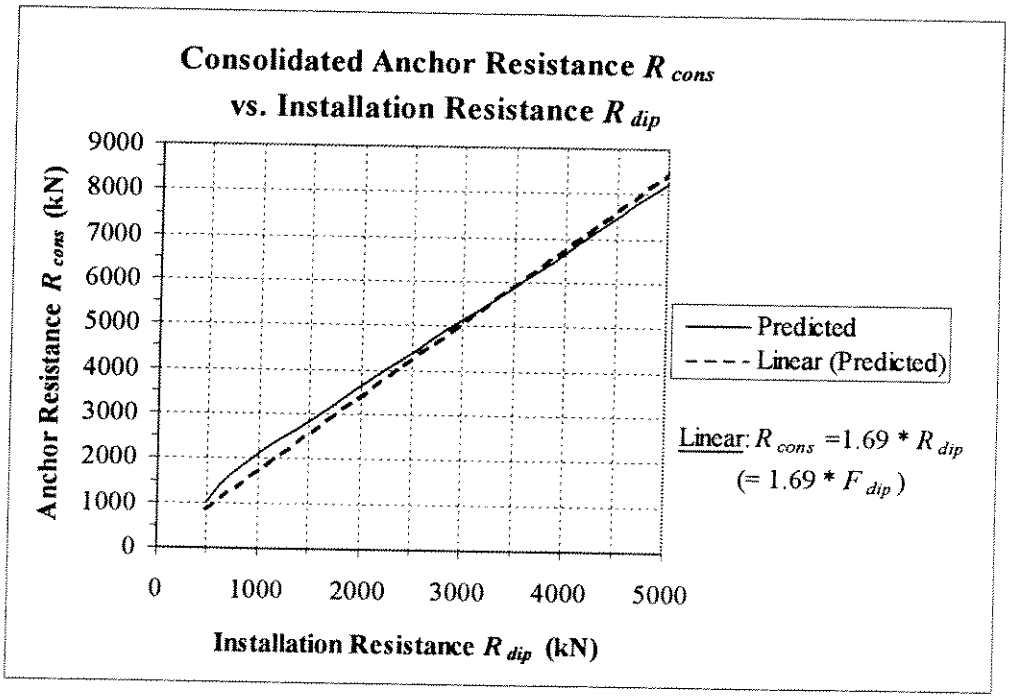

Figure 9.1 DIGIN computations of relationship between anchor resistance and installation load for best-estimates of intact and remoulded shear strength and zero uplift angle. Together with the computed relationship, a fitted linear trend line is included.

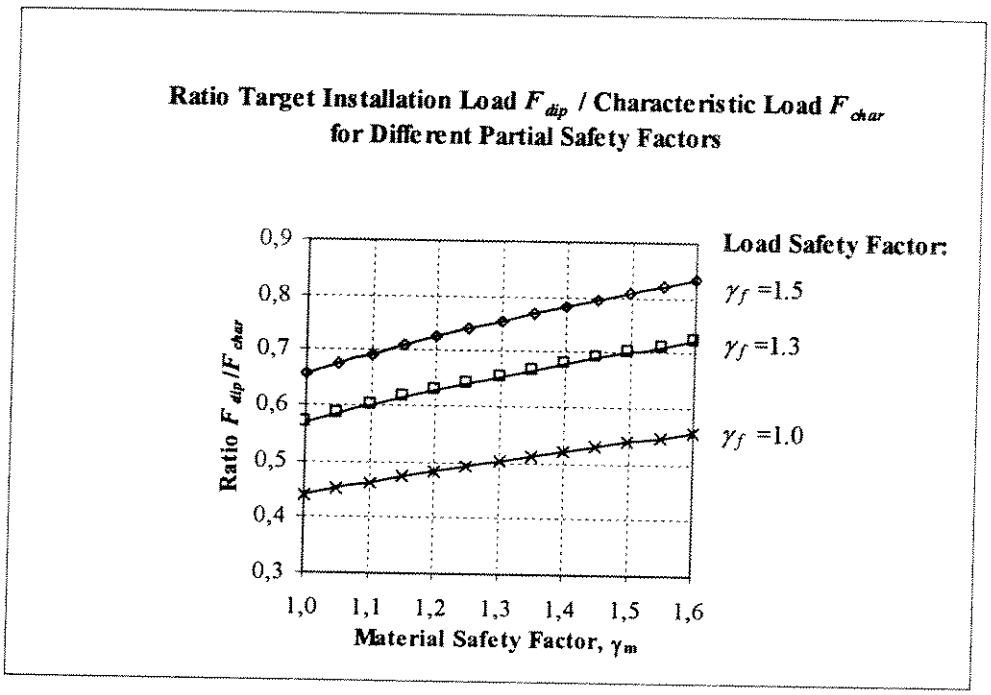

Figure 9.2 Required target installation load depending on choice of partial safety factors for proposed initial design equation.

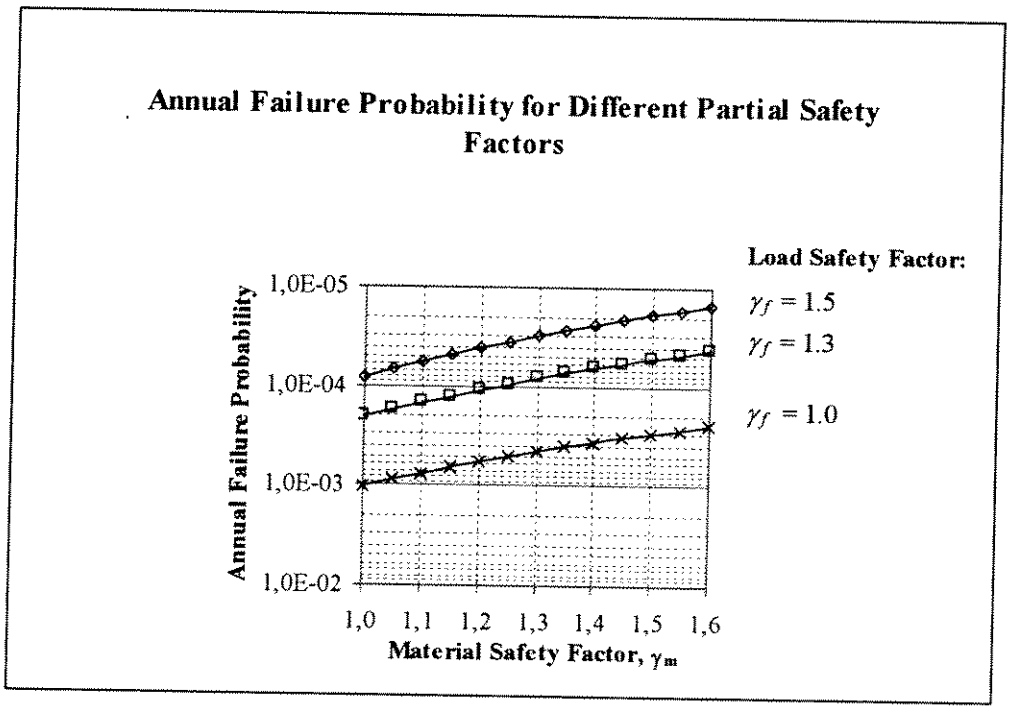

Figure 9.3 Estimated annual failure probability depending on choice of partial safety factors for proposed initial design equation.

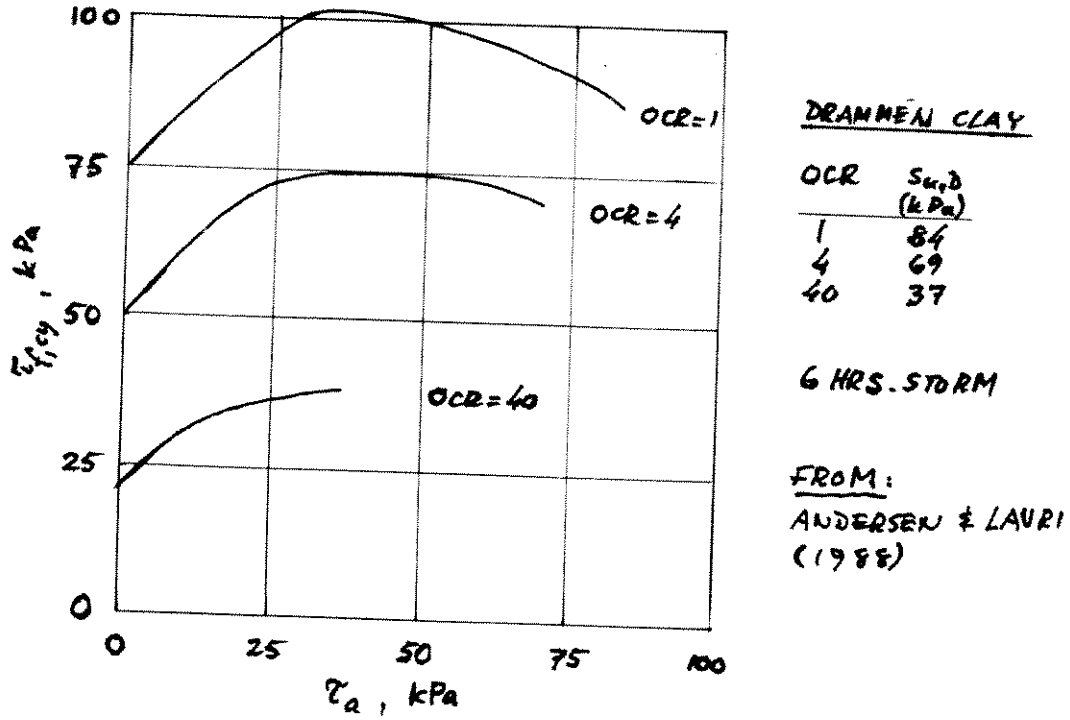

Figure 10.1 'Predicted' cyclic shear strength for Troll compared with reported Troll clay data (received after the reliability analysis) and Drammen clay data.

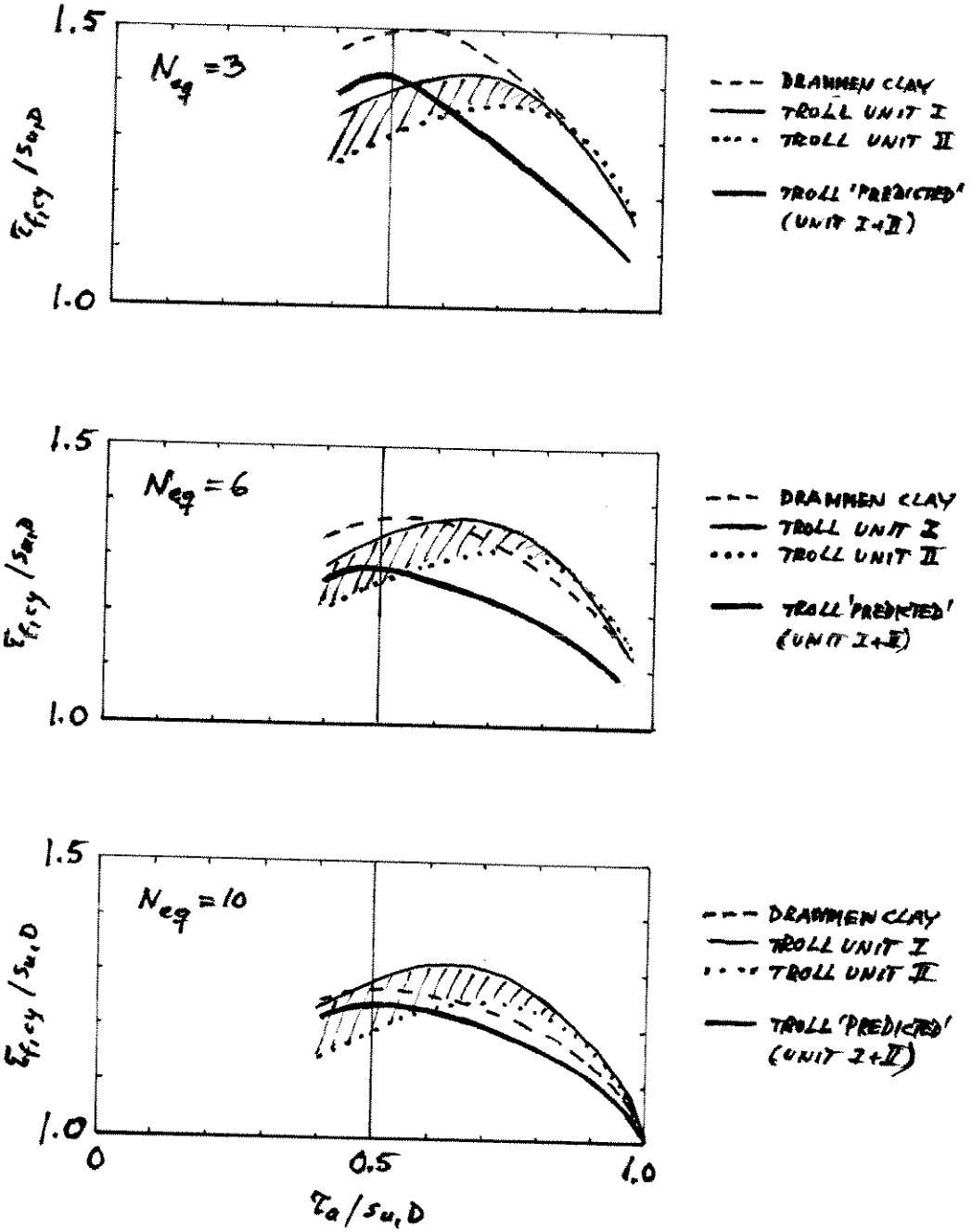

Figure 10.2 Cyclic shear strength $\tau_{f,cy}$ vs. average shear stress τ_a and *OCR*.

13 APPENDICES

APPENDIX
A
LINEAR REGRESSION ANALYSIS OF SOIL DATA

Appendix A: Linear Regression Analysis of Soil Data

In the following, the theoretical background for the development of two correlated linear regression lines for two sets of data points is described.

Two variables X and Y exhibit variations with the depth z. Here, X and Y denote intact and remoulded shear strength, respectively, for a clay. Data are given in terms of n triplets (z,x,y)i, i=1,...n, i.e., there are n pair-wise observations of X and Y, each pair being associated with a specific depth. Both X and Y are assumed on average to be linear functions of depth,

$$E[X]=b1+b2\cdot z \tag{A.1}$$

$$E[Y]=b3+b4\cdot z \tag{A.2}$$

which leads to two linear models

$$xi=b1+b2\cdot zi+\varepsilon xi, \quad i=1,...n \tag{A.3}$$

$$yi=b3+b4\cdot zi+\varepsilon yi, \quad i=1,...n \tag{A.4}$$

in which the residuals εxi and εyi, i=1,...n, are correlated with coefficient of correlation ρ, and $c=\sigma y/\sigma x$ is the ratio between the standard deviations of the residuals of Y and X, respectively. Standard methods of estimation can be used to estimate ρ, σx, and σy from the data.

A (2n)×(2n) covariance matrix Σ is established. It consists of four n×n sub-matrices, each of which contains n identical elements on the diagonal and each of which contains zeroes in all off-diagonal entries. For n=5, the matrix appears as follows

$$\Sigma=\left[\begin{array}{ccccc|ccccc} 1 & 0 & 0 & 0 & 0 & c\rho & 0 & 0 & 0 & 0 \\ 0 & 1 & 0 & 0 & 0 & 0 & c\rho & 0 & 0 & 0 \\ 0 & 0 & 1 & 0 & 0 & 0 & 0 & c\rho & 0 & 0 \\ 0 & 0 & 0 & 1 & 0 & 0 & 0 & 0 & c\rho & 0 \\ 0 & 0 & 0 & 0 & 1 & 0 & 0 & 0 & 0 & c\rho \\ \hline c\rho & 0 & 0 & 0 & 0 & c^2 & 0 & 0 & 0 & 0 \\ 0 & c\rho & 0 & 0 & 0 & 0 & c^2 & 0 & 0 & 0 \\ 0 & 0 & c\rho & 0 & 0 & 0 & 0 & c^2 & 0 & 0 \\ 0 & 0 & 0 & c\rho & 0 & 0 & 0 & 0 & c^2 & 0 \\ 0 & 0 & 0 & 0 & c\rho & 0 & 0 & 0 & 0 & c^2 \end{array}\right] \tag{A.5}$$

The two linear models for X and Y with respect to depth z can be combined and expressed on matrix form

$$x=ab+\varepsilon \tag{A.6}$$

in which $x=(x1,x2,...xn,y1,y2,...yn)^T$, $b=(b1,b2,b3,b4)^T$, and $\varepsilon=(\varepsilon x1,\varepsilon x2,...\varepsilon xn,\varepsilon y1,\varepsilon y2,...\varepsilon yn)T$. a is a (2n)×4 matrix defined as follows

$$a=\begin{bmatrix} 1 & z_1 & 0 & 0 \\ 1 & z_2 & 0 & 0 \\ \vdots & \vdots & \vdots & \vdots \\ \vdots & \vdots & \vdots & \vdots \\ 1 & z_n & 0 & 0 \\ 0 & 0 & 1 & z_1 \\ 0 & 0 & 1 & z_2 \\ \vdots & \vdots & \vdots & \vdots \\ \vdots & \vdots & \vdots & \vdots \\ 0 & 0 & 1 & z_n \end{bmatrix} \tag{A.7}$$

The vector of residuals has a covariance matrix $\sigma x2\Sigma$, and the sought-after vector b of coefficients is estimated by

$$\hat{\mathbf{b}} = (\mathbf{a}^T\boldsymbol{\Sigma}^{-1}\mathbf{a})^{-1}\mathbf{a}^T\boldsymbol{\Sigma}^{-1}\mathbf{x} \tag{A.8}$$

The covariance matrix for $\hat{\mathbf{b}}$ is

$$\mathbf{C}_{\hat{\mathbf{b}}} = \sigma_x^2 (\mathbf{a}^T \boldsymbol{\Sigma}^{-1} \mathbf{a})^{-1} \tag{A.9}$$

from which the standard deviation of $\hat{\mathbf{b}}$ and correlation matrix for $\hat{\mathbf{b}}$ can both be easily derived.

- o0o -

APPENDIX
B
ANALYSIS OF TWO-WAY CYCLIC LOADING

Appendix B Analysis of two-way cyclic loading ($\tau_a = 0$)

Clay subjected to constant-amplitude cyclic loading will respond by development of a cyclically varying shear strain. Starting from a small value at the initiation of the loading, the amplitude of this cyclic shear strain will increase as the loading proceeds. A load history may be represented so as to consist of a series of blocks of such constant-amplitude cyclic loading. The load history is for practical purposes arranged as an ordered series of stress blocks of increasing shear stress amplitude.

The instantaneous value of the cumulative shear strain amplitude response at any point in time proves to be dependent on the current stress level, i.e., it depends on the shear stress amplitude of the current stress cycle. This is reflected by a static strain increment, which is always added when the loading shifts from a lower stress level to a higher, such as when the loading from one stress block is followed by the loading from the next stress block. This static strain increment is known as the immediate strain. Whenever applied upon the initiation of the cyclic loading at a new stress level, the static strain increment is always followed by the further cyclic strain accumulation that is caused by the load cycles that take place at this new stress level.

The more severe the loading – in terms of larger stress amplitudes and higher number of stress cycles – the larger is the accumulated shear strain during the load history. An upper limit for the cyclic shear stress amplitude that can be mobilised in clay during the loading is reached at large such accumulated strains, thus indicating the occurrence of a failure condition. This upper limit for the shear stress may be interpreted as the available cyclic shear strength of the clay. Failure is defined to occur when the accumulated shear strain amplitude γ_c exceeds a critical level, γ_{cf}. Reasonable choices for the limiting value γ_{cf} ranges from about 3% to as much as 15% depending on the actual type of clay. As long as a sufficiently high value of γ_{cf} is chosen for the clay in question, the sensitivity to this choice will be small, see Ronold and Madsen (1987). The check of γ_c against γ_{cf} is performed for the value that γ_c has by the end of the ordered load history.

The strain-contour diagram gives the relation between the number of shear stress cycles N of constant shear stress amplitude τ necessary to reach a cyclic shear strain amplitude γ. Figure 5.1 in IR 203 shows an example from NGI (1975) of a strain-contour diagram, based on direct simple shear (DSS) tests on Drammen clay with an overconsolidation ratio OCR = 1, i.e. a normally consolidated clay. For a general introduction to the strain accumulation techniques reference is made to Foss et al. (1978).

The strain-contour diagram can be represented by the following relationship

$$\frac{\tau}{s_u} = \frac{\gamma}{a_1 + (a_2 + a_3 \log_{10} N + a_4 (\log_{10} N)^2)\gamma} \tag{B.1}$$

in which $a_1,...a_4$ are coefficients.

This gives a nonlinear model for the strain

$$\gamma_i = \frac{a_1 (\tau / s_u)_i}{1 - (\tau / s_u)_i (a_2 + a_3 \log_{10} N_i + a_4 (\log_{10} N_i)^2)} + \varepsilon_i \tag{B.2}$$

Mean values of $a_1,...a_4$ can be estimated together with the standard deviation σ of the residuals ε by a least-squares regression of γ on τ/s_u and N based on data triplets $((\tau/s_u)_i, N_i, \gamma_i)$ from direct simple shear tests. Their standard deviations and correlation matrix can be estimated by a resampling technique such as the jackknife and the bootstrap, see Efron and Tibshirani (1993).

The accumulated strain γ_c owing to a particular load history can be determined by application of the strain-contour diagram in conjunction with the strain accumulation method. The stress history is ordered as a sequence of n blocks of constant amplitude stress with increasing amplitude. Applying the number of cycles in the first stress block, the cyclic shear strain after this block is determined directly from the strain-contour diagram. By following a contour of constant strain in this diagram up to the stress level of the second stress block, an equivalent number of stress cycles at this stress level, owing to the preceding part of the stress history, is determined. The effects of the second stress block are now added: Initiation of this stress gives an immediate increment in the shear strain amplitude, depending on the previous stress level and the new stress level. The corresponding equivalent number of stress cycles at the stress level of the new stress block is then determined from the strain-contour diagram. To this number, the number of cycles in the second stress block is added, and the total accumulated strain after this block is determined from the strain-contour diagram. This procedure is repeated for the remaining stress blocks, and the strain determined after the nth stress block is thus the final accumulated strain γ_c due to the entire load history. Note that in this strain accumulation procedure, an improved calculation of the immediate strain according to a model by Ronold (1993) may be included when pore pressure measurement data from the direct simple shear tests are available.

A total of 82 triplets $((\tau/s_u)_i, N_i, \gamma_i)$ are available from 15 stress-controlled direct simple shear tests on test specimens of Troll clay. The four coefficients $a_1,...a_4$ can be estimated by means of a nonlinear regression analysis. For this purpose, it is assumed that observations of strain on the same test specimen are positively correlated, and the intra-specimen coefficient of correlation ρ is assumed to be reasonably well represented by a geometric decay model, $\rho=r^{\Delta\gamma}$, where $\Delta\gamma=|\gamma_i-\gamma_j|$ with γ_i and γ_j being two strain observations on the same soil specimen, and r is a base to be chosen. A base $r=10^{-300}$ proves to be a reasonable choice. It is also assumed that the standard deviation σ of the residuals ε is proportional to $\sqrt{\gamma}$, $\sigma=k\sqrt{\gamma}$. Reference is made to Ronold (1993). A jackknife technique as described by Efron and Tibshirani (1993) is used to estimate the standard deviation and correlation matrix for $a_1,...a_4$. The resulting estimates of the mean value, standard deviation, and correlation matrix for $a_1,...a_4$ from the non-linear regression and the jackknife are as follows

$$E\begin{bmatrix}\hat{a}_1\\ \hat{a}_2\\ \hat{a}_3\\ \hat{a}_4\end{bmatrix}=\begin{bmatrix}0.152\cdot10^{-2}\\ 0.885\\ 0.155\\ 0.378\cdot10^{-1}\end{bmatrix};\ D\begin{bmatrix}\hat{a}_1\\ \hat{a}_2\\ \hat{a}_3\\ \hat{a}_4\end{bmatrix}=\begin{bmatrix}0.661\cdot10^{-3}\\ 0.747\cdot10^{-1}\\ 0.908\cdot10^{-1}\\ 0.250\cdot10^{-1}\end{bmatrix}; \tag{B.3}$$

$$\tilde{\rho}=\begin{bmatrix}1.0000 & -0.5105 & 0.4420 & -0.4784\\ -0.5105 & 1.0000 & -0.9820 & 0.9258\\ 0.4420 & -0.9820 & 1.0000 & -0.9738\\ -0.4784 & 0.9258 & -0.9738 & 1.0000\end{bmatrix} \tag{B.4}$$

The standard deviation of the strain residuals results as a by-product of the regression as

$$\hat{\sigma}=0.131\sqrt{\gamma} \tag{B.5}$$

In the reliability analysis, the distribution of $a_1,...a_4$ is taken as a four-dimensional normal distribution. The residual ε is modelled as $\varepsilon=0.131U\sqrt{\gamma}$, where U is a standardised normally

distributed variable, and represents arbitrary variations about the average strain predictions that come out of the strain-contour diagram. Predictions of the accumulated strain γ_c by the strain accumulation method are encumbered with model uncertainty. The model uncertainty is represented by an unbiased random factor F which is modelled by a normally distributed variable with unit mean and 10% coefficient of variation, see Ronold and Madsen (1987).

When γ_c is the accumulated strain predicted as a function of $a_1,...a_4$ by the strain accumulation method as described above, then the 'true' accumulated strain $\gamma_{c,res}$ can be represented as

$$\gamma_{c,res} = F(\gamma_c + 0.131U\sqrt{\gamma_c}) \tag{B.6}$$

In this study, the cyclic-shear-strength-to-undrained-shear-strength ratio $\tau_{f,cy}/s_u$ and its distribution is sought-after. Therefore, all stress amplitudes in the load history representation, i.e., one stress amplitude per stress block, are scaled by the same factor which is chosen such that the resulting accumulated shear strain $\gamma_{c,res}$ owing to the load history becomes exactly equal to the failure strain γ_{cf}. In this scaled stress history, the stress amplitude value which is exceeded by exactly one stress cycle, is then interpreted as the cyclic-shear-strength-to-undrained-shear-strength ratio $\tau_{f,cy}/s_u$. In this study, the failure strain is taken as γ_{cf}=0.05.

When the load history is given, outcomes of the cyclic-shear-strength-to-undrained-shear-strength ratio $\tau_{f,cy}/s_u$ are simulated by Monte-Carlo simulation of outcomes of the six stochastic variables $a_1,...a_4$, U, and F. This gives a simulated distribution of the cyclic-shear-strength-to-undrained-shear-strength ratio $\tau_{f,cy}/s_u$, and the mean value, standard deviation, skewness, kurtosis, and coefficient of variation of the distribution are interpreted.

Nine different load histories are considered here as described in IR 203, and the simulation procedure is repeated for all nine histories to get distributions and statistical moments for the cyclic shear strength that corresponds to each of them. The results are given in Table B.1 below.

Table B.1 Results of simulation of $\tau_{f,cy}/s_u$ distribution.

Load case	Description	$\tau_{f,cy}/s_u$				
		Mean	St.dev.	Skewness	Kurtosis	CoV (%)
1	E1 WF	0.94	0.026	–1.64	7.1	2.8
2	E1 LF	1.02	0.045	–0.40	4.0	4.4
3	E1 LF+WF	1.01	0.041	–0.46	3.7	4.1
4	E2 WF	0.95	0.026	–1.51	6.8	2.7
5	E2 LF	1.01	0.044	–0.47	3.6	4.4
6	E2 LF+WF	1.01	0.043	–0.52	3.4	4.2
7	E3 WF	0.97	0.030	–1.30	5.5	3.1
8	E3 LF	1.01	0.042	–0.32	3.5	4.2
9	E3 LF+WF	1.01	0.041	–0.60	3.7	4.1

The results in Table B.1 indicates that the cyclic-shear-strength-to-undrained-shear-strength ratio $\tau_{f,cy}/s_u$ has a distribution with a coefficient of variation of about 3 to 5 %, which represents a fairly small uncertainty. This is considerably less than the uncertainty found for normally consolidated Drammen clay. As one of the major sources of uncertainty in $\tau_{f,cy}/s_u$ is the uncertainty in the strain-contour coefficients $a_1,...a_4$, this difference between the Troll clay and the Drammen clay may to a great extent be explained by the significantly larger uncertainty in a_2 found for Drammen clay relative to Troll clay. These findings are not totally unexpected, because more data are available for the estimation of Troll clay properties than there were for the estimation of Drammen clay properties, so the statistical uncertainty should be less for Troll clay properties than for Drammen clay properties.

The equivalent number of cycles to failure, N_{eq}, of amplitude $\tau_{f,cy}/s_u$ can be calculated from

$$\log_{10} N_{eq} = \frac{-a_3 + \sqrt{a_3^{\,2} - 4a_4\left(\frac{a_1}{\gamma} - \frac{1}{\tau_{f,cy}/s_u} + a_2\right)}}{2a_4} \tag{B.7}$$

in which γ is set equal to the failure strain γ_{cf}=0.05.

With the distribution of $\tau_{f,cy}/s_u$ given in terms of its first four statistical moments, this distribution can be represented by a fourth-moment Hermite polynomial expansion of a standard normal variable U as follows

$$\frac{\tau_{f,cy}}{s_u} = \mu + \kappa\sigma\left[U + c_3(U^2 - 1) + c_4(U^3 - 3U)\right] \tag{B.8}$$

with

$$c_4 = \frac{\sqrt{1+36h_4} - 1}{18}; \quad c_3 = \frac{h_3}{1+6c_4}; \quad \kappa = \frac{1}{\sqrt{1+2c_3^{\,2}+6c_4^{\,2}}}; \quad h_3 = \frac{\alpha_3}{6}; \quad h_4 = \frac{\alpha_4 - 3}{24} \tag{B.9}$$

in which μ, σ, α_3, and α_4 denote the first four statistical moments of $\tau_{f,cy}/s_u$. The distribution of the equivalent number of cycles can now be obtained by simulation of the standard Gaussian variable U in conjunction with use of Equations (B.7) through (B.9). This has been done for all the nine load cases considered. The results of these simulations are presented in Table B.2 in terms of the first four statistical moments of the equivalent number of cycles N_{eq}. Note that even if $\tau_{f,cy}/s_u$ has a coefficient of variation of only 3-5%, N_{eq} comes out with a much higher uncertainty. The skewness and kurtosis values reported in Table B.2 should be used with care. They are encumbered with considerable uncertainty owing to the limited number of simulations used for their estimation.

Table B.2 Results of simulation of N_{eq} distribution

Load case	Description	N_{eq}				
		Mean	St.dev.	Skewness	Kurtosis	CoV (%)
1	E1 WF	6.04	2.10	1.25	6.1	35
2	E1 LF	3.03	1.71	1.26	6.2	56
3	E1 LF+WF	3.15	1.59	0.90	4.2	51
4	E2 WF	5.52	1.85	0.84	4.9	34
5	E2 LF	3.16	1.73	1.05	4.5	55
6	E2 LF+WF	3.16	1.61	0.74	3.3	51
7	E3 WF	4.19	1.67	0.72	3.8	40
8	E3 LF	3.20	1.81	1.40	6.9	56
9	E3 LF+WF	3.29	1.69	1.14	4.7	52

- o0o -

APPENDIX
C
RESPONSE SURFACE DATA

Appendix C Response Surface Data

In the following, the data file applied in the response surface modelling is presented. The first 6 columns represent the input data to the response surface, while the last two columns represent the out data.

The following input variables are specified in the response surface interface file for in single layer of clay:

Input:

1. Intact, soil shear strength intercept at zero depth, $s_{u,0}$
2. Intact, soil shear strength gradient, k_u
3. Remoulded, soil shear strength intercept at zero depth, $s_{u,r,0}$
4. Remoulded, soil shear strength gradient, $k_{u,r}$
5. Installation load at the dip-down point, f_{dip}
6. Uplift angle under extreme load, θ_e

Output:

7. Penetration depth during installation, z
8. Consolidated anchor resistance at the dip down point, r_{cons}

s_u (kPa)	k_u (kPa/m)	$s_{u,r}$ (kPa)	$k_{u,r}$ (kPa/m)	F_{dip} (kN)	θ_e (deg)	z (m)	R_{cons} (kN)
-0.400	2.220	-7.880	1.280	5.7341E+02	0.0	2.0	1.3113E+03
-0.400	2.220	-7.880	1.280	7.9452E+02	0.0	3.0	1.9025E+03
-0.400	2.220	-7.880	1.280	1.0455E+03	0.0	4.0	2.3963E+03
-0.400	2.220	-7.880	1.280	1.3482E+03	0.0	5.0	2.8550E+03
-0.400	2.220	-7.880	1.280	1.6300E+03	0.0	6.0	3.3199E+03
-0.400	2.220	-7.880	1.280	1.9014E+03	0.0	7.0	3.7538E+03
-0.400	2.220	-7.880	1.280	2.1835E+03	0.0	8.0	4.2168E+03
-0.400	2.220	-7.880	1.280	2.4591E+03	0.0	9.0	4.6901E+03
-0.400	2.220	-7.880	1.280	2.7397E+03	0.0	10.0	5.1073E+03
-0.400	2.220	-7.880	1.280	3.0351E+03	0.0	11.0	5.5547E+03
-0.400	2.220	-7.880	1.280	3.3128E+03	0.0	12.0	5.9886E+03
-0.400	2.220	-7.880	1.280	3.5957E+03	0.0	13.0	6.4216E+03
-0.400	2.220	-7.880	1.280	3.8660E+03	0.0	14.0	6.8632E+03
-0.400	2.220	-7.880	1.280	4.2063E+03	0.0	15.0	7.3516E+03
-0.400	2.220	-7.880	1.280	4.4866E+03	0.0	16.0	7.8019E+03
-0.400	2.220	-7.880	1.280	4.7506E+03	0.0	17.0	8.2125E+03
-1.300	2.200	-6.700	1.300	4.9136E+02	0.0	2.0	1.0419E+03
-1.300	2.200	-6.700	1.300	7.4851E+02	0.0	3.0	1.6826E+03
-1.300	2.200	-6.700	1.300	1.0525E+03	0.0	4.0	2.1901E+03
-1.300	2.200	-6.700	1.300	1.3838E+03	0.0	5.0	2.6545E+03
-1.300	2.200	-6.700	1.300	1.6771E+03	0.0	6.0	3.1220E+03
-1.300	2.200	-6.700	1.300	1.9619E+03	0.0	7.0	3.5604E+03
-1.300	2.200	-6.700	1.300	2.2485E+03	0.0	8.0	4.0255E+03
-1.300	2.200	-6.700	1.300	2.5385E+03	0.0	9.0	4.4588E+03
-1.300	2.200	-6.700	1.300	2.8222E+03	0.0	10.0	4.9020E+03
-1.300	2.200	-6.700	1.300	3.1462E+03	0.0	11.0	5.3551E+03
-1.300	2.200	-6.700	1.300	3.4446E+03	0.0	12.0	5.8107E+03
-1.300	2.200	-6.700	1.300	3.7177E+03	0.0	13.0	6.2457E+03
-1.300	2.200	-6.700	1.300	4.0076E+03	0.0	14.0	6.6720E+03
-1.300	2.200	-6.700	1.300	4.2659E+03	0.0	15.0	7.0980E+03
-1.300	2.200	-6.700	1.300	4.5433E+03	0.0	16.0	7.5278E+03
-1.300	2.200	-6.700	1.300	4.8217E+03	0.0	17.0	7.9618E+03
-2.200	2.180	-5.520	1.320	5.1063E+03	0.0	18.0	8.3722E+03
-2.200	2.180	-5.520	1.320	6.7244E+02	1.0	3.0	1.4180E+03
-2.200	2.180	-5.520	1.320	1.0307E+03	1.0	4.0	1.9646E+03
-2.200	2.180	-5.520	1.320	1.4299E+03	1.0	5.0	2.4397E+03
-2.200	2.180	-5.520	1.320	1.7242E+03	1.0	6.0	2.9139E+03
-2.200	2.180	-5.520	1.320	2.0391E+03	1.0	7.0	3.3676E+03
-2.200	2.180	-5.520	1.320	2.3337E+03	1.0	8.0	3.7994E+03
-2.200	2.180	-5.520	1.320	2.6193E+03	1.0	9.0	4.2388E+03
-2.200	2.180	-5.520	1.320	2.9069E+03	1.0	10.0	4.7115E+03
-2.200	2.180	-5.520	1.320	3.2203E+03	1.0	11.0	5.1065E+03
-2.200	2.180	-5.520	1.320	3.5152E+03	1.0	12.0	5.5327E+03
-2.200	2.180	-5.520	1.320	3.7844E+03	1.0	13.0	5.9656E+03
-2.200	2.180	-5.520	1.320	4.0866E+03	1.0	14.0	6.4027E+03
-2.200	2.180	-5.520	1.320	4.3762E+03	1.0	15.0	6.8478E+03

s_u (kPa)	k_s (kPa/m)	$s_{u,r}$ (kPa)	$k_{s,r}$ (kPa/m)	F_{stg} (kN)	θ_s (deg)	z (m)	R_{case} (kN)
-2.200	2.180	-5.520	1.320	4.6698E+03	1.0	16.0	7.2571E+03
-2.200	2.180	-5.520	1.320	4.9476E+03	1.0	17.0	7.6726E+03
-2.200	2.180	-5.520	1.320	5.2279E+03	1.0	18.0	8.0903E+03
-2.200	2.180	-5.520	1.320	5.5320E+03	1.0	19.0	8.5757E+03
-2.200	2.180	-5.520	1.320	5.7960E+03	1.0	20.0	8.9978E+03
-2.200	2.180	-5.520	1.320	6.0848E+03	1.0	21.0	9.3967E+03
-3.100	2.160	-4.340	1.340	5.7733E+02	2.0	3.0	1.1492E+03
-3.100	2.160	-4.340	1.340	1.0504E+03	2.0	4.0	1.7320E+03
-3.100	2.160	-4.340	1.340	1.4607E+03	2.0	5.0	2.2140E+03
-3.100	2.160	-4.340	1.340	1.7687E+03	2.0	6.0	2.6790E+03
-3.100	2.160	-4.340	1.340	2.0812E+03	2.0	7.0	3.1328E+03
-3.100	2.160	-4.340	1.340	2.3853E+03	2.0	8.0	3.5645E+03
-3.100	2.160	-4.340	1.340	2.6880E+03	2.0	9.0	3.9998E+03
-3.100	2.160	-4.340	1.340	2.9928E+03	2.0	10.0	4.4453E+03
-3.100	2.160	-4.340	1.340	3.3040E+03	2.0	11.0	4.8969E+03
-3.100	2.160	-4.340	1.340	3.5934E+03	2.0	12.0	5.3309E+03
-3.100	2.160	-4.340	1.340	3.8848E+03	2.0	13.0	5.7644E+03
-3.100	2.160	-4.340	1.340	4.1958E+03	2.0	14.0	6.1561E+03
-3.100	2.160	-4.340	1.340	4.4964E+03	2.0	15.0	6.6449E+03
-3.100	2.160	-4.340	1.340	4.7859E+03	2.0	16.0	7.0514E+03
-3.100	2.160	-4.340	1.340	5.0943E+03	2.0	17.0	7.4623E+03
-3.100	2.160	-4.340	1.340	5.3667E+03	2.0	18.0	7.9165E+03
-3.100	2.160	-4.340	1.340	5.6630E+03	2.0	19.0	8.2879E+03
-3.100	2.160	-4.340	1.340	5.9628E+03	2.0	20.0	8.6978E+03
-3.100	2.160	-4.340	1.340	6.2430E+03	2.0	21.0	9.1181E+03
-3.100	2.160	-4.340	1.340	6.5268E+03	2.0	22.0	9.6130E+03
-3.100	2.160	-4.340	1.340	6.8129E+03	2.0	23.0	9.9884E+03
-3.100	2.160	-4.340	1.340	7.0783E+03	2.0	24.0	1.0375E+04
-4.000	2.140	-3.160	1.360	4.3482E+02	3.0	3.0	8.7645E+02
-4.000	2.140	-3.160	1.360	1.0330E+03	3.0	4.0	1.4651E+03
-4.000	2.140	-3.160	1.360	1.4750E+03	3.0	5.0	2.0030E+03
-4.000	2.140	-3.160	1.360	1.8056E+03	3.0	6.0	2.4668E+03
-4.000	2.140	-3.160	1.360	2.1388E+03	3.0	7.0	2.9196E+03
-4.000	2.140	-3.160	1.360	2.4574E+03	3.0	8.0	3.3421E+03
-4.000	2.140	-3.160	1.360	2.7690E+03	3.0	9.0	3.7951E+03
-4.000	2.140	-3.160	1.360	3.0711E+03	3.0	10.0	4.2607E+03
-4.000	2.140	-3.160	1.360	3.3897E+03	3.0	11.0	4.6367E+03
-4.000	2.140	-3.160	1.360	3.6988E+03	3.0	12.0	5.0773E+03
-4.000	2.140	-3.160	1.360	3.9824E+03	3.0	13.0	5.5309E+03
-4.000	2.140	-3.160	1.360	4.3008E+03	3.0	14.0	5.9432E+03
-4.000	2.140	-3.160	1.360	4.6076E+03	3.0	15.0	6.3645E+03
-4.000	2.140	-3.160	1.360	4.9206E+03	3.0	16.0	6.7878E+03
-4.000	2.140	-3.160	1.360	5.2159E+03	3.0	17.0	7.2226E+03
-4.000	2.140	-3.160	1.360	5.5141E+03	3.0	18.0	7.6081E+03
-4.000	2.140	-3.160	1.360	5.7712E+03	3.0	19.0	8.0420E+03
-4.000	2.140	-3.160	1.360	6.1013E+03	3.0	20.0	8.4323E+03
-4.000	2.140	-3.160	1.360	6.3610E+03	3.0	21.0	8.9400E+03
-4.000	2.140	-3.160	1.360	6.6490E+03	3.0	22.0	9.3362E+03
-4.000	2.140	-3.160	1.360	6.9380E+03	3.0	23.0	9.6804E+03
-4.000	2.140	-3.160	1.360	7.2310E+03	3.0	24.0	1.0075E+04
-4.000	2.140	-3.160	1.360	7.5571E+03	3.0	25.0	1.0610E+04
-4.000	2.140	-3.160	1.360	7.8560E+03	3.0	26.0	1.0955E+04
-4.000	2.140	-3.160	1.360	8.1320E+03	3.0	27.0	1.1352E+04
-4.900	2.120	-1.980	1.380	5.5856E+02	4.0	3.0	5.5249E+02
-4.900	2.120	-1.980	1.380	1.0771E+03	4.0	4.0	1.2391E+03
-4.900	2.120	-1.980	1.380	1.5087E+03	4.0	5.0	1.7909E+03
-4.900	2.120	-1.980	1.380	1.8529E+03	4.0	6.0	2.2444E+03
-4.900	2.120	-1.980	1.380	2.1887E+03	4.0	7.0	2.6988E+03
-4.900	2.120	-1.980	1.380	2.5197E+03	4.0	8.0	3.1552E+03
-4.900	2.120	-1.980	1.380	2.8550E+03	4.0	9.0	3.5715E+03
-4.900	2.120	-1.980	1.380	3.1677E+03	4.0	10.0	4.0102E+03
-4.900	2.120	-1.980	1.380	3.4988E+03	4.0	11.0	4.4635E+03
-4.900	2.120	-1.980	1.380	3.8029E+03	4.0	12.0	4.8475E+03
-4.900	2.120	-1.980	1.380	4.1236E+03	4.0	13.0	5.2725E+03
-4.900	2.120	-1.980	1.380	4.4546E+03	4.0	14.0	5.7055E+03
-4.900	2.120	-1.980	1.380	4.7704E+03	4.0	15.0	6.0940E+03
-4.900	2.120	-1.980	1.380	4.9977E+03	4.0	16.0	6.5259E+03
-4.900	2.120	-1.980	1.380	5.3648E+03	4.0	17.0	6.9233E+03
-4.900	2.120	-1.980	1.380	5.6672E+03	4.0	18.0	7.4338E+03
-4.900	2.120	-1.980	1.380	5.9706E+03	4.0	19.0	7.7698E+03
-4.900	2.120	-1.980	1.380	6.2787E+03	4.0	20.0	8.1708E+03
-4.900	2.120	-1.980	1.380	6.5899E+03	4.0	21.0	8.6467E+03
-4.900	2.120	-1.980	1.380	6.8791E+03	4.0	22.0	9.0019E+03
-4.900	2.120	-1.980	1.380	7.1956E+03	4.0	23.0	9.4064E+03
-4.900	2.120	-1.980	1.380	7.4889E+03	4.0	24.0	9.8178E+03
-4.900	2.120	-1.980	1.380	7.7843E+03	4.0	25.0	1.0311E+04
-4.900	2.120	-1.980	1.380	8.0819E+03	4.0	26.0	1.0672E+04
-4.900	2.120	-1.980	1.380	8.3515E+03	4.0	27.0	1.1026E+04
-4.900	2.120	-1.980	1.380	8.5574E+03	4.0	28.0	1.1539E+04
-4.900	2.120	-1.980	1.380	8.8296E+03	4.0	29.0	1.1899E+04
-5.800	2.100	-0.800	1.400	1.5547E+03	5.0	5.0	1.5498E+03
-5.800	2.100	-0.800	1.400	1.9241E+03	5.0	6.0	2.0409E+03
-5.800	2.100	-0.800	1.400	2.2720E+03	5.0	7.0	2.4893E+03
-5.800	2.100	-0.800	1.400	2.5972E+03	5.0	8.0	2.9204E+03
-5.800	2.100	-0.800	1.400	2.9373E+03	5.0	9.0	3.3375E+03
-5.800	2.100	-0.800	1.400	3.2543E+03	5.0	10.0	3.7829E+03
-5.800	2.100	-0.800	1.400	3.5741E+03	5.0	11.0	4.2052E+03
-5.800	2.100	-0.800	1.400	3.8764E+03	5.0	12.0	4.6354E+03
-5.800	2.100	-0.800	1.400	4.2195E+03	5.0	13.0	5.0267E+03
-5.800	2.100	-0.800	1.400	4.5096E+03	5.0	14.0	5.5120E+03
-5.800	2.100	-0.800	1.400	4.8274E+03	5.0	15.0	5.8620E+03
-5.800	2.100	-0.800	1.400	5.1469E+03	5.0	16.0	6.2653E+03
-5.800	2.100	-0.800	1.400	5.4718E+03	5.0	17.0	6.7316E+03
-5.800	2.100	-0.800	1.400	5.7470E+03	5.0	18.0	7.1327E+03

s_u (kPa)	k_u (kPa/m)	$s_{u,r}$ (kPa)	$k_{u,r}$ (kPa/m)	F_{up} (kN)	θ_i (deg)	z (m)	R_{conc} (kN)
-5.800	2.100	-0.800	1.400	6.0533E+03	5.0	19.0	7.5416E+03
-5.800	2.100	-0.800	1.400	6.3375E+03	5.0	20.0	7.9526E+03
-5.800	2.100	-0.800	1.400	6.6489E+03	5.0	21.0	8.3752E+03
-5.800	2.100	-0.800	1.400	6.9634E+03	5.0	22.0	8.7317E+03
-5.800	2.100	-0.800	1.400	7.2554E+03	5.0	23.0	9.2381E+03
-5.800	2.100	-0.800	1.400	7.5492E+03	5.0	24.0	9.6012E+03
-5.800	2.100	-0.800	1.400	7.8447E+03	5.0	25.0	9.9685E+03
-5.800	2.100	-0.800	1.400	8.1425E+03	5.0	26.0	1.0393E+04
-5.800	2.100	-0.800	1.400	8.4424E+03	5.0	27.0	1.0760E+04
-5.800	2.100	-0.800	1.400	8.7140E+03	5.0	28.0	1.1217E+04
-5.800	2.100	-0.800	1.400	9.0175E+03	5.0	29.0	1.1590E+04
-5.800	2.100	-0.800	1.400	9.3647E+03	5.0	30.0	1.1958E+04
-5.800	2.100	-0.800	1.400	9.6428E+03	5.0	31.0	1.2425E+04
-5.800	2.100	-0.800	1.400	9.9224E+03	5.0	32.0	1.2801E+04
-6.700	2.080	0.380	1.420	1.9922E+03	6.0	6.0	1.8220E+03
-6.700	2.080	0.380	1.420	2.3597E+03	6.0	7.0	2.2689E+03
-6.700	2.080	0.380	1.420	2.7016E+03	6.0	8.0	2.7135E+03
-6.700	2.080	0.380	1.420	3.0297E+03	6.0	9.0	3.1392E+03
-6.700	2.080	0.380	1.420	3.3813E+03	6.0	10.0	3.5450E+03
-6.700	2.080	0.380	1.420	3.6820E+03	6.0	11.0	3.9742E+03
-6.700	2.080	0.380	1.420	4.0065E+03	6.0	12.0	4.4068E+03
-6.700	2.080	0.380	1.420	4.2986E+03	6.0	13.0	4.8000E+03
-6.700	2.080	0.380	1.420	4.6510E+03	6.0	14.0	5.2456E+03
-6.700	2.080	0.380	1.420	4.9741E+03	6.0	15.0	5.6065E+03
-6.700	2.080	0.380	1.420	5.2684E+03	6.0	16.0	6.0670E+03
-6.700	2.080	0.380	1.420	5.5719E+03	6.0	17.0	6.4791E+03
-6.700	2.080	0.380	1.420	5.9039E+03	6.0	18.0	6.8926E+03
-6.700	2.080	0.380	1.420	6.2109E+03	6.0	19.0	7.3149E+03
-6.700	2.080	0.380	1.420	6.5471E+03	6.0	20.0	7.6814E+03
-6.700	2.080	0.380	1.420	6.7791E+03	6.0	21.0	8.0579E+03
-6.700	2.080	0.380	1.420	7.0949E+03	6.0	22.0	8.4789E+03
-6.700	2.080	0.380	1.420	7.3884E+03	6.0	23.0	8.9183E+03
-6.700	2.080	0.380	1.420	7.7100E+03	6.0	24.0	9.2919E+03
-6.700	2.080	0.380	1.420	8.0076E+03	6.0	25.0	9.6645E+03
-6.700	2.080	0.380	1.420	8.3070E+03	6.0	26.0	1.0194E+04
-6.700	2.080	0.380	1.420	8.5800E+03	6.0	27.0	1.0569E+04
-6.700	2.080	0.380	1.420	8.8830E+03	6.0	28.0	1.0946E+04
-6.700	2.080	0.380	1.420	9.1840E+03	6.0	29.0	1.1257E+04
-6.700	2.080	0.380	1.420	9.5365E+03	6.0	30.0	1.1734E+04
-6.700	2.080	0.380	1.420	9.8166E+03	6.0	31.0	1.2110E+04
-6.700	2.080	0.380	1.420	1.0094E+04	6.0	32.0	1.2493E+04
-6.700	2.080	0.380	1.420	1.0411E+04	6.0	33.0	1.2981E+04
-6.700	2.080	0.380	1.420	1.1060E+04	6.0	35.0	1.3672E+04
-7.600	2.060	1.560	1.440	2.4737E+03	7.0	7.0	2.0621E+03
-7.600	2.060	1.560	1.440	2.8180E+03	7.0	8.0	2.5051E+03
-7.600	2.060	1.560	1.440	3.1505E+03	7.0	9.0	2.9173E+03
-7.600	2.060	1.560	1.440	3.5032E+03	7.0	10.0	3.3488E+03
-7.600	2.060	1.560	1.440	3.8039E+03	7.0	11.0	3.7552E+03
-7.600	2.060	1.560	1.440	4.1300E+03	7.0	12.0	4.1654E+03
-7.600	2.060	1.560	1.440	4.4414E+03	7.0	13.0	4.5956E+03
-7.600	2.060	1.560	1.440	4.7805E+03	7.0	14.0	5.0079E+03
-7.600	2.060	1.560	1.440	5.1250E+03	7.0	15.0	5.4209E+03
-7.600	2.060	1.560	1.440	5.4745E+03	7.0	16.0	5.8354E+03
-7.600	2.060	1.560	1.440	5.6943E+03	7.0	17.0	6.2139E+03
-7.600	2.060	1.560	1.440	6.0324E+03	7.0	18.0	6.6292E+03
-7.600	2.060	1.560	1.440	6.3411E+03	7.0	19.0	7.0074E+03
-7.600	2.060	1.560	1.440	6.6793E+03	7.0	20.0	7.4251E+03
-7.600	2.060	1.560	1.440	6.9970E+03	7.0	21.0	7.8024E+03
-7.600	2.060	1.560	1.440	7.2280E+03	7.0	22.0	8.2587E+03
-7.600	2.060	1.560	1.440	7.5485E+03	7.0	23.0	8.6888E+03
-7.600	2.060	1.560	1.440	7.8452E+03	7.0	24.0	9.0143E+03
-7.600	2.060	1.560	1.440	8.1438E+03	7.0	25.0	9.3819E+03
-7.600	2.060	1.560	1.440	8.4442E+03	7.0	26.0	9.9161E+03
-7.600	2.060	1.560	1.440	8.7465E+03	7.0	27.0	1.0228E+04
-7.600	2.060	1.560	1.440	9.0477E+03	7.0	28.0	1.0608E+04
-7.600	2.060	1.560	1.440	9.4304E+03	7.0	29.0	1.1000E+04
-7.600	2.060	1.560	1.440	9.7083E+03	7.0	30.0	1.1483E+04
-7.600	2.060	1.560	1.440	9.9917E+03	7.0	31.0	1.1791E+04
-7.600	2.060	1.560	1.440	1.0300E+04	7.0	32.0	1.2186E+04
-7.600	2.060	1.560	1.440	1.0582E+04	7.0	33.0	1.2610E+04
-7.600	2.060	1.560	1.440	1.0871E+04	7.0	34.0	1.3000E+04
-7.600	2.060	1.560	1.440	1.1240E+04	7.0	35.0	1.3503E+04
-7.600	2.060	1.560	1.440	1.1525E+04	7.0	36.0	1.3821E+04
-7.600	2.060	1.560	1.440	1.1815E+04	7.0	37.0	1.4135E+04
-8.500	2.040	2.740	1.460	2.9692E+03	8.0	8.0	2.2766E+03
-8.500	2.040	2.740	1.460	3.2996E+03	8.0	9.0	2.7012E+03
-8.500	2.040	2.740	1.460	3.6200E+03	8.0	10.0	3.1317E+03
-8.500	2.040	2.740	1.460	3.9816E+03	8.0	11.0	3.5215E+03
-8.500	2.040	2.740	1.460	4.2644E+03	8.0	12.0	3.9524E+03
-8.500	2.040	2.740	1.460	4.5935E+03	8.0	13.0	4.3608E+03
-8.500	2.040	2.740	1.460	4.8869E+03	8.0	14.0	4.7742E+03
-8.500	2.040	2.740	1.460	5.2561E+03	8.0	15.0	5.1932E+03
-8.500	2.040	2.740	1.460	5.5291E+03	8.0	16.0	5.5731E+03
-8.500	2.040	2.740	1.460	5.8822E+03	8.0	17.0	5.9897E+03
-8.500	2.040	2.740	1.460	6.1589E+03	8.0	18.0	6.3696E+03
-8.500	2.040	2.740	1.460	6.5577E+03	8.0	19.0	6.7500E+03
-8.500	2.040	2.740	1.460	6.8127E+03	8.0	20.0	7.1772E+03
-8.500	2.040	2.740	1.460	7.1320E+03	8.0	21.0	7.5577E+03
-8.500	2.040	2.740	1.460	7.4537E+03	8.0	22.0	7.9383E+03
-8.500	2.040	2.740	1.460	7.7778E+03	8.0	23.0	8.3874E+03
-8.500	2.040	2.740	1.460	8.1047E+03	8.0	24.0	8.7783E+03
-8.500	2.040	2.740	1.460	8.5101E+03	8.0	25.0	9.2478E+03
-8.500	2.040	2.740	1.460	8.6369E+03	8.0	26.0	9.5739E+03
-8.500	2.040	2.740	1.460	8.9410E+03	8.0	27.0	9.9477E+03

s_u (kPa)	k_u (kPa/m)	$s_{u,r}$ (kPa)	$k_{u,r}$ (kPa/m)	F_{dip} (kN)	θ_s (deg)	z (m)	R_{conn} (kN)
-8.500	2.040	2.740	1.460	9.2429E+03	8.0	28.0	1.0345E+04
-8.500	2.040	2.740	1.460	9.6344E+03	8.0	29.0	1.0657E+04
-8.500	2.040	2.740	1.460	9.9107E+03	8.0	30.0	1.1141E+04
-8.500	2.040	2.740	1.460	1.0225E+04	8.0	31.0	1.1465E+04
-8.500	2.040	2.740	1.460	1.0477E+04	8.0	32.0	1.1865E+04
-8.500	2.040	2.740	1.460	1.0790E+04	8.0	33.0	1.2283E+04
-8.500	2.040	2.740	1.460	1.1078E+04	8.0	34.0	1.2686E+04
-8.500	2.040	2.740	1.460	1.1361E+04	8.0	35.0	1.3119E+04
-8.500	2.040	2.740	1.460	1.1616E+04	8.0	36.0	1.3441E+04
-8.500	2.040	2.740	1.460	1.2027E+04	8.0	37.0	1.3836E+04
-8.500	2.040	2.740	1.460	1.2282E+04	8.0	38.0	1.4274E+04
-8.500	2.040	2.740	1.460	1.2539E+04	8.0	39.0	1.4594E+04
-9.400	2.020	3.920	1.480	3.5911E+03	9.0	9.0	2.4790E+03
-9.400	2.020	3.920	1.480	3.8010E+03	9.0	10.0	2.9051E+03
-9.400	2.020	3.920	1.480	4.1196E+03	9.0	11.0	3.3198E+03
-9.400	2.020	3.920	1.480	4.4714E+03	9.0	12.0	3.7249E+03
-9.400	2.020	3.920	1.480	4.7461E+03	9.0	13.0	4.1361E+03
-9.400	2.020	3.920	1.480	5.1161E+03	9.0	14.0	4.5205E+03
-9.400	2.020	3.920	1.480	5.4920E+03	9.0	15.0	4.9338E+03
-9.400	2.020	3.920	1.480	5.7109E+03	9.0	16.0	5.3544E+03
-9.400	2.020	3.920	1.480	6.0083E+03	9.0	17.0	5.7348E+03
-9.400	2.020	3.920	1.480	6.3462E+03	9.0	18.0	6.1182E+03
-9.400	2.020	3.920	1.480	6.6874E+03	9.0	19.0	6.4980E+03
-9.400	2.020	3.920	1.480	6.9652E+03	9.0	20.0	6.8792E+03
-9.400	2.020	3.920	1.480	7.2865E+03	9.0	21.0	7.3806E+03
-9.400	2.020	3.920	1.480	7.6100E+03	9.0	22.0	7.7138E+03
-9.400	2.020	3.920	1.480	7.9361E+03	9.0	23.0	8.0973E+03
-9.400	2.020	3.920	1.480	8.2653E+03	9.0	24.0	8.4808E+03
-9.400	2.020	3.920	1.480	8.5977E+03	9.0	25.0	8.8732E+03
-9.400	2.020	3.920	1.480	8.8731E+03	9.0	26.0	9.2846E+03
-9.400	2.020	3.920	1.480	9.2094E+03	9.0	27.0	9.6701E+03
-9.400	2.020	3.920	1.480	9.5207E+03	9.0	28.0	1.0006E+04
-9.400	2.020	3.920	1.480	9.8323E+03	9.0	29.0	1.0385E+04
-9.400	2.020	3.920	1.480	1.0110E+04	9.0	30.0	1.0883E+04
-9.400	2.020	3.920	1.480	1.0540E+04	9.0	31.0	1.1201E+04
-9.400	2.020	3.920	1.480	1.0830E+04	9.0	32.0	1.1630E+04
-9.400	2.020	3.920	1.480	1.0993E+04	9.0	33.0	1.2038E+04
-9.400	2.020	3.920	1.480	1.1278E+04	9.0	34.0	1.2364E+04
-9.400	2.020	3.920	1.480	1.1564E+04	9.0	35.0	1.2789E+04
-9.400	2.020	3.920	1.480	1.1944E+04	9.0	36.0	1.3113E+04
-9.400	2.020	3.920	1.480	1.2143E+04	9.0	37.0	1.3648E+04
-9.400	2.020	3.920	1.480	1.2490E+04	9.0	38.0	1.3972E+04
-9.400	2.020	3.920	1.480	1.2782E+04	9.0	39.0	1.4296E+04
-9.400	2.020	3.920	1.480	1.3040E+04	9.0	40.0	1.4732E+04
-10.300	2.000	5.100	1.500	4.3714E+03	10.0	11.0	3.1016E+03
-10.300	2.000	5.100	1.500	4.6303E+03	10.0	12.0	3.4887E+03
-10.300	2.000	5.100	1.500	4.9705E+03	10.0	13.0	3.8935E+03
-10.300	2.000	5.100	1.500	5.3070E+03	10.0	14.0	4.3099E+03
-10.300	2.000	5.100	1.500	5.5411E+03	10.0	15.0	4.6923E+03
-10.300	2.000	5.100	1.500	5.9206E+03	10.0	16.0	5.1108E+03
-10.300	2.000	5.100	1.500	6.2230E+03	10.0	17.0	5.4934E+03
-10.300	2.000	5.100	1.500	6.5846E+03	10.0	18.0	5.8780E+03
-10.300	2.000	5.100	1.500	6.8385E+03	10.0	19.0	6.2618E+03
-10.300	2.000	5.100	1.500	7.1199E+03	10.0	20.0	6.6448E+03
-10.300	2.000	5.100	1.500	7.4382E+03	10.0	21.0	7.0279E+03
-10.300	2.000	5.100	1.500	7.7870E+03	10.0	22.0	7.4163E+03
-10.300	2.000	5.100	1.500	8.1134E+03	10.0	23.0	7.8219E+03
-10.300	2.000	5.100	1.500	8.4470E+03	10.0	24.0	8.2063E+03
-10.300	2.000	5.100	1.500	8.7788E+03	10.0	25.0	8.5998E+03
-10.300	2.000	5.100	1.500	9.0583E+03	10.0	26.0	9.0132E+03
-10.300	2.000	5.100	1.500	9.3709E+03	10.0	27.0	9.4111E+03
-10.300	2.000	5.100	1.500	9.6257E+03	10.0	28.0	9.7342E+03
-10.300	2.000	5.100	1.500	1.0015E+04	10.0	29.0	1.0231E+04
-10.300	2.000	5.100	1.500	1.0331E+04	10.0	30.0	1.0553E+04
-10.300	2.000	5.100	1.500	1.0618E+04	10.0	31.0	1.0883E+04
-10.300	2.000	5.100	1.500	1.0898E+04	10.0	32.0	1.1393E+04
-10.300	2.000	5.100	1.500	1.1216E+04	10.0	33.0	1.1724E+04
-10.300	2.000	5.100	1.500	1.1502E+04	10.0	34.0	1.2041E+04
-10.300	2.000	5.100	1.500	1.1917E+04	10.0	35.0	1.2490E+04
-10.300	2.000	5.100	1.500	1.2173E+04	10.0	36.0	1.2806E+04
-10.300	2.000	5.100	1.500	1.2467E+04	10.0	37.0	1.3344E+04
-10.300	2.000	5.100	1.500	1.2756E+04	10.0	38.0	1.3581E+04
-10.300	2.000	5.100	1.500	1.3147E+04	10.0	39.0	1.3907E+04
-10.300	2.000	5.100	1.500	1.3443E+04	10.0	40.0	1.4455E+04
-11.200	1.980	6.280	1.520	5.2399E+03	11.0	13.0	3.6729E+03
-11.200	1.980	6.280	1.520	5.5118E+03	11.0	14.0	4.0562E+03
-11.200	1.980	6.280	1.520	5.8303E+03	11.0	15.0	4.4724E+03
-11.200	1.980	6.280	1.520	6.1533E+03	11.0	16.0	4.8540E+03
-11.200	1.980	6.280	1.520	6.4421E+03	11.0	17.0	5.2391E+03
-11.200	1.980	6.280	1.520	6.7200E+03	11.0	18.0	5.6234E+03
-11.200	1.980	6.280	1.520	6.9953E+03	11.0	19.0	6.0071E+03
-11.200	1.980	6.280	1.520	7.3688E+03	11.0	20.0	6.3904E+03
-11.200	1.980	6.280	1.520	7.7213E+03	11.0	21.0	6.7741E+03
-11.200	1.980	6.280	1.520	8.0514E+03	11.0	22.0	7.2348E+03
-11.200	1.980	6.280	1.520	8.4104E+03	11.0	23.0	7.5724E+03
-11.200	1.980	6.280	1.520	8.6368E+03	11.0	24.0	7.9643E+03
-11.200	1.980	6.280	1.520	8.9436E+03	11.0	25.0	8.3771E+03
-11.200	1.980	6.280	1.520	9.2785E+03	11.0	26.0	8.7754E+03
-11.200	1.980	6.280	1.520	9.5045E+03	11.0	27.0	9.1031E+03
-11.200	1.980	6.280	1.520	9.9026E+03	11.0	28.0	9.4385E+03
-11.200	1.980	6.280	1.520	1.0210E+04	11.0	29.0	9.8359E+03
-11.200	1.980	6.280	1.520	1.0438E+04	11.0	30.0	1.0258E+04
-11.200	1.980	6.280	1.520	1.0843E+04	11.0	31.0	1.0591E+04
-11.200	1.980	6.280	1.520	1.1162E+04	11.0	32.0	1.1029E+04

s_u (kPa)	k_s (kPa/m)	$s_{u,r}$ (kPa)	$k_{u,r}$ (kPa/m)	F_{dp} (kN)	θ_c (deg)	z (m)	R_{conc} (kN)
-11.200	1.980	6.280	1.520	1.1410E+04	11.0	33.0	1.1435E+04
-11.200	1.980	6.280	1.520	1.1731E+04	11.0	34.0	1.1766E+04
-11.200	1.980	6.280	1.520	1.2019E+04	11.0	35.0	1.2095E+04
-11.200	1.980	6.280	1.520	1.2440E+04	11.0	36.0	1.2543E+04
-11.200	1.980	6.280	1.520	1.2732E+04	11.0	37.0	1.2870E+04
-11.200	1.980	6.280	1.520	1.2989E+04	11.0	38.0	1.3323E+04
-11.200	1.980	6.280	1.520	1.3283E+04	11.0	39.0	1.3652E+04
-11.200	1.980	6.280	1.520	1.3542E+04	11.0	40.0	1.4110E+04
-12.100	1.960	7.460	1.540	6.1588E+03	12.0	15.0	4.2365E+03
-12.100	1.960	7.460	1.540	6.4011E+03	12.0	16.0	4.6177E+03
-12.100	1.960	7.460	1.540	6.6989E+03	12.0	17.0	5.0027E+03
-12.100	1.960	7.460	1.540	6.9989E+03	12.0	18.0	5.3871E+03
-12.100	1.960	7.460	1.540	7.2630E+03	12.0	19.0	5.7712E+03
-12.100	1.960	7.460	1.540	7.5960E+03	12.0	20.0	6.1591E+03
-12.100	1.960	7.460	1.540	7.8984E+03	12.0	21.0	6.5665E+03
-12.100	1.960	7.460	1.540	8.2566E+03	12.0	22.0	6.9534E+03
-12.100	1.960	7.460	1.540	8.4775E+03	12.0	23.0	7.2947E+03
-12.100	1.960	7.460	1.540	8.8162E+03	12.0	24.0	7.6831E+03
-12.100	1.960	7.460	1.540	9.1501E+03	12.0	25.0	8.1014E+03
-12.100	1.960	7.460	1.540	9.4868E+03	12.0	26.0	8.4146E+03
-12.100	1.960	7.460	1.540	9.8286E+03	12.0	27.0	8.8326E+03
-12.100	1.960	7.460	1.540	1.0229E+04	12.0	28.0	9.1661E+03
-12.100	1.960	7.460	1.540	1.0545E+04	12.0	29.0	9.6620E+03
-12.100	1.960	7.460	1.540	1.0767E+04	12.0	30.0	9.9980E+03
-12.100	1.960	7.460	1.540	1.1052E+04	12.0	31.0	1.0333E+04
-12.100	1.960	7.460	1.540	1.1338E+04	12.0	32.0	1.0656E+04
-12.100	1.960	7.460	1.540	1.1657E+04	12.0	33.0	1.1096E+04
-12.100	1.960	7.460	1.540	1.1945E+04	12.0	34.0	1.1428E+04
-12.100	1.960	7.460	1.540	1.2233E+04	12.0	35.0	1.1874E+04
-12.100	1.960	7.460	1.540	1.2523E+04	12.0	36.0	1.2206E+04
-12.100	1.960	7.460	1.540	1.2986E+04	12.0	37.0	1.2547E+04
-12.100	1.960	7.460	1.540	1.3243E+04	12.0	38.0	1.2988E+04
-12.100	1.960	7.460	1.540	1.3531E+04	12.0	39.0	1.3331E+04
-12.100	1.960	7.460	1.540	1.3833E+04	12.0	40.0	1.3791E+04
-13.000	1.940	8.640	1.560	7.0735E+03	13.0	17.0	4.7576E+03
-13.000	1.940	8.640	1.560	7.2603E+03	13.0	18.0	5.1409E+03
-13.000	1.940	8.640	1.560	7.5318E+03	13.0	19.0	5.5243E+03
-13.000	1.940	8.640	1.560	7.9230E+03	13.0	20.0	5.9117E+03
-13.000	1.940	8.640	1.560	8.1879E+03	13.0	21.0	6.3182E+03
-13.000	1.940	8.640	1.560	8.4395E+03	13.0	22.0	6.6417E+03
-13.000	1.940	8.640	1.560	8.7723E+03	13.0	23.0	7.0508E+03
-13.000	1.940	8.640	1.560	9.0207E+03	13.0	24.0	7.3902E+03
-13.000	1.940	8.640	1.560	9.3621E+03	13.0	25.0	7.7784E+03
-13.000	1.940	8.640	1.560	9.7022E+03	13.0	26.0	8.2006E+03
-13.000	1.940	8.640	1.560	1.0014E+04	13.0	27.0	8.5368E+03
-13.000	1.940	8.640	1.560	1.0329E+04	13.0	28.0	8.8741E+03
-13.000	1.940	8.640	1.560	1.0644E+04	13.0	29.0	9.2723E+03
-13.000	1.940	8.640	1.560	1.0994E+04	13.0	30.0	9.6981E+03
-13.000	1.940	8.640	1.560	1.1281E+04	13.0	31.0	1.0034E+04
-13.000	1.940	8.640	1.560	1.1601E+04	13.0	32.0	1.0368E+04
-13.000	1.940	8.640	1.560	1.2054E+04	13.0	33.0	1.0805E+04
-13.000	1.940	8.640	1.560	1.2314E+04	13.0	34.0	1.1139E+04
-13.000	1.940	8.640	1.560	1.2475E+04	13.0	35.0	1.1482E+04
-13.000	1.940	8.640	1.560	1.2790E+04	13.0	36.0	1.1930E+04
-13.000	1.940	8.640	1.560	1.3089E+04	13.0	37.0	1.2385E+04
-13.000	1.940	8.640	1.560	1.3383E+04	13.0	38.0	1.2635E+04
-13.000	1.940	8.640	1.560	1.3822E+04	13.0	39.0	1.2965E+04
-13.000	1.940	8.640	1.560	1.4084E+04	13.0	40.0	1.3425E+04
-13.900	1.920	9.820	1.580	8.2373E+03	14.0	20.0	5.6480E+03
-13.900	1.920	9.820	1.580	8.5071E+03	14.0	21.0	6.0972E+03
-13.900	1.920	9.820	1.580	8.7553E+03	14.0	22.0	6.3764E+03
-13.900	1.920	9.820	1.580	9.1155E+03	14.0	23.0	6.7877E+03
-13.900	1.920	9.820	1.580	9.3373E+03	14.0	24.0	7.1777E+03
-13.900	1.920	9.820	1.580	9.7074E+03	14.0	25.0	7.5150E+03
-13.900	1.920	9.820	1.580	9.9182E+03	14.0	26.0	7.9365E+03
-13.900	1.920	9.820	1.580	1.0232E+04	14.0	27.0	8.2769E+03
-13.900	1.920	9.820	1.580	1.0577E+04	14.0	28.0	8.6153E+03
-13.900	1.920	9.820	1.580	1.0894E+04	14.0	29.0	8.9480E+03
-13.900	1.920	9.820	1.580	1.1212E+04	14.0	30.0	9.3778E+03
-13.900	1.920	9.820	1.580	1.1531E+04	14.0	31.0	9.7136E+03
-13.900	1.920	9.820	1.580	1.1852E+04	14.0	32.0	1.0151E+04
-13.900	1.920	9.820	1.580	1.2168E+04	14.0	33.0	1.0486E+04
-13.900	1.920	9.820	1.580	1.2428E+04	14.0	34.0	1.0820E+04
-13.900	1.920	9.820	1.580	1.2755E+04	14.0	35.0	1.1266E+04
-13.900	1.920	9.820	1.580	1.3082E+04	14.0	36.0	1.1600E+04
-13.900	1.920	9.820	1.580	1.3336E+04	14.0	37.0	1.1944E+04
-13.900	1.920	9.820	1.580	1.3782E+04	14.0	38.0	1.2318E+04
-13.900	1.920	9.820	1.580	1.4074E+04	14.0	39.0	1.2649E+04
-13.900	1.920	9.820	1.580	1.4376E+04	14.0	40.0	1.2993E+04
-14.800	1.900	11.000	1.600	9.2469E+03	15.0	22.0	6.1708E+03
-14.800	1.900	11.000	1.600	9.4850E+03	15.0	23.0	6.4953E+03
-14.800	1.900	11.000	1.600	9.6925E+03	15.0	24.0	6.9000E+03
-14.800	1.900	11.000	1.600	9.9320E+03	15.0	25.0	7.2415E+03
-14.800	1.900	11.000	1.600	1.0276E+04	15.0	26.0	7.6610E+03
-14.800	1.900	11.000	1.600	1.0623E+04	15.0	27.0	8.0016E+03
-14.800	1.900	11.000	1.600	1.0803E+04	15.0	28.0	8.3402E+03
-14.800	1.900	11.000	1.600	1.1148E+04	15.0	29.0	8.6766E+03
-14.800	1.900	11.000	1.600	1.1433E+04	15.0	30.0	9.1058E+03
-14.800	1.900	11.000	1.600	1.1788E+04	15.0	31.0	9.4422E+03
-14.800	1.900	11.000	1.600	1.2109E+04	15.0	32.0	9.7775E+03
-14.800	1.900	11.000	1.600	1.2398E+04	15.0	33.0	1.0216E+04
-14.800	1.900	11.000	1.600	1.2725E+04	15.0	34.0	1.0551E+04
-14.800	1.900	11.000	1.600	1.3046E+04	15.0	35.0	1.0892E+04
-14.800	1.900	11.000	1.600	1.3376E+04	15.0	36.0	1.1263E+04

s_u (kPa)	k_u (kPa/m)	$s_{u,r}$ (kPa)	$k_{u,r}$ (kPa/m)	F_{dp} (kN)	θ_i (deg)	z (m)	R_{comp} (kN)
-14.800	1.900	11.000	1.600	1.3630E+04	15.0	37.0	1.1595E+04
-14.800	1.900	11.000	1.600	1.3925E+04	15.0	38.0	1.2048E+04
-14.800	1.900	11.000	1.600	1.4363E+04	15.0	39.0	1.2393E+04
-14.800	1.900	11.000	1.600	1.4668E+04	15.0	40.0	1.2770E+04
-3.550	2.200	-6.700	1.300	5.6436E+02	0.0	3.0	1.0534E+03
-3.550	2.200	-6.700	1.300	8.3187E+02	0.0	4.0	1.6652E+03
-3.550	2.200	-6.700	1.300	1.1883E+03	0.0	5.0	2.1703E+03
-3.550	2.200	-6.700	1.300	1.5191E+03	0.0	6.0	2.6392E+03
-3.550	2.200	-6.700	1.300	1.8125E+03	0.0	7.0	3.1064E+03
-3.550	2.200	-6.700	1.300	2.0968E+03	0.0	8.0	3.5607E+03
-3.550	2.200	-6.700	1.300	2.4114E+03	0.0	9.0	4.0255E+03
-3.550	2.200	-6.700	1.300	2.7141E+03	0.0	10.0	4.4382E+03
-3.550	2.200	-6.700	1.300	3.0000E+03	0.0	11.0	4.8987E+03
-3.550	2.200	-6.700	1.300	3.2747E+03	0.0	12.0	5.3503E+03
-3.550	2.200	-6.700	1.300	3.5637E+03	0.0	13.0	5.7827E+03
-3.550	2.200	-6.700	1.300	3.8572E+03	0.0	14.0	6.2261E+03
-3.550	2.200	-6.700	1.300	4.1230E+03	0.0	15.0	6.6666E+03
-3.550	2.200	-6.700	1.300	4.4059E+03	0.0	16.0	7.0919E+03
-3.550	2.200	-6.700	1.300	4.6926E+03	0.0	17.0	7.5210E+03
-3.550	2.200	-6.700	1.300	5.0026E+03	0.0	18.0	7.9541E+03
-3.550	2.200	-6.700	1.300	5.2578E+03	0.0	19.0	8.3636E+03
-3.550	2.200	-6.700	1.300	5.5773E+03	0.0	20.0	8.7761E+03
-3.550	2.200	-6.700	1.300	5.8573E+03	0.0	21.0	9.2706E+03
-5.800	2.200	-6.700	1.300	5.8028E+02	0.0	4.0	1.0352E+03
-5.800	2.200	-6.700	1.300	9.0574E+02	0.0	5.0	1.6511E+03
-5.800	2.200	-6.700	1.300	1.3309E+03	0.0	6.0	2.1606E+03
-5.800	2.200	-6.700	1.300	1.6473E+03	0.0	7.0	2.6294E+03
-5.800	2.200	-6.700	1.300	1.9397E+03	0.0	8.0	3.0983E+03
-5.800	2.200	-6.700	1.300	2.2357E+03	0.0	9.0	3.5373E+03
-5.800	2.200	-6.700	1.300	2.5251E+03	0.0	10.0	4.0028E+03
-5.800	2.200	-6.700	1.300	2.8274E+03	0.0	11.0	4.4369E+03
-5.800	2.200	-6.700	1.300	3.1137E+03	0.0	12.0	4.8808E+03
-5.800	2.200	-6.700	1.300	3.4017E+03	0.0	13.0	5.3328E+03
-5.800	2.200	-6.700	1.300	3.7092E+03	0.0	14.0	5.7914E+03
-5.800	2.200	-6.700	1.300	3.9924E+03	0.0	15.0	6.2085E+03
-5.800	2.200	-6.700	1.300	4.2963E+03	0.0	16.0	6.6592E+03
-5.800	2.200	-6.700	1.300	4.5872E+03	0.0	17.0	7.0822E+03
-5.800	2.200	-6.700	1.300	4.8654E+03	0.0	18.0	7.5133E+03
-5.800	2.200	-6.700	1.300	5.1638E+03	0.0	19.0	7.9216E+03
-5.800	2.200	-6.700	1.300	5.4275E+03	0.0	20.0	8.3603E+03
-5.800	2.200	-6.700	1.300	5.7141E+03	0.0	21.0	8.7750E+03
-5.800	2.200	-6.700	1.300	6.0037E+03	0.0	22.0	9.2730E+03
-5.800	2.200	-6.700	1.300	6.2757E+03	0.0	23.0	9.6666E+03
-8.050	2.200	-6.700	1.300	5.7011E+02	0.0	5.0	1.0234E+03
-8.050	2.200	-6.700	1.300	1.0334E+03	0.0	6.0	1.6133E+03
-8.050	2.200	-6.700	1.300	1.4476E+03	0.0	7.0	2.1481E+03
-8.050	2.200	-6.700	1.300	1.7551E+03	0.0	8.0	2.6293E+03
-8.050	2.200	-6.700	1.300	2.0617E+03	0.0	9.0	3.0832E+03
-8.050	2.200	-6.700	1.300	2.3713E+03	0.0	10.0	3.5380E+03
-8.050	2.200	-6.700	1.300	2.6615E+03	0.0	11.0	4.0033E+03
-8.050	2.200	-6.700	1.300	2.9646E+03	0.0	12.0	4.4169E+03
-8.050	2.200	-6.700	1.300	3.2512E+03	0.0	13.0	4.8782E+03
-8.050	2.200	-6.700	1.300	3.5537E+03	0.0	14.0	5.3308E+03
-8.050	2.200	-6.700	1.300	3.8616E+03	0.0	15.0	5.7642E+03
-8.050	2.200	-6.700	1.300	4.1343E+03	0.0	16.0	6.2007E+03
-8.050	2.200	-6.700	1.300	4.4214E+03	0.0	17.0	6.6505E+03
-8.050	2.200	-6.700	1.300	4.7137E+03	0.0	18.0	7.0770E+03
-8.050	2.200	-6.700	1.300	4.9933E+03	0.0	19.0	7.5074E+03
-8.050	2.200	-6.700	1.300	5.2938E+03	0.0	20.0	7.9150E+03
-8.050	2.200	-6.700	1.300	5.5806E+03	0.0	21.0	8.3529E+03
-8.050	2.200	-6.700	1.300	5.8697E+03	0.0	22.0	8.7382E+03
-8.050	2.200	-6.700	1.300	6.1634E+03	0.0	23.0	9.2636E+03
-8.050	2.200	-6.700	1.300	6.4404E+03	0.0	24.0	9.6889E+03
-8.050	2.200	-6.700	1.300	6.7201E+03	0.0	25.0	1.0082E+04
-10.300	2.200	-6.700	1.300	5.4479E+02	0.0	6.0	8.8698E+02
-10.300	2.200	-6.700	1.300	1.1295E+03	0.0	7.0	1.5985E+03
-10.300	2.200	-6.700	1.300	1.5379E+03	0.0	8.0	2.1356E+03
-10.300	2.200	-6.700	1.300	1.8537E+03	0.0	9.0	2.6139E+03
-10.300	2.200	-6.700	1.300	2.1706E+03	0.0	10.0	3.0810E+03
-10.300	2.200	-6.700	1.300	2.4837E+03	0.0	11.0	3.5187E+03
-10.300	2.200	-6.700	1.300	2.7921E+03	0.0	12.0	3.9825E+03
-10.300	2.200	-6.700	1.300	3.1051E+03	0.0	13.0	4.4149E+03
-10.300	2.200	-6.700	1.300	3.3984E+03	0.0	14.0	4.8568E+03
-10.300	2.200	-6.700	1.300	3.6979E+03	0.0	15.0	5.3086E+03
-10.300	2.200	-6.700	1.300	3.9869E+03	0.0	16.0	5.7627E+03
-10.300	2.200	-6.700	1.300	4.2943E+03	0.0	17.0	6.2048E+03
-10.300	2.200	-6.700	1.300	4.5909E+03	0.0	18.0	6.6218E+03
-10.300	2.200	-6.700	1.300	4.8739E+03	0.0	19.0	7.0467E+03
-10.300	2.200	-6.700	1.300	5.1788E+03	0.0	20.0	7.4754E+03
-10.300	2.200	-6.700	1.300	5.4700E+03	0.0	21.0	7.9081E+03
-10.300	2.200	-6.700	1.300	5.7238E+03	0.0	22.0	8.3174E+03
-10.300	2.200	-6.700	1.300	6.0205E+03	0.0	23.0	8.7296E+03
-10.300	2.200	-6.700	1.300	6.2997E+03	0.0	24.0	9.2537E+03
-10.300	2.200	-6.700	1.300	6.5825E+03	0.0	25.0	9.6783E+03
-10.300	2.200	-6.700	1.300	6.8680E+03	0.0	26.0	1.0071E+04
-10.300	2.200	-6.700	1.300	7.2044E+03	0.0	27.0	1.0429E+04
-10.300	2.200	-6.700	1.300	7.4971E+03	0.0	28.0	1.0858E+04
-12.550	2.200	-6.700	1.300	7.3008E+02	0.0	7.0	9.7659E+02
-12.550	2.200	-6.700	1.300	1.2885E+03	0.0	8.0	1.6096E+03
-12.550	2.200	-6.700	1.300	1.6477E+03	0.0	9.0	2.1231E+03
-12.550	2.200	-6.700	1.300	1.9794E+03	0.0	10.0	2.6016E+03
-12.550	2.200	-6.700	1.300	2.3014E+03	0.0	11.0	3.0628E+03
-12.550	2.200	-6.700	1.300	2.6163E+03	0.0	12.0	3.5020E+03
-12.550	2.200	-6.700	1.300	2.9216E+03	0.0	13.0	3.9826E+03

s_u (kPa)	k_u (kPa/m)	$s_{u,r}$ (kPa)	$k_{u,r}$ (kPa/m)	F_{ap} (kN)	θ_i (deg)	z (m)	$R_{res,r}$ (kN)
-12.550	2.200	-6.700	1.300	3.2291E+03	0.0	14.0	4.3945E+03
-12.550	2.200	-6.700	1.300	3.5246E+03	0.0	15.0	4.8535E+03
-12.550	2.200	-6.700	1.300	3.8226E+03	0.0	16.0	5.3037E+03
-12.550	2.200	-6.700	1.300	4.1435E+03	0.0	17.0	5.7587E+03
-12.550	2.200	-6.700	1.300	4.4480E+03	0.0	18.0	6.1694E+03
-12.550	2.200	-6.700	1.300	4.7171E+03	0.0	19.0	6.6166E+03
-12.550	2.200	-6.700	1.300	5.0285E+03	0.0	20.0	7.0407E+03
-12.550	2.200	-6.700	1.300	5.3275E+03	0.0	21.0	7.4686E+03
-12.550	2.200	-6.700	1.300	5.6262E+03	0.0	22.0	7.8961E+03
-12.550	2.200	-6.700	1.300	5.8801E+03	0.0	23.0	8.3090E+03
-12.550	2.200	-6.700	1.300	6.2096E+03	0.0	24.0	8.7204E+03
-12.550	2.200	-6.700	1.300	6.4938E+03	0.0	25.0	9.2431E+03
-12.550	2.200	-6.700	1.300	6.7800E+03	0.0	26.0	9.6669E+03
-12.550	2.200	-6.700	1.300	7.0109E+03	0.0	27.0	1.0059E+04
-12.550	2.200	-6.700	1.300	7.2994E+03	0.0	28.0	1.0545E+04
-12.550	2.200	-6.700	1.300	7.5905E+03	0.0	29.0	1.0941E+04
-14.800	2.200	-6.700	1.300	9.4952E+02	0.0	8.0	8.3881E+02
-14.800	2.200	-6.700	1.300	1.4364E+03	0.0	9.0	1.5812E+03
-14.800	2.200	-6.700	1.300	1.7909E+03	0.0	10.0	2.1119E+03
-14.800	2.200	-6.700	1.300	2.1284E+03	0.0	11.0	2.5903E+03
-14.800	2.200	-6.700	1.300	2.4597E+03	0.0	12.0	3.0576E+03
-14.800	2.200	-6.700	1.300	2.7590E+03	0.0	13.0	3.4959E+03
-14.800	2.200	-6.700	1.300	3.0813E+03	0.0	14.0	3.9601E+03
-14.800	2.200	-6.700	1.300	3.3941E+03	0.0	15.0	4.3906E+03
-14.800	2.200	-6.700	1.300	3.6783E+03	0.0	16.0	4.8358E+03
-14.800	2.200	-6.700	1.300	3.9791E+03	0.0	17.0	5.2868E+03
-14.800	2.200	-6.700	1.300	4.2827E+03	0.0	18.0	5.7441E+03
-14.800	2.200	-6.700	1.300	4.5946E+03	0.0	19.0	6.1828E+03
-14.800	2.200	-6.700	1.300	4.8857E+03	0.0	20.0	6.6053E+03
-14.800	2.200	-6.700	1.300	5.1788E+03	0.0	21.0	7.0315E+03
-14.800	2.200	-6.700	1.300	5.4822E+03	0.0	22.0	7.4614E+03
-14.800	2.200	-6.700	1.300	5.7843E+03	0.0	23.0	7.8955E+03
-14.800	2.200	-6.700	1.300	6.0373E+03	0.0	24.0	8.3062E+03
-14.800	2.200	-6.700	1.300	6.3733E+03	0.0	25.0	8.7198E+03
-14.800	2.200	-6.700	1.300	6.6599E+03	0.0	26.0	9.1365E+03
-14.800	2.200	-6.700	1.300	6.9489E+03	0.0	27.0	9.6410E+03
-14.800	2.200	-6.700	1.300	7.1808E+03	0.0	28.0	1.0037E+04
-14.800	2.200	-6.700	1.300	7.4724E+03	0.0	29.0	1.0520E+04
-14.800	2.200	-6.700	1.300	7.8274E+03	0.0	30.0	1.0919E+04
-14.800	2.200	-6.700	1.300	8.0348E+03	0.0	31.0	1.1358E+04
-1.300	2.150	-6.700	1.300	4.6774E+02	0.0	2.0	1.0017E+03
-1.300	2.150	-6.700	1.300	7.3059E+02	0.0	3.0	1.6302E+03
-1.300	2.150	-6.700	1.300	1.0177E+03	0.0	4.0	2.1302E+03
-1.300	2.150	-6.700	1.300	1.3571E+03	0.0	5.0	2.5939E+03
-1.300	2.150	-6.700	1.300	1.6496E+03	0.0	6.0	3.0366E+03
-1.300	2.150	-6.700	1.300	1.9325E+03	0.0	7.0	3.4816E+03
-1.300	2.150	-6.700	1.300	2.2171E+03	0.0	8.0	3.9371E+03
-1.300	2.150	-6.700	1.300	2.5046E+03	0.0	9.0	4.3412E+03
-1.300	2.150	-6.700	1.300	2.8303E+03	0.0	10.0	4.7931E+03
-1.300	2.150	-6.700	1.300	3.0963E+03	0.0	11.0	5.2359E+03
-1.300	2.150	-6.700	1.300	3.3901E+03	0.0	12.0	5.6621E+03
-1.300	2.150	-6.700	1.300	3.6590E+03	0.0	13.0	6.0951E+03
-1.300	2.150	-6.700	1.300	3.9444E+03	0.0	14.0	6.5036E+03
-1.300	2.150	-6.700	1.300	4.2160E+03	0.0	15.0	6.9442E+03
-1.300	2.150	-6.700	1.300	4.5074E+03	0.0	16.0	7.3652E+03
-1.300	2.150	-6.700	1.300	4.7857E+03	0.0	17.0	7.7638E+03
-1.300	2.150	-6.700	1.300	5.0653E+03	0.0	18.0	8.1648E+03
-1.300	2.150	-6.700	1.300	5.3281E+03	0.0	19.0	8.5688E+03
-1.300	2.100	-6.700	1.300	4.5341E+02	0.0	2.0	9.7916E+02
-1.300	2.100	-6.700	1.300	7.0478E+02	0.0	3.0	1.5700E+03
-1.300	2.100	-6.700	1.300	9.9257E+02	0.0	4.0	2.0755E+03
-1.300	2.100	-6.700	1.300	1.3303E+03	0.0	5.0	2.5193E+03
-1.300	2.100	-6.700	1.300	1.6205E+03	0.0	6.0	2.9636E+03
-1.300	2.100	-6.700	1.300	1.8992E+03	0.0	7.0	3.3828E+03
-1.300	2.100	-6.700	1.300	2.1794E+03	0.0	8.0	3.8244E+03
-1.300	2.100	-6.700	1.300	2.4625E+03	0.0	9.0	4.2388E+03
-1.300	2.100	-6.700	1.300	2.7825E+03	0.0	10.0	4.6647E+03
-1.300	2.100	-6.700	1.300	3.0691E+03	0.0	11.0	5.0971E+03
-1.300	2.100	-6.700	1.300	3.3334E+03	0.0	12.0	5.5334E+03
-1.300	2.100	-6.700	1.300	3.5980E+03	0.0	13.0	5.9349E+03
-1.300	2.100	-6.700	1.300	3.8786E+03	0.0	14.0	6.3568E+03
-1.300	2.100	-6.700	1.300	4.1631E+03	0.0	15.0	6.7641E+03
-1.300	2.100	-6.700	1.300	4.4323E+03	0.0	16.0	7.1751E+03
-1.300	2.100	-6.700	1.300	4.7051E+03	0.0	17.0	7.5643E+03
-1.300	2.100	-6.700	1.300	5.0208E+03	0.0	18.0	7.9824E+03
-1.300	2.100	-6.700	1.300	5.3022E+03	0.0	19.0	8.3776E+03
-1.300	2.100	-6.700	1.300	5.5626E+03	0.0	20.0	8.7758E+03
-1.300	2.050	-6.700	1.300	4.3069E+02	0.0	2.0	9.4635E+02
-1.300	2.050	-6.700	1.300	6.8558E+02	0.0	3.0	1.5263E+03
-1.300	2.050	-6.700	1.300	9.5810E+02	0.0	4.0	2.0065E+03
-1.300	2.050	-6.700	1.300	1.3029E+03	0.0	5.0	2.4532E+03
-1.300	2.050	-6.700	1.300	1.5918E+03	0.0	6.0	2.8772E+03
-1.300	2.050	-6.700	1.300	1.8680E+03	0.0	7.0	3.3039E+03
-1.300	2.050	-6.700	1.300	2.1508E+03	0.0	8.0	3.7229E+03
-1.300	2.050	-6.700	1.300	2.4635E+03	0.0	9.0	4.1265E+03
-1.300	2.050	-6.700	1.300	2.7332E+03	0.0	10.0	4.5443E+03
-1.300	2.050	-6.700	1.300	3.0046E+03	0.0	11.0	4.9686E+03
-1.300	2.050	-6.700	1.300	3.2894E+03	0.0	12.0	5.3769E+03
-1.300	2.050	-6.700	1.300	3.5638E+03	0.0	13.0	5.7914E+03
-1.300	2.050	-6.700	1.300	3.8413E+03	0.0	14.0	6.1832E+03
-1.300	2.050	-6.700	1.300	4.1229E+03	0.0	15.0	6.6059E+03
-1.300	2.050	-6.700	1.300	4.3904E+03	0.0	16.0	6.9855E+03
-1.300	2.050	-6.700	1.300	4.6768E+03	0.0	17.0	7.3924E+03
-1.300	2.050	-6.700	1.300	4.9515E+03	0.0	18.0	7.7774E+03

z_u (kPa)	k_u (kPa/m)	$z_{u'}$ (kPa)	$k_{u'}$ (kPa/m)	F_{dp} (kN)	θ_i (deg)	z (m)	R_{cone} (kN)
-1.300	2.050	-6.700	1.300	5.2081E+03	0.0	19.0	8.1654E+03
-1.300	2.050	-6.700	1.300	5.4848E+03	0.0	20.0	8.5562E+03
-1.300	2.000	-6.700	1.300	4.0873E+02	0.0	2.0	9.0591E+02
-1.300	2.000	-6.700	1.300	6.5772E+02	0.0	3.0	1.4783E+03
-1.300	2.000	-6.700	1.300	9.3230E+02	0.0	4.0	1.9486E+03
-1.300	2.000	-6.700	1.300	1.2656E+03	0.0	5.0	2.3841E+03
-1.300	2.000	-6.700	1.300	1.5608E+03	0.0	6.0	2.7976E+03
-1.300	2.000	-6.700	1.300	1.8355E+03	0.0	7.0	3.2135E+03
-1.300	2.000	-6.700	1.300	2.1159E+03	0.0	8.0	3.6218E+03
-1.300	2.000	-6.700	1.300	2.4176E+03	0.0	9.0	4.0177E+03
-1.300	2.000	-6.700	1.300	2.6828E+03	0.0	10.0	4.4224E+03
-1.300	2.000	-6.700	1.300	2.9730E+03	0.0	11.0	4.8345E+03
-1.300	2.000	-6.700	1.300	3.2291E+03	0.0	12.0	5.2528E+03
-1.300	2.000	-6.700	1.300	3.4985E+03	0.0	13.0	5.6294E+03
-1.300	2.000	-6.700	1.300	3.8017E+03	0.0	14.0	6.0444E+03
-1.300	2.000	-6.700	1.300	4.0798E+03	0.0	15.0	6.4304E+03
-1.300	2.000	-6.700	1.300	4.3601E+03	0.0	16.0	6.8238E+03
-1.300	2.000	-6.700	1.300	4.6295E+03	0.0	17.0	7.1965E+03
-1.300	2.000	-6.700	1.300	4.8961E+03	0.0	18.0	7.5716E+03
-1.300	2.000	-6.700	1.300	5.1712E+03	0.0	19.0	7.9494E+03
-1.300	2.000	-6.700	1.300	5.4464E+03	0.0	20.0	8.3284E+03
-1.300	2.000	-6.700	1.300	5.7021E+03	0.0	21.0	8.7593E+03
-1.300	1.950	-6.700	1.300	4.2137E+02	0.0	2.0	8.6769E+02
-1.300	1.950	-6.700	1.300	6.3736E+02	0.0	3.0	1.4271E+03
-1.300	1.950	-6.700	1.300	8.9642E+02	0.0	4.0	1.8963E+03
-1.300	1.950	-6.700	1.300	1.2360E+03	0.0	5.0	2.3106E+03
-1.300	1.950	-6.700	1.300	1.5297E+03	0.0	6.0	2.7137E+03
-1.300	1.950	-6.700	1.300	1.7994E+03	0.0	7.0	3.1228E+03
-1.300	1.950	-6.700	1.300	2.0996E+03	0.0	8.0	3.5221E+03
-1.300	1.950	-6.700	1.300	2.3703E+03	0.0	9.0	3.9071E+03
-1.300	1.950	-6.700	1.300	2.6429E+03	0.0	10.0	4.3060E+03
-1.300	1.950	-6.700	1.300	2.9153E+03	0.0	11.0	4.7097E+03
-1.300	1.950	-6.700	1.300	3.1921E+03	0.0	12.0	5.0993E+03
-1.300	1.950	-6.700	1.300	3.4734E+03	0.0	13.0	5.4915E+03
-1.300	1.950	-6.700	1.300	3.7436E+03	0.0	14.0	5.8731E+03
-1.300	1.950	-6.700	1.300	4.0169E+03	0.0	15.0	6.2504E+03
-1.300	1.950	-6.700	1.300	4.2922E+03	0.0	16.0	6.6351E+03
-1.300	1.950	-6.700	1.300	4.5581E+03	0.0	17.0	6.9997E+03
-1.300	1.950	-6.700	1.300	4.8227E+03	0.0	18.0	7.3666E+03
-1.300	1.950	-6.700	1.300	5.0890E+03	0.0	19.0	7.8318E+03
-1.300	1.950	-6.700	1.300	5.4012E+03	0.0	20.0	8.2074E+03
-1.300	1.950	-6.700	1.300	5.6538E+03	0.0	21.0	8.5279E+03
-1.300	1.950	-6.700	1.300	5.9089E+03	0.0	22.0	8.9070E+03
-1.300	1.900	-6.700	1.300	4.0460E+02	0.0	2.0	8.3365E+02
-1.300	1.900	-6.700	1.300	6.0871E+02	0.0	3.0	1.3831E+03
-1.300	1.900	-6.700	1.300	8.7088E+02	0.0	4.0	1.8342E+03
-1.300	1.900	-6.700	1.300	1.2080E+03	0.0	5.0	2.2377E+03
-1.300	1.900	-6.700	1.300	1.5008E+03	0.0	6.0	2.6449E+03
-1.300	1.900	-6.700	1.300	1.7693E+03	0.0	7.0	3.0307E+03
-1.300	1.900	-6.700	1.300	2.0627E+03	0.0	8.0	3.4207E+03
-1.300	1.900	-6.700	1.300	2.3302E+03	0.0	9.0	3.8012E+03
-1.300	1.900	-6.700	1.300	2.6081E+03	0.0	10.0	4.1868E+03
-1.300	1.900	-6.700	1.300	2.8683E+03	0.0	11.0	4.5795E+03
-1.300	1.900	-6.700	1.300	3.1415E+03	0.0	12.0	4.9628E+03
-1.300	1.900	-6.700	1.300	3.4322E+03	0.0	13.0	5.3481E+03
-1.300	1.900	-6.700	1.300	3.6858E+03	0.0	14.0	5.7195E+03
-1.300	1.900	-6.700	1.300	3.9556E+03	0.0	15.0	6.0887E+03
-1.300	1.900	-6.700	1.300	4.2467E+03	0.0	16.0	6.4426E+03
-1.300	1.900	-6.700	1.300	4.5243E+03	0.0	17.0	6.8221E+03
-1.300	1.900	-6.700	1.300	4.7880E+03	0.0	18.0	7.1813E+03
-1.300	1.900	-6.700	1.300	5.0547E+03	0.0	19.0	7.5432E+03
-1.300	1.900	-6.700	1.300	5.3019E+03	0.0	20.0	7.9784E+03
-1.300	1.900	-6.700	1.300	5.5718E+03	0.0	21.0	8.2910E+03
-1.300	1.900	-6.700	1.300	5.8681E+03	0.0	22.0	8.6660E+03
-1.300	1.900	-6.700	1.300	6.1206E+03	0.0	23.0	9.0124E+03
-1.300	2.200	-3.750	1.300	4.6975E+02	0.0	2.0	1.0419E+03
-1.300	2.200	-3.750	1.300	8.7229E+02	0.0	3.0	1.6826E+03
-1.300	2.200	-3.750	1.300	1.3396E+03	0.0	4.0	2.1901E+03
-1.300	2.200	-3.750	1.300	1.6579E+03	0.0	5.0	2.6545E+03
-1.300	2.200	-3.750	1.300	1.9609E+03	0.0	6.0	3.1220E+03
-1.300	2.200	-3.750	1.300	2.2674E+03	0.0	7.0	3.5604E+03
-1.300	2.200	-3.750	1.300	2.5553E+03	0.0	8.0	4.0255E+03
-1.300	2.200	-3.750	1.300	2.8676E+03	0.0	9.0	4.4588E+03
-1.300	2.200	-3.750	1.300	3.1486E+03	0.0	10.0	4.9020E+03
-1.300	2.200	-3.750	1.300	3.4439E+03	0.0	11.0	5.3551E+03
-1.300	2.200	-3.750	1.300	3.7443E+03	0.0	12.0	5.8107E+03
-1.300	2.200	-3.750	1.300	4.0500E+03	0.0	13.0	6.2457E+03
-1.300	2.200	-3.750	1.300	4.3079E+03	0.0	14.0	6.6720E+03
-1.300	2.200	-3.750	1.300	4.6028E+03	0.0	15.0	7.0980E+03
-1.300	2.200	-3.750	1.300	4.9005E+03	0.0	16.0	7.5278E+03
-1.300	2.200	-3.750	1.300	5.1856E+03	0.0	17.0	7.9618E+03
-1.300	2.200	-3.750	1.300	5.4691E+03	0.0	18.0	8.3722E+03
-1.300	2.200	-3.750	1.300	5.7574E+03	0.0	19.0	8.7855E+03
-1.300	2.200	-3.750	1.300	6.0256E+03	0.0	20.0	9.1994E+03
-1.300	2.200	-3.750	1.300	6.3193E+03	0.0	21.0	9.6740E+03
-1.300	2.200	-0.800	1.300	7.5203E+02	0.0	2.0	1.0419E+03
-1.300	2.200	-0.800	1.300	1.2738E+03	0.0	3.0	1.6826E+03
-1.300	2.200	-0.800	1.300	1.6249E+03	0.0	4.0	2.1901E+03
-1.300	2.200	-0.800	1.300	1.9525E+03	0.0	5.0	2.6545E+03
-1.300	2.200	-0.800	1.300	2.2567E+03	0.0	6.0	3.1220E+03
-1.300	2.200	-0.800	1.300	2.5771E+03	0.0	7.0	3.5604E+03
-1.300	2.200	-0.800	1.300	2.8814E+03	0.0	8.0	4.0255E+03
-1.300	2.200	-0.800	1.300	3.1883E+03	0.0	9.0	4.4588E+03
-1.300	2.200	-0.800	1.300	3.4986E+03	0.0	10.0	4.9020E+03

s_u (kPa)	k_s (kPa/m)	$s_{u,r}$ (kPa)	$k_{s,r}$ (kPa/m)	F_{dp} (kN)	θ_i (deg)	z (m)	R_{case} (kN)
-1.300	2.200	-0.800	1.300	3.7806E+03	0.0	11.0	5.3551E+03
-1.300	2.200	-0.800	1.300	4.0990E+03	0.0	12.0	5.8107E+03
-1.300	2.200	-0.800	1.300	4.3668E+03	0.0	13.0	6.2457E+03
-1.300	2.200	-0.800	1.300	4.6736E+03	0.0	14.0	6.6720E+03
-1.300	2.200	-0.800	1.300	4.9675E+03	0.0	15.0	7.0980E+03
-1.300	2.200	-0.800	1.300	5.2645E+03	0.0	16.0	7.5278E+03
-1.300	2.200	-0.800	1.300	5.5622E+03	0.0	17.0	7.9618E+03
-1.300	2.200	-0.800	1.300	5.8648E+03	0.0	18.0	8.3722E+03
-1.300	2.200	-0.800	1.300	6.1448E+03	0.0	19.0	8.7855E+03
-1.300	2.200	-0.800	1.300	6.4287E+03	0.0	20.0	9.1994E+03
-1.300	2.200	-0.800	1.300	6.7129E+03	0.0	21.0	9.6740E+03
-1.300	2.200	-0.800	1.300	7.0009E+03	0.0	22.0	1.0101E+04
-1.300	2.200	-0.800	1.300	7.2910E+03	0.0	23.0	1.0531E+04
-1.300	2.200	-0.800	1.300	7.5571E+03	0.0	24.0	1.0891E+04
-1.300	2.200	2.150	1.300	1.6051E+03	0.0	3.0	1.6826E+03
-1.300	2.200	2.150	1.300	1.9602E+03	0.0	4.0	2.1901E+03
-1.300	2.200	2.150	1.300	2.2598E+03	0.0	5.0	2.6545E+03
-1.300	2.200	2.150	1.300	2.5818E+03	0.0	6.0	3.1220E+03
-1.300	2.200	2.150	1.300	2.9293E+03	0.0	7.0	3.5604E+03
-1.300	2.200	2.150	1.300	3.2435E+03	0.0	8.0	4.0255E+03
-1.300	2.200	2.150	1.300	3.5447E+03	0.0	9.0	4.4588E+03
-1.300	2.200	2.150	1.300	3.8828E+03	0.0	10.0	4.9020E+03
-1.300	2.200	2.150	1.300	4.1316E+03	0.0	11.0	5.3551E+03
-1.300	2.200	2.150	1.300	4.5021E+03	0.0	12.0	5.8107E+03
-1.300	2.200	2.150	1.300	4.7321E+03	0.0	13.0	6.2457E+03
-1.300	2.200	2.150	1.300	5.0480E+03	0.0	14.0	6.6720E+03
-1.300	2.200	2.150	1.300	5.3476E+03	0.0	15.0	7.0980E+03
-1.300	2.200	2.150	1.300	5.6226E+03	0.0	16.0	7.5278E+03
-1.300	2.200	2.150	1.300	5.9024E+03	0.0	17.0	7.9618E+03
-1.300	2.200	2.150	1.300	6.2085E+03	0.0	18.0	8.3722E+03
-1.300	2.200	2.150	1.300	6.4939E+03	0.0	19.0	8.7855E+03
-1.300	2.200	2.150	1.300	6.7810E+03	0.0	20.0	9.1994E+03
-1.300	2.200	2.150	1.300	7.0705E+03	0.0	21.0	9.6740E+03
-1.300	2.200	2.150	1.300	7.3882E+03	0.0	22.0	1.0101E+04
-1.300	2.200	2.150	1.300	7.6540E+03	0.0	23.0	1.0531E+04
-1.300	2.200	2.150	1.300	7.9502E+03	0.0	24.0	1.0891E+04
-1.300	2.200	2.150	1.300	8.2204E+03	0.0	25.0	1.1385E+04
-1.300	2.200	2.150	1.300	8.5207E+03	0.0	26.0	1.1793E+04
-1.300	2.200	5.100	1.300	2.3334E+03	0.0	4.0	2.1901E+03
-1.300	2.200	5.100	1.300	2.6483E+03	0.0	5.0	2.6545E+03
-1.300	2.200	5.100	1.300	2.9568E+03	0.0	6.0	3.1220E+03
-1.300	2.200	5.100	1.300	3.2703E+03	0.0	7.0	3.5604E+03
-1.300	2.200	5.100	1.300	3.5886E+03	0.0	8.0	4.0255E+03
-1.300	2.200	5.100	1.300	3.8916E+03	0.0	9.0	4.4588E+03
-1.300	2.200	5.100	1.300	4.2001E+03	0.0	10.0	4.9020E+03
-1.300	2.200	5.100	1.300	4.5336E+03	0.0	11.0	5.3551E+03
-1.300	2.200	5.100	1.300	4.8091E+03	0.0	12.0	5.8107E+03
-1.300	2.200	5.100	1.300	5.1016E+03	0.0	13.0	6.2457E+03
-1.300	2.200	5.100	1.300	5.4051E+03	0.0	14.0	6.6720E+03
-1.300	2.200	5.100	1.300	5.7314E+03	0.0	15.0	7.0980E+03
-1.300	2.200	5.100	1.300	6.0396E+03	0.0	16.0	7.5278E+03
-1.300	2.200	5.100	1.300	6.3253E+03	0.0	17.0	7.9618E+03
-1.300	2.200	5.100	1.300	6.5818E+03	0.0	18.0	8.3722E+03
-1.300	2.200	5.100	1.300	6.9564E+03	0.0	19.0	8.7855E+03
-1.300	2.200	5.100	1.300	7.1902E+03	0.0	20.0	9.1994E+03
-1.300	2.200	5.100	1.300	7.4853E+03	0.0	21.0	9.6740E+03
-1.300	2.200	5.100	1.300	7.7824E+03	0.0	22.0	1.0101E+04
-1.300	2.200	5.100	1.300	8.1480E+03	0.0	23.0	1.0531E+04
-1.300	2.200	5.100	1.300	8.4229E+03	0.0	24.0	1.0891E+04
-1.300	2.200	5.100	1.300	8.7282E+03	0.0	25.0	1.1385E+04
-1.300	2.200	5.100	1.300	9.0039E+03	0.0	26.0	1.1793E+04
-1.300	2.200	5.100	1.300	9.2830E+03	0.0	27.0	1.2160E+04
-1.300	2.200	5.100	1.300	9.5632E+03	0.0	28.0	1.2668E+04
-1.300	2.200	5.100	1.300	9.8476E+03	0.0	29.0	1.3082E+04
-1.300	2.200	8.050	1.300	3.0680E+03	0.0	5.0	2.6545E+03
-1.300	2.200	8.050	1.300	3.3627E+03	0.0	6.0	3.1220E+03
-1.300	2.200	8.050	1.300	3.6604E+03	0.0	7.0	3.5604E+03
-1.300	2.200	8.050	1.300	3.9849E+03	0.0	8.0	4.0255E+03
-1.300	2.200	8.050	1.300	4.2967E+03	0.0	9.0	4.4588E+03
-1.300	2.200	8.050	1.300	4.6072E+03	0.0	10.0	4.9020E+03
-1.300	2.200	8.050	1.300	4.9026E+03	0.0	11.0	5.3551E+03
-1.300	2.200	8.050	1.300	5.1978E+03	0.0	12.0	5.8107E+03
-1.300	2.200	8.050	1.300	5.5254E+03	0.0	13.0	6.2457E+03
-1.300	2.200	8.050	1.300	5.7790E+03	0.0	14.0	6.6720E+03
-1.300	2.200	8.050	1.300	6.1152E+03	0.0	15.0	7.0980E+03
-1.300	2.200	8.050	1.300	6.4259E+03	0.0	16.0	7.5278E+03
-1.300	2.200	8.050	1.300	6.7183E+03	0.0	17.0	7.9618E+03
-1.300	2.200	8.050	1.300	6.9759E+03	0.0	18.0	8.3722E+03
-1.300	2.200	8.050	1.300	7.2707E+03	0.0	19.0	8.7855E+03
-1.300	2.200	8.050	1.300	7.5942E+03	0.0	20.0	9.1994E+03
-1.300	2.200	8.050	1.300	7.8941E+03	0.0	21.0	9.6740E+03
-1.300	2.200	8.050	1.300	8.1961E+03	0.0	22.0	1.0101E+04
-1.300	2.200	8.050	1.300	8.4716E+03	0.0	23.0	1.0531E+04
-1.300	2.200	8.050	1.300	8.7774E+03	0.0	24.0	1.0891E+04
-1.300	2.200	8.050	1.300	8.9843E+03	0.0	25.0	1.1385E+04
-1.300	2.200	8.050	1.300	9.2607E+03	0.0	26.0	1.1793E+04
-1.300	2.200	8.050	1.300	9.5405E+03	0.0	27.0	1.2160E+04
-1.300	2.200	8.050	1.300	9.8971E+03	0.0	28.0	1.2668E+04
-1.300	2.200	8.050	1.300	1.0181E+04	0.0	29.0	1.3082E+04
-1.300	2.200	8.050	1.300	1.0470E+04	0.0	30.0	1.3422E+04
-1.300	2.200	11.000	1.300	3.6424E+03	0.0	5.0	2.6545E+03
-1.300	2.200	11.000	1.300	3.8342E+03	0.0	6.0	3.1220E+03
-1.300	2.200	11.000	1.300	4.1027E+03	0.0	7.0	3.5604E+03
-1.300	2.200	11.000	1.300	4.4339E+03	0.0	8.0	4.0255E+03

s_u (kPa)	k_s (kPa/m)	$s_{u,r}$ (kPa)	$k_{s,r}$ (kPa/m)	F_{dp} (kN)	θ_i (deg)	z (m)	R_{case} (kN)
-1.300	2.200	11.000	1.300	4.6932E+03	0.0	9.0	4.4588E+03
-1.300	2.200	11.000	1.300	5.0071E+03	0.0	10.0	4.9020E+03
-1.300	2.200	11.000	1.300	5.3017E+03	0.0	11.0	5.3551E+03
-1.300	2.200	11.000	1.300	5.6372E+03	0.0	12.0	5.8107E+03
-1.300	2.200	11.000	1.300	5.9703E+03	0.0	13.0	6.2457E+03
-1.300	2.200	11.000	1.300	6.2497E+03	0.0	14.0	6.6720E+03
-1.300	2.200	11.000	1.300	6.5061E+03	0.0	15.0	7.0980E+03
-1.300	2.200	11.000	1.300	6.8253E+03	0.0	16.0	7.5278E+03
-1.300	2.200	11.000	1.300	7.0826E+03	0.0	17.0	7.9618E+03
-1.300	2.200	11.000	1.300	7.3799E+03	0.0	18.0	8.3722E+03
-1.300	2.200	11.000	1.300	7.7057E+03	0.0	19.0	8.7855E+03
-1.300	2.200	11.000	1.300	7.9385E+03	0.0	20.0	9.1994E+03
-1.300	2.200	11.000	1.300	8.2409E+03	0.0	21.0	9.6740E+03
-1.300	2.200	11.000	1.300	8.5172E+03	0.0	22.0	1.0101E+04
-1.300	2.200	11.000	1.300	8.8234E+03	0.0	23.0	1.0531E+04
-1.300	2.200	11.000	1.300	9.1321E+03	0.0	24.0	1.0891E+04
-1.300	2.200	11.000	1.300	9.4125E+03	0.0	25.0	1.1385E+04
-1.300	2.200	11.000	1.300	9.7250E+03	0.0	26.0	1.1793E+04
-1.300	2.200	11.000	1.300	9.9759E+03	0.0	27.0	1.2160E+04
-1.300	2.200	11.000	1.300	1.0230E+04	0.0	28.0	1.2668E+04
-1.300	2.200	11.000	1.300	1.0544E+04	0.0	29.0	1.3082E+04
-1.300	2.200	11.000	1.300	1.0834E+04	0.0	30.0	1.3422E+04
-1.300	2.200	11.000	1.300	1.1090E+04	0.0	31.0	1.3945E+04
-1.300	2.200	-6.700	1.350	4.8713E+02	0.0	2.0	1.0419E+03
-1.300	2.200	-6.700	1.350	7.5950E+02	0.0	3.0	1.6826E+03
-1.300	2.200	-6.700	1.350	1.0706E+03	0.0	4.0	2.1901E+03
-1.300	2.200	-6.700	1.350	1.4239E+03	0.0	5.0	2.6545E+03
-1.300	2.200	-6.700	1.350	1.7215E+03	0.0	6.0	3.1220E+03
-1.300	2.200	-6.700	1.350	2.0152E+03	0.0	7.0	3.5604E+03
-1.300	2.200	-6.700	1.350	2.3149E+03	0.0	8.0	4.0255E+03
-1.300	2.200	-6.700	1.350	2.6476E+03	0.0	9.0	4.4588E+03
-1.300	2.200	-6.700	1.350	2.9328E+03	0.0	10.0	4.9020E+03
-1.300	2.200	-6.700	1.350	3.2199E+03	0.0	11.0	5.3551E+03
-1.300	2.200	-6.700	1.350	3.5062E+03	0.0	12.0	5.8107E+03
-1.300	2.200	-6.700	1.350	3.7815E+03	0.0	13.0	6.2457E+03
-1.300	2.200	-6.700	1.350	4.0736E+03	0.0	14.0	6.6720E+03
-1.300	2.200	-6.700	1.350	4.3697E+03	0.0	15.0	7.0980E+03
-1.300	2.200	-6.700	1.350	4.6497E+03	0.0	16.0	7.5278E+03
-1.300	2.200	-6.700	1.350	4.9539E+03	0.0	17.0	7.9618E+03
-1.300	2.200	-6.700	1.350	5.2625E+03	0.0	18.0	8.3722E+03
-1.300	2.200	-6.700	1.350	5.5549E+03	0.0	19.0	8.7855E+03
-1.300	2.200	-6.700	1.350	5.8481E+03	0.0	20.0	9.1994E+03
-1.300	2.200	-6.700	1.400	4.8159E+02	0.0	2.0	1.0419E+03
-1.300	2.200	-6.700	1.400	7.5911E+02	0.0	3.0	1.6826E+03
-1.300	2.200	-6.700	1.400	1.0880E+03	0.0	4.0	2.1901E+03
-1.300	2.200	-6.700	1.400	1.4632E+03	0.0	5.0	2.6545E+03
-1.300	2.200	-6.700	1.400	1.7667E+03	0.0	6.0	3.1220E+03
-1.300	2.200	-6.700	1.400	2.0654E+03	0.0	7.0	3.5604E+03
-1.300	2.200	-6.700	1.400	2.4015E+03	0.0	8.0	4.0255E+03
-1.300	2.200	-6.700	1.400	2.7009E+03	0.0	9.0	4.4588E+03
-1.300	2.200	-6.700	1.400	2.9889E+03	0.0	10.0	4.9020E+03
-1.300	2.200	-6.700	1.400	3.2785E+03	0.0	11.0	5.3551E+03
-1.300	2.200	-6.700	1.400	3.5828E+03	0.0	12.0	5.8107E+03
-1.300	2.200	-6.700	1.400	3.8757E+03	0.0	13.0	6.2457E+03
-1.300	2.200	-6.700	1.400	4.1894E+03	0.0	14.0	6.6720E+03
-1.300	2.200	-6.700	1.400	4.5085E+03	0.0	15.0	7.0980E+03
-1.300	2.200	-6.700	1.400	4.7785E+03	0.0	16.0	7.5278E+03
-1.300	2.200	-6.700	1.400	5.0639E+03	0.0	17.0	7.9618E+03
-1.300	2.200	-6.700	1.400	5.3990E+03	0.0	18.0	8.3722E+03
-1.300	2.200	-6.700	1.400	5.6945E+03	0.0	19.0	8.7855E+03
-1.300	2.200	-6.700	1.400	5.9934E+03	0.0	20.0	9.1994E+03
-1.300	2.200	-6.700	1.400	6.2713E+03	0.0	21.0	9.6740E+03
-1.300	2.200	-6.700	1.450	4.7966E+02	0.0	2.0	1.0419E+03
-1.300	2.200	-6.700	1.450	7.6704E+02	0.0	3.0	1.6826E+03
-1.300	2.200	-6.700	1.450	1.1078E+03	0.0	4.0	2.1901E+03
-1.300	2.200	-6.700	1.450	1.4937E+03	0.0	5.0	2.6545E+03
-1.300	2.200	-6.700	1.450	1.8117E+03	0.0	6.0	3.1220E+03
-1.300	2.200	-6.700	1.450	2.1162E+03	0.0	7.0	3.5604E+03
-1.300	2.200	-6.700	1.450	2.4519E+03	0.0	8.0	4.0255E+03
-1.300	2.200	-6.700	1.450	2.7458E+03	0.0	9.0	4.4588E+03
-1.300	2.200	-6.700	1.450	3.0450E+03	0.0	10.0	4.9020E+03
-1.300	2.200	-6.700	1.450	3.3635E+03	0.0	11.0	5.3551E+03
-1.300	2.200	-6.700	1.450	3.6730E+03	0.0	12.0	5.8107E+03
-1.300	2.200	-6.700	1.450	3.9875E+03	0.0	13.0	6.2457E+03
-1.300	2.200	-6.700	1.450	4.2893E+03	0.0	14.0	6.6720E+03
-1.300	2.200	-6.700	1.450	4.5946E+03	0.0	15.0	7.0980E+03
-1.300	2.200	-6.700	1.450	4.9041E+03	0.0	16.0	7.5278E+03
-1.300	2.200	-6.700	1.450	5.2367E+03	0.0	17.0	7.9618E+03
-1.300	2.200	-6.700	1.450	5.5386E+03	0.0	18.0	8.3722E+03
-1.300	2.200	-6.700	1.450	5.8363E+03	0.0	19.0	8.7855E+03
-1.300	2.200	-6.700	1.450	6.1385E+03	0.0	20.0	9.1994E+03
-1.300	2.200	-6.700	1.450	6.4443E+03	0.0	21.0	9.6740E+03
-1.300	2.200	-6.700	1.450	6.7291E+03	0.0	22.0	1.0101E+04
-1.300	2.200	-6.700	1.500	4.7634E+02	0.0	2.0	1.0419E+03
-1.300	2.200	-6.700	1.500	7.6669E+02	0.0	3.0	1.6826E+03
-1.300	2.200	-6.700	1.500	1.1286E+03	0.0	4.0	2.1901E+03
-1.300	2.200	-6.700	1.500	1.5338E+03	0.0	5.0	2.6545E+03
-1.300	2.200	-6.700	1.500	1.8485E+03	0.0	6.0	3.1220E+03
-1.300	2.200	-6.700	1.500	2.1869E+03	0.0	7.0	3.5604E+03
-1.300	2.200	-6.700	1.500	2.5023E+03	0.0	8.0	4.0255E+03
-1.300	2.200	-6.700	1.500	2.8976E+03	0.0	9.0	4.4588E+03
-1.300	2.200	-6.700	1.500	3.1256E+03	0.0	10.0	4.9020E+03
-1.300	2.200	-6.700	1.500	3.4494E+03	0.0	11.0	5.3551E+03
-1.300	2.200	-6.700	1.500	3.7640E+03	0.0	12.0	5.8107E+03

z_a (kPa)	k_a (kPa/m)	$z_{a,r}$ (kPa)	$k_{a,r}$ (kPa/m)	F_{ap} (kN)	θ_i (deg)	z (m)	R_{conc} (kN)
-1.300	2.200	-6.700	1.500	4.0834E+03	0.0	13.0	6.2457E+03
-1.300	2.200	-6.700	1.500	4.3898E+03	0.0	14.0	6.6720E+03
-1.300	2.200	-6.700	1.500	4.6996E+03	0.0	15.0	7.0980E+03
-1.300	2.200	-6.700	1.500	5.0128E+03	0.0	16.0	7.5278E+03
-1.300	2.200	-6.700	1.500	5.3295E+03	0.0	17.0	7.9618E+03
-1.300	2.200	-6.700	1.500	5.6768E+03	0.0	18.0	8.3722E+03
-1.300	2.200	-6.700	1.500	5.9799E+03	0.0	19.0	8.7855E+03
-1.300	2.200	-6.700	1.500	6.2855E+03	0.0	20.0	9.1994E+03
-1.300	2.200	-6.700	1.500	6.5955E+03	0.0	21.0	9.6740E+03
-1.300	2.200	-6.700	1.500	6.8837E+03	0.0	22.0	1.0101E+04
-1.300	2.200	-6.700	1.500	7.2539E+03	0.0	23.0	1.0531E+04
-1.300	2.200	-6.700	1.500	7.5479E+03	0.0	24.0	1.0891E+04
-1.300	2.200	-6.700	1.550	4.8287E+02	0.0	2.0	1.0419E+03
-1.300	2.200	-6.700	1.550	7.6781E+02	0.0	3.0	1.6826E+03
-1.300	2.200	-6.700	1.550	1.1522E+03	0.0	4.0	2.1901E+03
-1.300	2.200	-6.700	1.550	1.5696E+03	0.0	5.0	2.6545E+03
-1.300	2.200	-6.700	1.550	1.9052E+03	0.0	6.0	3.1220E+03
-1.300	2.200	-6.700	1.550	2.2276E+03	0.0	7.0	3.5604E+03
-1.300	2.200	-6.700	1.550	2.5523E+03	0.0	8.0	4.0255E+03
-1.300	2.200	-6.700	1.550	2.8842E+03	0.0	9.0	4.4588E+03
-1.300	2.200	-6.700	1.550	3.2098E+03	0.0	10.0	4.9020E+03
-1.300	2.200	-6.700	1.550	3.5261E+03	0.0	11.0	5.3551E+03
-1.300	2.200	-6.700	1.550	3.8630E+03	0.0	12.0	5.8107E+03
-1.300	2.200	-6.700	1.550	4.1894E+03	0.0	13.0	6.2457E+03
-1.300	2.200	-6.700	1.550	4.5046E+03	0.0	14.0	6.6720E+03
-1.300	2.200	-6.700	1.550	4.8191E+03	0.0	15.0	7.0980E+03
-1.300	2.200	-6.700	1.550	5.1389E+03	0.0	16.0	7.5278E+03
-1.300	2.200	-6.700	1.550	5.4616E+03	0.0	17.0	7.9618E+03
-1.300	2.200	-6.700	1.550	5.8155E+03	0.0	18.0	8.3722E+03
-1.300	2.200	-6.700	1.550	6.1255E+03	0.0	19.0	8.7855E+03
-1.300	2.200	-6.700	1.550	6.4386E+03	0.0	20.0	9.1994E+03
-1.300	2.200	-6.700	1.550	6.7528E+03	0.0	21.0	9.6740E+03
-1.300	2.200	-6.700	1.550	7.0467E+03	0.0	22.0	1.0101E+04
-1.300	2.200	-6.700	1.550	7.3673E+03	0.0	23.0	1.0531E+04
-1.300	2.200	-6.700	1.550	7.7234E+03	0.0	24.0	1.0891E+04
-1.300	2.200	-6.700	1.550	8.0246E+03	0.0	25.0	1.1385E+04
-1.300	2.200	-6.700	1.600	4.7761E+02	0.0	2.0	1.0419E+03
-1.300	2.200	-6.700	1.600	7.7917E+02	0.0	3.0	1.6826E+03
-1.300	2.200	-6.700	1.600	1.1744E+03	0.0	4.0	2.1901E+03
-1.300	2.200	-6.700	1.600	1.6095E+03	0.0	5.0	2.6545E+03
-1.300	2.200	-6.700	1.600	1.9483E+03	0.0	6.0	3.1220E+03
-1.300	2.200	-6.700	1.600	2.2798E+03	0.0	7.0	3.5604E+03
-1.300	2.200	-6.700	1.600	2.6105E+03	0.0	8.0	4.0255E+03
-1.300	2.200	-6.700	1.600	2.9479E+03	0.0	9.0	4.4588E+03
-1.300	2.200	-6.700	1.600	3.2783E+03	0.0	10.0	4.9020E+03
-1.300	2.200	-6.700	1.600	3.6146E+03	0.0	11.0	5.3551E+03
-1.300	2.200	-6.700	1.600	3.9573E+03	0.0	12.0	5.8107E+03
-1.300	2.200	-6.700	1.600	4.2863E+03	0.0	13.0	6.2457E+03
-1.300	2.200	-6.700	1.600	4.6267E+03	0.0	14.0	6.6720E+03
-1.300	2.200	-6.700	1.600	4.9465E+03	0.0	15.0	7.0980E+03
-1.300	2.200	-6.700	1.600	5.2708E+03	0.0	16.0	7.5278E+03
-1.300	2.200	-6.700	1.600	5.6001E+03	0.0	17.0	7.9618E+03
-1.300	2.200	-6.700	1.600	5.9584E+03	0.0	18.0	8.3722E+03
-1.300	2.200	-6.700	1.600	6.2729E+03	0.0	19.0	8.7855E+03
-1.300	2.200	-6.700	1.600	6.5902E+03	0.0	20.0	9.1994E+03
-1.300	2.200	-6.700	1.600	6.9101E+03	0.0	21.0	9.6740E+03
-1.300	2.200	-6.700	1.600	7.2310E+03	0.0	22.0	1.0101E+04
-1.300	2.200	-6.700	1.600	7.6148E+03	0.0	23.0	1.0531E+04
-1.300	2.200	-6.700	1.600	7.9181E+03	0.0	24.0	1.0891E+04
-1.300	2.200	-6.700	1.600	8.2228E+03	0.0	25.0	1.1385E+04
-1.300	2.200	-6.700	1.600	8.5296E+03	0.0	26.0	1.1793E+04
-1.300	2.200	-6.700	1.300	4.9136E+02	2.5	2.0	1.0702E+03
-1.300	2.200	-6.700	1.300	7.4851E+02	2.5	3.0	1.7004E+03
-1.300	2.200	-6.700	1.300	1.0525E+03	2.5	4.0	2.2026E+03
-1.300	2.200	-6.700	1.300	1.3838E+03	2.5	5.0	2.6688E+03
-1.300	2.200	-6.700	1.300	1.6771E+03	2.5	6.0	3.1237E+03
-1.300	2.200	-6.700	1.300	1.9619E+03	2.5	7.0	3.5714E+03
-1.300	2.200	-6.700	1.300	2.2485E+03	2.5	8.0	4.0308E+03
-1.300	2.200	-6.700	1.300	2.5385E+03	2.5	9.0	4.4671E+03
-1.300	2.200	-6.700	1.300	2.8222E+03	2.5	10.0	4.9088E+03
-1.300	2.200	-6.700	1.300	3.1462E+03	2.5	11.0	5.3559E+03
-1.300	2.200	-6.700	1.300	3.4446E+03	2.5	12.0	5.7693E+03
-1.300	2.200	-6.700	1.300	3.7177E+03	2.5	13.0	6.2356E+03
-1.300	2.200	-6.700	1.300	4.0076E+03	2.5	14.0	6.6983E+03
-1.300	2.200	-6.700	1.300	4.2659E+03	2.5	15.0	7.1257E+03
-1.300	2.200	-6.700	1.300	4.5433E+03	2.5	16.0	7.5554E+03
-1.300	2.200	-6.700	1.300	4.8217E+03	2.5	17.0	7.9871E+03
-1.300	2.200	-6.700	1.300	5.1063E+03	2.5	18.0	8.3762E+03
-1.300	2.200	-6.700	1.300	4.9136E+02	5.0	2.0	1.1470E+03
-1.300	2.200	-6.700	1.300	7.4851E+02	5.0	3.0	1.7351E+03
-1.300	2.200	-6.700	1.300	1.0525E+03	5.0	4.0	2.2353E+03
-1.300	2.200	-6.700	1.300	1.3838E+03	5.0	5.0	2.6939E+03
-1.300	2.200	-6.700	1.300	1.6771E+03	5.0	6.0	3.1584E+03
-1.300	2.200	-6.700	1.300	1.9619E+03	5.0	7.0	3.5752E+03
-1.300	2.200	-6.700	1.300	2.2485E+03	5.0	8.0	4.0480E+03
-1.300	2.200	-6.700	1.300	2.5385E+03	5.0	9.0	4.4912E+03
-1.300	2.200	-6.700	1.300	2.8222E+03	5.0	10.0	4.9027E+03
-1.300	2.200	-6.700	1.300	3.1462E+03	5.0	11.0	5.3525E+03
-1.300	2.200	-6.700	1.300	3.4446E+03	5.0	12.0	5.7743E+03
-1.300	2.200	-6.700	1.300	3.7177E+03	5.0	13.0	6.2300E+03
-1.300	2.200	-6.700	1.300	4.0076E+03	5.0	14.0	6.6533E+03
-1.300	2.200	-6.700	1.300	4.2659E+03	5.0	15.0	7.0738E+03
-1.300	2.200	-6.700	1.300	4.5433E+03	5.0	16.0	7.4991E+03
-1.300	2.200	-6.700	1.300	4.8217E+03	5.0	17.0	7.9353E+03

s_u (kPa)	k_u (kPa/m)	$s_{u,r}$ (kPa)	$k_{u,r}$ (kPa/m)	F_{dp} (kN)	θ_i (deg)	z (m)	R_{case} (kN)
-1.300	2.200	-6.700	1.300	5.1063E+03	5.0	18.0	8.4368E+03
-1.300	2.200	-6.700	1.300	4.9136E+02	7.5	2.0	1.2361E+03
-1.300	2.200	-6.700	1.300	7.4851E+02	7.5	3.0	1.8029E+03
-1.300	2.200	-6.700	1.300	1.0525E+03	7.5	4.0	2.2760E+03
-1.300	2.200	-6.700	1.300	1.3838E+03	7.5	5.0	2.7274E+03
-1.300	2.200	-6.700	1.300	1.6771E+03	7.5	6.0	3.1633E+03
-1.300	2.200	-6.700	1.300	1.9619E+03	7.5	7.0	3.6228E+03
-1.300	2.200	-6.700	1.300	2.2485E+03	7.5	8.0	4.0642E+03
-1.300	2.200	-6.700	1.300	2.5385E+03	7.5	9.0	4.5253E+03
-1.300	2.200	-6.700	1.300	2.8222E+03	7.5	10.0	4.9689E+03
-1.300	2.200	-6.700	1.300	3.1462E+03	7.5	11.0	5.3654E+03
-1.300	2.200	-6.700	1.300	3.4446E+03	7.5	12.0	5.8064E+03
-1.300	2.200	-6.700	1.300	3.7177E+03	7.5	13.0	6.3120E+03
-1.300	2.200	-6.700	1.300	4.0076E+03	7.5	14.0	6.7156E+03
-1.300	2.200	-6.700	1.300	4.2659E+03	7.5	15.0	7.1730E+03
-1.300	2.200	-6.700	1.300	4.5433E+03	7.5	16.0	7.5743E+03
-1.300	2.200	-6.700	1.300	4.8217E+03	7.5	17.0	7.9813E+03
-1.300	2.200	-6.700	1.300	5.1063E+03	7.5	18.0	8.3879E+03
-1.300	2.200	-6.700	1.300	4.9136E+02	10.0	2.0	1.3209E+03
-1.300	2.200	-6.700	1.300	7.4851E+02	10.0	3.0	1.8666E+03
-1.300	2.200	-6.700	1.300	1.0525E+03	10.0	4.0	2.3290E+03
-1.300	2.200	-6.700	1.300	1.3838E+03	10.0	5.0	2.7621E+03
-1.300	2.200	-6.700	1.300	1.6771E+03	10.0	6.0	3.2117E+03
-1.300	2.200	-6.700	1.300	1.9619E+03	10.0	7.0	3.6649E+03
-1.300	2.200	-6.700	1.300	2.2485E+03	10.0	8.0	4.1187E+03
-1.300	2.200	-6.700	1.300	2.5385E+03	10.0	9.0	4.5331E+03
-1.300	2.200	-6.700	1.300	2.8222E+03	10.0	10.0	4.9961E+03
-1.300	2.200	-6.700	1.300	3.1462E+03	10.0	11.0	5.4039E+03
-1.300	2.200	-6.700	1.300	3.4446E+03	10.0	12.0	5.8809E+03
-1.300	2.200	-6.700	1.300	3.7177E+03	10.0	13.0	6.3060E+03
-1.300	2.200	-6.700	1.300	4.0076E+03	10.0	14.0	6.7273E+03
-1.300	2.200	-6.700	1.300	4.2659E+03	10.0	15.0	7.1502E+03
-1.300	2.200	-6.700	1.300	4.5433E+03	10.0	16.0	7.5724E+03
-1.300	2.200	-6.700	1.300	4.8217E+03	10.0	17.0	7.9946E+03
-1.300	2.200	-6.700	1.300	5.1063E+03	10.0	18.0	8.4198E+03
-1.300	2.200	-6.700	1.300	4.9136E+02	12.5	2.0	1.4185E+03
-1.300	2.200	-6.700	1.300	7.4851E+02	12.5	3.0	1.9401E+03
-1.300	2.200	-6.700	1.300	1.0525E+03	12.5	4.0	2.3885E+03
-1.300	2.200	-6.700	1.300	1.3838E+03	12.5	5.0	2.8312E+03
-1.300	2.200	-6.700	1.300	1.6771E+03	12.5	6.0	3.2746E+03
-1.300	2.200	-6.700	1.300	1.9619E+03	12.5	7.0	3.7078E+03
-1.300	2.200	-6.700	1.300	2.2485E+03	12.5	8.0	4.1434E+03
-1.300	2.200	-6.700	1.300	2.5385E+03	12.5	9.0	4.5727E+03
-1.300	2.200	-6.700	1.300	2.8222E+03	12.5	10.0	5.0055E+03
-1.300	2.200	-6.700	1.300	3.1462E+03	12.5	11.0	5.4377E+03
-1.300	2.200	-6.700	1.300	3.4446E+03	12.5	12.0	5.8694E+03
-1.300	2.200	-6.700	1.300	3.7177E+03	12.5	13.0	6.3011E+03
-1.300	2.200	-6.700	1.300	4.0076E+03	12.5	14.0	6.7401E+03
-1.300	2.200	-6.700	1.300	4.2659E+03	12.5	15.0	7.1948E+03
-1.300	2.200	-6.700	1.300	4.5433E+03	12.5	16.0	7.6301E+03
-1.300	2.200	-6.700	1.300	4.8217E+03	12.5	17.0	8.0184E+03
-1.300	2.200	-6.700	1.300	5.1063E+03	12.5	18.0	8.4526E+03
-1.300	2.200	-6.700	1.300	4.9136E+02	15.0	2.0	1.5105E+03
-1.300	2.200	-6.700	1.300	7.4851E+02	15.0	3.0	2.0179E+03
-1.300	2.200	-6.700	1.300	1.0525E+03	15.0	4.0	2.4466E+03
-1.300	2.200	-6.700	1.300	1.3838E+03	15.0	5.0	2.8761E+03
-1.300	2.200	-6.700	1.300	1.6771E+03	15.0	6.0	3.3386E+03
-1.300	2.200	-6.700	1.300	1.9619E+03	15.0	7.0	3.7539E+03
-1.300	2.200	-6.700	1.300	2.2485E+03	15.0	8.0	4.2300E+03
-1.300	2.200	-6.700	1.300	2.5385E+03	15.0	9.0	4.6442E+03
-1.300	2.200	-6.700	1.300	2.8222E+03	15.0	10.0	5.0932E+03
-1.300	2.200	-6.700	1.300	3.1462E+03	15.0	11.0	5.4803E+03
-1.300	2.200	-6.700	1.300	3.4446E+03	15.0	12.0	5.9387E+03
-1.300	2.200	-6.700	1.300	3.7177E+03	15.0	13.0	6.3856E+03
-1.300	2.200	-6.700	1.300	4.0076E+03	15.0	14.0	6.7838E+03
-1.300	2.200	-6.700	1.300	4.2659E+03	15.0	15.0	7.1826E+03
-1.300	2.200	-6.700	1.300	4.5433E+03	15.0	16.0	7.7099E+03
-1.300	2.200	-6.700	1.300	4.8217E+03	15.0	17.0	8.1035E+03
-1.300	2.200	-6.700	1.300	5.1063E+03	15.0	18.0	8.4987E+03

- o0o -

APPENDIX
D
SHEAR STRENGTH DATA

Appendix D Shear Strength Data

D.1 Measured Shear Strength Data

Input file to REGRESS2. Measured intact and remoulded shear strength at considered location.

Depth (m)	Intact shear strength (kPa)	Remld. shear strength (kPa)
1	6	0.5
3	9.5	1.5
5	10	2
7	21	3
9	14.5	3
11	20	3
13	21	4
15	30	6.4
15	29	4
16	34	9
16	28	5.5
17	44	19
18	40	27
19	42	21
20	36	18
21	44	18
22	49	30
23	53	24
24	48	27
25	54	38
26	58	30
27	62	36
28	55	30
29	62	31
29	63	27
31	72	31
31	69	28
33	70	39
34	81	38
36	80	39

D.2 Modelled Shear Strength

Output file to REGRESS2. Computed mean values, standard deviations and correlation coefficient matrix for the four intercept values and gradients for the intact and remoulded trend lines, in addition to standard deviation and correlation coefficient for the residuals.

```
          TROLL DATA
    Applied in Probabilistic Analysis

X AND Y ARE CORRELATED AND VARY LINEARLY WITH DEPTH Z

X = A1 + A2 * Z
Y = A3 + A4 * Z

CONSTANT STANDARD DEVIATION OF RESIDUALS WITH DEPTH

MAXIMUM LIKELIHOOD ESTIMATOR FOR A1-A4:
A1= -0.6684E+01
A2=  0.1314E+01
A3= -0.1302E+01
A4=  0.2225E+01

STANDARD DEVIATIONS FOR A1-A4:
D(A1)=  0.2354E+01
D(A2)=  0.1061E+00
D(A3)=  0.1786E+01
D(A4)=  0.8047E-01

C.o.V. FOR A1-A4:
CoV(A1)= -0.3522E+00
CoV(A2)=  0.8074E-01
CoV(A3)= -0.1372E+01
CoV(A4)=  0.3616E-01

COVARIANCE MATRIX FOR A1-A4:
             0.554E+01  -0.226E+00    0.183E+01     -0.748E-01
            -0.226E+00   0.112E-01   -0.748E-01      0.372E-02
             0.183E+01  -0.748E-01    0.319E+01     -0.130E+00
            -0.748E-01   0.372E-02   -0.130E+00      0.648E-02

CORRELATION MATRIX FOR A1-A4:
              1.0000    -0.9071       0.4355  -0.3950
             -0.9071     1.0000      -0.3950   0.4355
              0.4355    -0.3950       1.0000  -0.9071
             -0.3950     0.4355      -0.9071   1.0000

STANDARD DEVIATIONS OF RESIDUALS:
ST.DEV. IN RES.(X)=   0.543E+01
ST.DEV. IN RES.(Y)=   0.412E+01

CORR. COEF. BETWEEN RESIDUALS = 0.435E+00
```

- o0o -

APPENDIX
E
UPDATED ESTIMATES FOR THE FAILURE PROBABILITY AFTER INSTALLATION

Appendix E Updated Estimates for the Failure Probability After Installation

After installation, more information about the system is available than at the design stage. E.g., if the installation was logged measured actual penetration depth or drag length of the anchor could be available. This one-site information, accounting for possible measurement uncertainties and uncertainty associated with the determining the actual drag length prior to start of penetration of anchor, can be utilised in modifying the estimated characteristic anchor resistance R_{char} and thereby the annual failure probability due to an extreme line tension.

The reliability formulations made have been defined such that it is simple to account for the additional information in the estimation of the annual failure probability. The additional information about the drag length and/or penetration depth is included in the formulation through conditioning, applying Bayesian updating.

The reliability formulation accounting for additional information about penetration depth and drag length after installation reads,

$$P_F = P\left(g(x) \le 0 \mid z_{pred} - z_{meas} = 0 \cap d_{i-pred} - d_{i-meas} = 0\right) \qquad \text{(E.1)}$$

where the limit state function g(x) is given by equation 4.10.

The predicted penetration depth (z_{pred}) and drag length ($d_{i\text{-}pred}$) are given directly from the response surface function, Equations (5.1) and (5.2). The predicted penetration depth, the drag length and the anchor resistance are directly available through the modelled response surface, as *cmb-pendep*, *cmb-drglen* and *cmb-hold*, respectively in the PROBAN input file.

The measured penetration depth (z_{meas}) and the measured drag length ($d_{i\text{-}meas}$) are equal to the measured values, modelled as stochastic if the measurements are associated with uncertainty. If, e.g. there is uncertainty as to how long the anchor dragged prior to start of penetration, this must be accounted for in the modelling since there is only the drag after penetration that is represented in the response surface. The updating event for drag length is then formulated as,

$$d_{i-pred} - \left(d_{i-meas} - d_{bedding-in}\right) = 0 \qquad \text{(E.2)}$$

where $d_{bedding\text{-}in}$ is the estimated drag length for the anchor to get sufficient embedment (bedding-in) to start the actual penetration, typically associated with large uncertainty.

The formulations for updating of the estimated annual failure probability after installation are included here to show that such an updating is possible to carry out applying probabilistic methods. Such an updating could be of interest, e.g. if the anchor installation operation was not accomplished as initially planned, or if the anchor system is to be upgraded to higher design loads during operation, (e.g. due to new mooring configurations or more harsh environmental conditions).

- o0o -

APPENDIX
F
DWA INPUT TO PROBAN RUNS

Appendix F DWA PROBAN Runs

```
% DWA II PROJECT, Report TR-205, Pilot Reliability Analysis of a Fluke Anchor
%--Input file for DIGIN runs applied in report DNV Rep.No 98-3034, rev. 01,
% Espen Cramer, 26/1 98
%
%--Definition of input variables----------
%
% Define uncertainty to the prediceted linear trend line for shear capacity
%
CREATE VARIABLE s_tr0 'Remoulded shear strength trend intercept (kPa)' DISTRIBUTION Normal Mean-StD -6.68 2.35
CREATE VARIABLE k_r 'Remoulded shear strength gradient (kPa/m)' DISTRIBUTION Normal Mean-StD 1.314 0.1061
CREATE VARIABLE s_ti0 'Intact shear strength trend intercept (kPa)' DISTRIBUTION Normal Mean-StD -1.30 1.78
CREATE VARIABLE k_i 'Intact shear strength gradient (kPa/m)' DISTRIBUTION Normal Mean-StD 2.225 0.0805
%
% Define residuals arround the trend line
%
CREATE VARIABLE e_r 'Residuals remoulded shear strength (kPa/m)' DISTRIBUTION Normal Mean-StD 0.0 5.43
CREATE VARIABLE e_i 'Residuals intact shear strength (kPa/m)' DISTRIBUTION Normal Mean-StD 0.0 4.12
%
% Define Correlation Matrix for trend line and residuals
%
% Trend line:
ASSIGN CORRELATION ( ONLY s_tr0 k_r ) BASIC -0.907
ASSIGN CORRELATION ( ONLY s_ti0 k_i ) BASIC -0.907
% Residuals
ASSIGN CORRELATION ( ONLY e_r e_i ) BASIC 0.435
% Trend lines
ASSIGN CORRELATION ( ONLY s_tr0 s_ti0 ) BASIC 0.435
ASSIGN CORRELATION ( ONLY k_r k_i ) BASIC 0.435
ASSIGN CORRELATION ( ONLY s_tr0 k_i ) BASIC -0.395
ASSIGN CORRELATION ( ONLY s_ti0 k_r ) BASIC -0.395
%
% Define acting shear-strength intercept
%
CREATE VARIABLE s_r0 'Residuals intact shear strength (kPa/m)' FUNCTION SUM (s_tr0 e_r)
CREATE VARIABLE s_i0 'Residuals intact shear strength (kPa/m)' FUNCTION SUM (s_ti0 e_i)
%
% Define influence of Loading Rate and Degradation
%
%Equivalent number of stress cycles
CREATE VARIABLE Neq 'Equivalent number of cycles' DISTRIBUTION Weibull Mean-StD-Low 3.16 1.61 0.25
%Loading rage and degradatin factor for b=0.7
CREATE VARIABLE dum1 '1.5212*N**(-0.0883)' FUNCTION POWER Neq -0.0883
CREATE VARIABLE u07fcy 'One-way cyclic stress for b=0.7' FUNCTION Product (1.5212 dum1)
%Influence of b=(0.6-0.8) on loading rate and degradation factor
CREATE VARIABLE b 'Rate of average stress' DISTRIBUTION Uniform Limits 0.6 0.8
CREATE VARIABLE b2 'b*b' FUNCTION Product (b b)
CREATE VARIABLE Xb 'Influence of b different from 0.7' FUNCTION Linear-Comb (-0.3831 b2 0.2299 b 1.0268 1.0 )
%
%Influence of modelling uncertainty on Ufcy for given Neq and b
CREATE VARIABLE Xfcy 'Modelling uncert on curve' DISTRIBUTION Normal Mean-StD 1.0 0.025
%
CREATE VARIABLE u_fcy 'One-way cyclic stress' FUNCTION Product (Xfcy Xb u07fcy)
%
% Define modelling uncertainty on DIGIN Computations
%
CREATE VARIABLE u_hold 'Model uncertainty on holding capacity' DISTRIBUTION Normal Mean-StD 1.0 0.15
CREATE VARIABLE u_pendep 'Model uncertainty on penetration depth' DISTRIBUTION Normal Mean-StD 1.0 0.15
CREATE VARIABLE u_drglen 'Model uncertainty on drag length' DISTRIBUTION Normal Mean-StD 1.0 0.15
%
% Annual extreme applied tension (kN)
%
CREATE VARIABLE l_e 'Estimated annual extreme tension (kN)' DISTRIBUTION Weibull Alp-Beta-Low 120.0 0.6 1300.0
%
% Define modelling uncertainty on applied annual extreme tension
%
CREATE VARIABLE u_le 'Modelling uncertainty on annual tension' DISTRIBUTION Normal Mean-CoV 1.0 0.15
%
CREATE VARIABLE annl_tension 'Applied annual extreme tension with model uncert' FUNCTION PROD (u_le l_e )
%
% Define Uplift angle under annual extreme tension
%
CREATE VARIABLE theta_e 'Uplift angle (deg)' FIXED 0.0
%
% Define Installation tension (kN)
```

```
%
CREATE VARIABLE I_i  'Installation tension (kN)' FIXED 3500.0
%
% Computed variables from response surface function
% fun(1) = cmb-pendep : Penetration depth
% fun(2) = cmb-drglen : Drag length
% fun(3) = cmb-hold   : Holding capacity
%
CREATE VARIABLE cmb 'Vector of installation results from interface'
  FUNCTION getcmb
   s_i0 k_i  s_r0 k_r  I_i theta_e
  -1.5  2.2  -2.2 1.3  I_i    0
   4.0  0.1   4.0  0.1  1000.0  5.0
   3 1 1
   40.0 200.0 10000.0
%
% Combined holding capacity
%
CREATE VARIABLE hold_fcy  'Holding capacity with cyclic effect'  FUNCTION product (only cmb-hold u_fcy )
%
CREATE VARIABLE hold_inc 'Increase in holding power after installation'  FUNCTION Difference hold_fcy I_i
%
CREATE VARIABLE hold_cap 'Total hold capacity '  FUNCTION Linear-Comb (only  u_hold hold_inc  I_i 1.0)
%
% Account for uncertainty on Drag Length and Holding Capacity
%
CREATE VARIABLE pendep 'penetration depth' FUNCTION PRODUCT (u_pendep cmb-pendep)
CREATE VARIABLE drglen 'drag length'      FUNCTION PRODUCT (u_drglen cmb-drglen)
%
% Defines threshold values for determination of Cummulative distributions
%
CREATE VARIABLE hold_t   'Holding capacity threshold' FIXED 6000.0
CREATE VARIABLE pendep_t 'Penetration depth threshold' FIXED 15.0
CREATE VARIABLE drglen_t 'Drag length threshold' FIXED 60.0
%
% Limit state function for holding capacity:
%
CREATE VARIABLE lim_failure 'Limit state for annual Pf: drag '  FUNCTION Difference   hold_cap  annl_tension
%
% Limit state function for determination of cummulative distributions
% Include modelling uncertainty in holding capacity only
%
CREATE VARIABLE cum_pendep 'Limit state penetration depth'  FUNCTION Difference  cmb-pendep  pendep_t
%
CREATE VARIABLE cum_drglen 'Limit state penetration depth'  FUNCTION Difference  cmb-drglen  drglen_t
%
CREATE VARIABLE cum_hold 'Limit state holding capacity '  FUNCTION Difference  hold_cap  hold_t
%
%--Definition of events-----------------------------------
%
CREATE EVENT Pf-annual  'Pf annual: drag of anchor'  SINGLE lim_failure < 0.0
CREATE EVENT Cum-pendep 'Cum dist penetration depth' SINGLE cum_pendep < 0.0
CREATE EVENT Cum-drglen 'Cum dist drag length'      SINGLE cum_drglen < 0.0
CREATE EVENT Cum-hold   'Cum dist for hold capacity' SINGLE cum_hold < 0.0
%
%--Settings-----------------------------------------------
ASSIGN STARTING-POINT VARIABLE I_e 6000.0
%
% Extension of work:
% Include variables for updating based on measured drag length or penetration depth
% Define measured penetration depth or drag length
 CREATE VARIABLE mes-pendep 'measured actual depth' DISTRIBUTION NORMAL MEAN-COV 20.0 0.05
 CREATE VARIABLE mes-drglen 'measured actual drag'  DISTRIBUTION NORMAL MEAN-COV 80.0 0.10
% Define measured event.
 CREATE VARIABLE upd-pendep 'actual depth' FUNCTION DIFFERENCE pendep mes-pendep
 CREATE VARIABLE upd-drglen 'actual depth' FUNCTION DIFFERENCE drglen mes-drglen
 CREATE EVENT  Mes-pendep 'depth equal measured depth'      SINGLE upd-pendep = 0.0
 CREATE EVENT  Mes-drglen 'drag length equal measured length' SINGLE upd-drglen = 0.0
% Define conditinal events accounting for the measured values
 CREATE EVENT  Upd-Pf-pendep 'Updated PF from depth measurment' CONDITIONED Pf-annual Mes-pendep
 CREATE EVENT  Upd-Pf-drglen 'Updated PF from drag measurment'  CONDITIONED Pf-annual Mes-drglen
```

- o0o -

APPENDIX
G
DWA RESULT FILE FROM PROBAN

Appendix G: DWA Result File from PROBAN.

```
      ******       ******       ******       ******       ** ***  ****
     ********     ********     ********     ********     **********
    **      **   **      **   **      **   **      **     **    **    **
    **           **      **   **                  **     **    **    **
     *******     **********    *******      *********     **    **    **
      *******    *********      *******     **********    **    **    **
            **   **                    **   **      **    **    **    **
    **      **   **      **    **      **   **      **    **    **    **
     ********     ********     ********     *********     **    **    **
      ******       ******       ******       ****** **    **    **    **
         ************************************************************
         *                                                          *
         *                                                          *
         *                      P R O B A N                         *
         *                                                          *
         *    General Purpose Probabilistic Analysis Program        *
         *                                                          *
         ************************************************************

                    Marketing and Support by DNV Sesam
 Program id    : 4.2-01                  Computer          : sun4u
 Release date  :  9-OCT-1996             Impl. update      :
 Access time   : 28-JAN-1998 10:20:01    Operating system  : SunOS 5.5.1 Generi
 User id       : espen                   CPU id            : 0008584856
 Account       : 1031116                 Installation      : DNV titanic

 Copyright DET NORSKE VERITAS SESAM AS, P.O.Box 300, N-1322 Hovik, Norway

                   FORM/SORM ANALYSIS                          SUB PAGE:
                 +-----------------------------------------------+
                 ! Probability of   : Pf-annual                  !
                 !                    Pf annual: drag of anchor  !
                 ! Analysis method  : FORM                      !
                 +-----------------------------------------------+

                   FORM Probability:                4.60647E-05

                   FORM Reliability index:             3.9104

                            Importance factors

                           Variable     Importance
                           ------------------------
                           l_e                86.0
                           ImpGroup-2          6.6
                           u_le                4.7
                           u_hold              1.5
                           Neq                 0.5
                           ImpGroup-1          0.3
                           Xfcy                0.2
                           b                   0.2

 ImpGroup-1  :  k_i          k_r          s_ti0        s_tr0
 ImpGroup-2  :  e_i          e_r
```

Linearization point

Variable	Type	Value	Prob	
u_le	Normal	1.127652148E+00	0.802619	+
l_e	Weibull	5.839475976E+03	0.999856	+++
theta_e	Constant	0.000000000E+00		
Xfcy	Normal	9.961390508E-01	0.438632	-
u_hold	Normal	9.270632018E-01	0.313397	-
l_i	Constant	3.500000000E+03		
b	Uniform	7.122260342E-01	0.561130	+
Neq	Weibull	3.426284520E+00	0.610339	+
k_i	Normal	2.224712164E+00	0.498574	-
k_r	Normal	1.303714011E+00	0.461385	-
s_ti0	Normal	-1.296526230E+00	0.500779	+
s_tr0	Normal	-6.310348574E+00	0.562495	+
e_i	Normal	-5.428451097E-02	0.494744	-
e_r	Normal	4.894396035E+00	0.816302	+
s_i0	Sum	-1.350810741E+00		
s_r0	Sum	-1.415952539E+00		
annl_tension	Product	6.584897625E+03		
b2	Product	5.072659238E-01		
dum1	Power	8.969641628E-01		
cmb	getcmb	1.019056234E+01		
		3.245315507E+01		
		5.042387487E+03		
Xb	Linear-Comb	9.962071899E-01		
u07fcy	Product	1.364461884E+00		
u_fcy	Product	1.354038603E+00		
hold_fcy	Product	6.827587306E+03		
hold_inc	Difference	3.327587306E+03		
hold_cap	Linear-Comb	6.584883742E+03		
lim_failure	Difference	-1.388294505E-02		

- o0o -